MICROBIOLOGICAL REVIEWS, Dec. 1980, p. 572-630
0146-0749/80/04-0572/59$02.00/0

Vol. 44, No. 4

Light Antennas in Phototactic Algae

KENNETH W. FOSTER[1]* AND ROBERT D. SMYTH[2]

Department of Pharmacology, Mount Sinai School of Medicine of the City University of New York, New York, New York 10029[1]; and Division of Biology, California Institute of Technology, Pasadena, California 91125[2]

It's my experience that everyone who has a device like a tracker in mind wants to use it ... where the range is maximum, the signals are small, and the going is tough.

Lucien M. Biberman (19)

INTRODUCTION

All photosynthetic organisms have evolved specialized means of regulating their exposure to sunlight. One form this adaptation has taken among the flagellated algae is their phototactic response, the ability to swim toward or away from a source of light. The response is found among representatives of all of the major algal groups except the Cyanophyta and the Rhodophyceae, which entirely lack flagellated forms. (We use the provisional classification of Dodge [58] in which most groups are not referred to above the level of class because of present uncertainties of relationships. This classification follows botanical rather than zoological nomenclature.) The response was first observed by Treviranus in 1817 in zoospores released from the filamentous alga *Draparnaldia* (239). Leading biologists studied the response in the nineteenth and early twentieth centuries, a period of investigation that culminated in Buder's definitive paper on algal phototaxis in 1917 (31). After a period of relative neglect, phototaxis has been under active investigation in a number of laboratories in recent years. Earlier work is thoroughly reviewed by Haupt (106); later work is covered by Feinleib and Curry (75), Forward (80), Lenci and Colombetti (146), Diehn (54), and Nultsch and Häder (200). Here, we apply physical principles to obtain new information from the results of physiological experiments and ultrastructural studies of algae reported in the literature. The purpose of our analysis is to explain phototaxis better and to suggest new approaches for studying the problem.

Buder (31) demonstrated that phototactic algal flagellates orient to the direction of a beam of light, provided its intensity is within the behavioral range of the cell. (We use the familiar term light intensity. More and more frequently irradiance is used instead.) This behavior is illustrated in Fig. 1, which shows the swimming path of a single cell. At B, light was turned on from below. The cell altered its path, locked on to the beam, and swam directly toward its source. At C, the light was turned off, and the cell drifted away. By means of converging and diverging lenses, Buder proved that the cell responds to light direction, not an external gradient of light intensity. In other words, a positively phototactic cell swims toward a light source whether the external light intensity increases, decreases, or remains the same. Buder examined the swimming paths and aggregation patterns of a variety of algae, including *Chlamydomonas, Carteria, Euglena, Trachelomonas,* colonial algae, and swarm cells of filamentous forms. He found that these algae orient to steady illumination and concluded that this behavior is the biologically significant photoresponse. In short, flagellated algae are specialized for tracking light direction.

The geometry of both the cell and its swimming path are important for phototaxis. When the cell changes its orientation to light, the distribution of light within the cell changes. Jennings (131) and Buder (31) recognized that the cell uses this change as a signal of how the cell has deviated from the light direction and what corrective response is needed. However, detailed

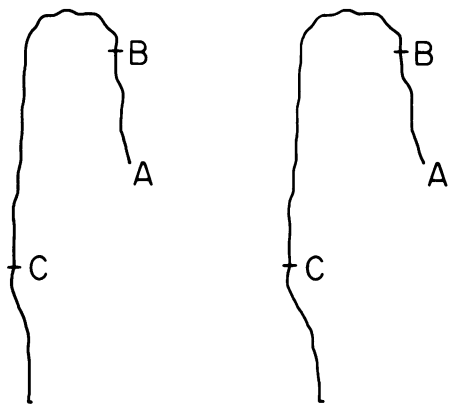

FIG. 1. *Stereo plot of the path of an alga showing phototactic attraction to light. The path appears in correct three-dimensional perspective when the image of the right-hand plot seen by right eye is superimposed on image of left-hand plot seen by left eye. A single cell of Chlamydomonas reinhardtii (strain 137c, mating type +) was followed for 12.0 s in the tracking microscope (16). Dim red light, which causes no response, was used for tracking. The position of the cell was recorded every 42 ms. The track starts at A. At B, blue stimulating light from below was turned on. At C, the stimulating light was turned off. Path length, 1.9 mm; average speed, 159 ± 14 μm/s.*

information about the signal and the response has proved difficult to obtain. After considering phototaxis from as many viewpoints as possible, we concluded that specialized structures independent of the photosynthetic apparatus are used for phototaxis, and that these structures are best thought of as directional light wave antennas. We call them antennas because, like radio wave antennas, their optical characteristics are dominated by interference and diffraction. In both algal and radio antennas this is a consequence of their size, which is of the same order as the electromagnetic waves they receive. In both cases the size of the structures is less than 50 wavelengths. (Larger radio antennas are properly called telescopes and can be described in familiar optical terms.)

Usually, an algal antenna is an eyespot plus associated structures. Algae control phototactic behavior by scanning their environment with the antennas. In our discussion, we follow a philosophy used in determining performance criteria of man-made antennas, in which emphasis is on optimum design for some intended function (224). In biological terms, this means that we must consider the environment, the signal received by the photoreceptor, signal processing, and the response in addition to the properties of the photoreceptor structure. Relevant information on phototaxis is limited, but by integrating details from a variety of algae, comparing them with other organisms, and considering the requirements for signal processing, we can map out the general principles of algal phototactic behavior.

One of our aims is to provide the reader with an intuitive sense of how phototaxis works. For this purpose certain dimensions must be kept in mind. Typical swimming speeds are 100 μm/s for unicellular algae and up to 1,000 μm/s for large colonial algae. Swimming is caused by the flagellar beat. As the organisms swim, their cell bodies rotate at frequencies in the range 0.2 to 2.0 Hz. The flagellar beat frequency is 10 to 100 times greater than the rotation frequency. Phototactic algae range from the size of bacteria to colonial algae containing thousands of cells and having a diameter up to 1 mm. Bacteria are typically a few micrometers in length.

This increased size relative to bacteria is important to the way that flagellated algae carry out phototaxis. Bacteria are too small to track light. One reason for this is that they cannot create within their bodies a sufficient gradient of light intensity to obtain accurate clues about light direction from changes in light intensity caused by their own motion. Furthermore, the swimming direction of bacteria is rapidly randomized by rotational Brownian motion. Motile bacteria have overcome this problem to some extent by evolving rod and spiral shapes. Even so, bacteria show at most a limited ability to orient parallel or perpendicular to a light beam (K. W. Foster and H. C. Berg, manuscript in preparation). They cannot sense light direction and cannot track. For most phototactic algae, the increase in size makes rotational Brownian motion insignificant. For example, Brownian motion randomizes the orientation of a sphere 10 μm in diameter, a common size for unicellular algae, in about 6.5 min (relaxation time). This is much longer than the reaction time of the cell. Furthermore, internal gradients of light intensity can be created in a surprising number of ways (see Antenna Structures). (The behavior of the smaller phototactic algae has not been studied in detail. The smallest is *Micromonas pusilla*, a monoflagellate 1 to 3 μm long and 0.75 to 1.0 μm wide with a volume of 1 to 2 μm^3 [158, 164, 237]. Like bacteria, this organism swims rapidly [50 body lengths per s] and changes direction frequently.)

Tracking is a sophisticated form of behavior involving problems of timing, stability, and noise. Acquisition of this ability required the evolution of complex cellular machinery and integration of the specialized components into an effective design. Tracking cannot be the incidental by-product of responses primarily used for other purposes. One biological purpose of phototaxis is to move the organism as rapidly as possible into the proper intensity of sunlight. The cells may also orient to optimize their rate of photosynthesis. Some algae appear to use light direction to find a place to mate or germinate. One indication that algae are under strong selective pressure to develop phototactic behavior is the spectacular convergent evolution that has occurred in different algal groups. As we will see, many examples are known of diverse elements that have been adapted to serve much the same function by different algae.

The Problem: Detecting Light Direction in the Native Environment

We have seen that algae regulate their exposure to light by swimming toward or away from the light source. To do this they detect a pattern in the distribution of light reaching them. The point is obvious when we consider that orientation would be impossible if the light were uniformly distributed. Light in natural environments has three physical properties (namely, color, polarization, and intensity) whose distribution pattern could be used. There is no evidence that algae orient by either color or polarization, even though they have some sensitivity

to both qualities. They orient to the intensity pattern.

The simplest possible pattern is parallel light, but natural light, especially under water, is diffuse, coming from different directions. The organism therefore must orient toward the average, or resultant, light direction. We are speaking now of the intensity of light at a single point and how it is distributed as a function of the angle of incidence. We are not speaking of a spatial gradient of light intensity. The distribution of light intensity must be sensed in such a way that the organism receives a signal telling it how to make a precise correction, a correction of the right magnitude in the right direction. For greatest effectiveness, the organism should respond correctly from any orientation.

Four severe constraints are placed on the design of the light detector: it must find the signal in a background of noise, it must operate over most of the range of light intensities found in the native environments, it must have the proper spectral sensitivity to detect the wavelengths of light that reach the algae, and it must communicate rapidly to the response apparatus. The design of a detector that extracts useful signals from noise is complex and calls for a detailed discussion here of the noise problem.

At least five sources of noise seem important in phototaxis. (i) Rotational diffusion is one source of noise. As already discussed, algae are so large that rotational Brownian motion, which results from thermal bombardment of the organism by water molecules, is insignificant. This is not the only cause of rotational diffusion. The motility of the organism itself has a random component that constantly alters its orientation. Repetitive beating of the flagella moves the organism. If all flagellar beat cycles were identical, the organism would be driven along a uniform helical path (153) perturbed only by the other sources of noise. This is partly what occurs, but random variation from one beat to the next introduces rotational and translational diffusion. The effect is accentuated by the low Reynolds number associated with cell motion; that is, inertial forces are negligible compared with viscous forces. This has the consequence of transmitting every motion of the flagella to motion of the body, causing it to move back and forth with each flagellar beat. In *Chlamydomonas*, where it has been measured, rotational diffusion is great enough so that course corrections are continuously required, but it does not prevent tracking. (*Chlamydomonas* has a Reynolds number of 10^{-3}. It rotates in a left-hand helix at about 2 Hz. Superimposed upon the rotation is rotational diffusion with a relaxation time of 2 s [R. D. Smyth and H. C. Berg, manuscript in preparation]. The flagellar beat frequency has been measured at 25 Hz [125] and 50 Hz [227] with different conditions and strains. In one beat cycle, rotational diffusion causes the cell to turn an average of 8°. The swimming speed is typically 100 μm/s. We have in our possession high-speed motion pictures of swimming *Chlamydomonas* cells. These films, made in the laboratory of T. L. Jahn by J. F. Fonseca, show that during one beat cycle the cell goes forward about 4 μm and backward about 2 μm. During one beat cycle the cell may turn back and forth through an angle of up to 20 or 30°.) (ii) A second noise source is convection currents. In shallow water, heating on the bottom causes water to rise to the surface. This creates a series of circulation paths that continuously cycle the water from the bottom to the surface and back to the bottom again. The algae must be able to reorient as this convective flow carries them off course. Both convection currents and rotational diffusion differ from the following sources of noise in that the signal is altered by actual variation in the orientation of the organism to the light. (iii) A third noise source is external fluctuation in light intensity. Waves on the surface of any body of water act as lenses that partly focus light below the surface. As the waves move, bright bars of light move with them, causing the light below the surface to fluctuate. The phenomenon can be seen by looking at ripples in shallow water in direct sunlight. Measurements made using large sensors in large bodies of water exposed to direct sunlight (51, 195 and references therein, 225) indicate that the fluctuations are large. For example, in the upper few meters the variation may be as much as 80 to 90% of the mean intensity and is maximum in the frequency range 0.4 to 1.0 Hz. This is somewhat below the rotation frequency of unicellular algae. Measurements with sensors the size of algal sensors are needed of the magnitude of light fluctuation as a function of frequency in algal environments. We predict that appropriate measurement will show that external fluctuation in light intensity constitutes an important source of noise. (iv) Shot noise is caused by statistical fluctuation in the number of excitations of photoreceptor pigment, and its magnitude depends on the amount of pigment and the amount of light. (v) Internal noise is noise produced within the organism by such factors as concentration fluctuations and fluctuations in membrane potential. This noise occurs at all stages, from signal reception through response. We know from the relatively small number of molecules involved in biochemical processes that these fluctuations must be large and must therefore introduce appreciable noise into phototaxis, but at present we have no

adequate measure or good theoretical estimate of this noise.

The Solution: a Directional Antenna Designed to Match the Environment of the Organism

Phototactic algae solve the problem of finding the light direction by scanning their environment with an antenna sensitive to light. The antenna must be integrated with the response mechanism of the cell so as to produce an effective overall design. Consider unicellular forms first. Despite their enormous diversity of form, they use the same basic scheme for phototaxis. The extent to which their antenna design matches requirements determines how effectively they track.

Figure 2 shows a diagram of *Chlamydomonas* that illustrates the principle. The cell has a red spot on its side, the eyespot. The eyespot and associated structures form a directional antenna (see Antenna Structures). (Most of the algae we discuss have eyespots. This means that one of the components of the antenna is visibly pigmented. However, the visible pigment is not the photoreceptor pigment, which is present in too small an amount to be seen in the microscope. It is not essential that the antenna have a visibly pigmented structure, and algae exist that have antennas but not eyespots. We use the words eyespot and stigma synonymously.) The antenna senses light most strongly when the light is normal to the outer surface of the antenna and least when it strikes the antenna from the side or the back. The cell swims with its flagella forward, rotating approximately twice a second as it swims. This rotation causes the antenna to scan the environment. If the swimming path were held parallel to the light direction, the antenna would receive nearly constant illumination throughout the scan cycle. But noise quickly causes the cell to deviate from the aligned orientation. When the swimming path becomes sufficiently inclined to the light direction, the light intensity seen by the antenna becomes periodic. This results from the variation in angle between the antenna and the light direction that occurs during the rotation cycle. The cell processes this periodic signal to determine when to make a corrective response that will realign the path to the light. The response of the flagella, by changing the orientation of the cell, changes the shape of the signal during the next scan cycle. The sequence of events thus forms a closed loop, the tracking servo loop diagrammed in Fig. 3.

We thus see that rotation of the cell gives a temporal pattern to the light intensity sensed by the antenna (see Signal Production). The fact

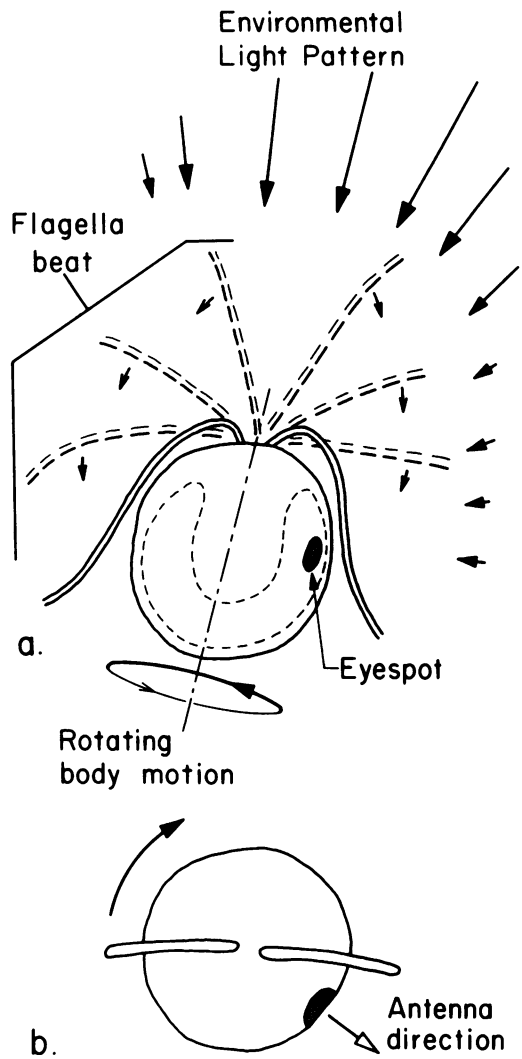

FIG. 2. *Design principles of phototaxis in Chlamydomonas. (a) Side view of cell; (b) end view. The incident light pattern is indicated by solid arrows. The eyespot, which lies inside the chloroplast (dashed line), forms part of the antenna. Rotation of the cell causes the antenna to scan the incident light. This produces a signal that controls the flagellar beat (see Fig. 3). The antenna direction (open arrow) is normal to the cell surface. The antenna is most sensitive to light coming from this direction. Successive positions of the flagella during the power stroke are shown. Flagellar motion causes the cell to translate with the flagellar end forward and to rotate in the left-hand sense.*

that the cell receives a patterned signal is central to phototaxis. The pattern is used in at least three important ways: for the information it contains about orientation, for noise suppression, and for extension of the effective intensity range. We describe each of these uses briefly

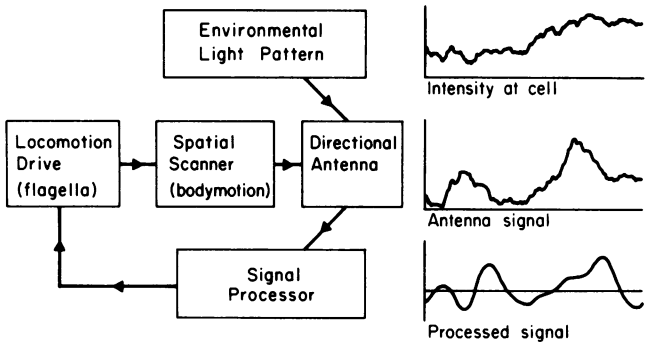

FIG. 3. *Control loop for phototaxis showing environmental stimulus and the signal at two stages of processing. The signal intensity (ordinate) during two rotations of the antenna is plotted against time (abscissa). The signal drifts because of noise, but the processed signal has two well-defined maxima phased with the rotation of the cell. Signals were computer simulated without attempting realistic noise simulation.*

here, and analyze them in detail when we discuss antenna function (see Signal Processing).

All tracking devices work by processing some form of error signal that is generated when the tracker drifts off target. To be useful for tracking, the error signal must contain information about the direction of deviation from the target. The quality of tracking can be improved if the error signal also contains information about the magnitude of the deviation. Probably the most familiar kind of tracker is a man-made one in which an array of sensors points toward the source being tracked. Each sensor points in a slightly different direction. When the tracker drifts off target, the pattern of stimulation of the sensors changes; the signal processor then analyzes the pattern of change and figures out in what direction and how fast it must move the tracker to return it to the target. Unicellular algae have only one sensor (see Antenna Structures). In a single-sensor tracker it would be useless to point the sensor at the target, because then the signal change produced upon deviation would contain no directional information. Instead, the sensor must point off to the side of the target, and its direction must be varied systematically to produce a periodic signal. The phase of the signal contains information about the error direction, and its amplitude contains information about the error magnitude. The error information can be used by the cell if the cell makes a fixed response that is phased with the error signal and proportional in magnitude to its amplitude.

For the rotation of the cell to produce a usefully patterned temporal signal at the sensor, the antenna must be directional. By this we mean that the intensity sensed by the antenna must vary with the angle of incidence of the light reaching the antenna. Merely having a small sensor asymmetrically located in the cell produces some directionality. Increased directionality is achieved by specialized antenna structures which employ a variety of optical principles (see Antenna Structures). This increases the amplitude of the signal with concomitant improvement in tracking.

What pattern of directionality in the antenna produces the maximum amplitude of signal? Qualitatively, we can see that a narrow directionality would make it difficult for the antenna to track a broad source, because the antenna would wander around on the source without detecting much change in intensity. By the same reasoning, a wide antenna would be poor for tracking a point source. The optimum design is to match the directionality of the antenna to the distribution of the light it tracks. For the ideal tracker, in other words, a plot of the relative sensitivity of the antenna in all directions would be congruent with a plot of the light intensity in all directions. We would predict, therefore, a rough match between the directionality of the antenna and the light distribution that it is most advantageous for the organism to detect (see Signal Production).

The second use that the cell makes of the temporal pattern of stimulation is noise suppression. Finding an appropriate signal in the midst of noise is never a trivial task. The problem is simplified when the detector can take advantage of some known characteristic of the signal. A familiar example is AM radio, in which the receiver can be tuned to the frequency of the transmitting station. Even if the signal does not already have a useful characteristic to aid detection when it arrives, such a characteristic can sometimes be imparted to it before it reaches the sensor. This is the scheme employed by phototactic algae. They use their own rotation

to give the light received by the sensor a known temporal pattern that can be matched with a signal processor (see Signal Production).

When considering noise, it is convenient to think of the input stimulus in a way that a signal is commonly analyzed in electronics, namely, as the sum of a series of sine waves of different frequencies. The amplitudes of the sine waves are different at different frequencies and, taken together, determine the form of the input stimulus. From this point of view we can say that cell rotation greatly enriches the sensed light intensity for certain frequencies. The signal processor then acts as a band-pass filter to select those frequencies and suppress others.

The filter used by the signal processor is more than just a band-pass filter. We show later that its precise form can be found experimentally by measuring the impulse response, the time course of response after a pulse stimulus (see Signal Processing). The filter performs two functions: (i) signal matching and (ii) differentiation.

By signal matching, we mean that the detector is especially sensitive to a particular shape of input signal, not merely to a particular frequency range. One expects a rough match between the processing filter and some stimulus pattern that can be produced by the rotation of the cell and by the directional properties of the antenna.

Differentiation is important in suppressing low-frequency noise. Low-frequency noise is troublesome because it represents a shifting base line upon which the signal is superimposed and renders absolute measurements meaningless. The rate of change of the signal (the derivative) is highly insensitive to this form of noise. Many biological sensors therefore measure the derivative rather than the absolute level of the signal. Some well-studied examples are bacterial chemotaxis (30), the light-growth response of *Phycomyces* (82, 150), the electroreceptors of the ampullae of Lorenzini in dogfish (192), some mechanoreceptors in skin (33), and carotid baroreceptors (204). In algae, the antenna signal is also processed to detect the rate of change of the signal.

In receptors, high-frequency noise (frequencies above the band-pass region) is suppressed by averaging the input stimulus over a time longer than the period of the high-frequency noise. In other words, the signal is integrated over the memory time of the receptor. Applied to algae, this means that the response at any time is determined by information collected throughout the rotation cycle. This suppresses noise, but creates a delay in the response that must be compensated for in the design (see Signal Processing). (The input signal possesses one high-frequency component with known characteristics, namely, the signal caused by the flagellar beat. Later we discuss how this might be used in signal detection [see Signal Processing].)

We can ask why evolution has selected the particular rotation frequencies observed. They probably represent, at least partly, a compromise with the frequency spectrum of the noise. The longer the rotation time, the more accurately the signal can be known. A limit to the length of the rotation period is set by low-frequency noise, in particular noise caused by external fluctuation in light intensity and rotational diffusion. Rotational diffusion eventually renders old information invalid. We suspect that noise from these souces rises at frequencies lower than the observed rotation frequency, and that the rotation frequency has been set close to the lowest frequency where phototaxis is possible.

The scheme of signal modulation and processing described so far is precisely that which has been demonstrated in the phototropic response of the fungus *Phycomyces* (50, 82), although the time scale for algal phototaxis is shorter by a factor of 10^3.

The third use mentioned above for a patterned signal is range extension. We have seen that the processor acts as a differentiator. Besides suppressing low-frequency noise, differentiation also makes the processed signal relatively independent of the average intensity of the incident light. The intensity range for algal phototaxis is best documented for *Chlamydomonas* (76, 201), which is phototactic over a 10^4 range of intensity extending from 10^{11} to 10^{15} quanta cm^{-2} s^{-1} at 500 nm.

This operating range must match the range relevant to the survival of the organism in its natural environment. Its lower limit is set by several factors, including the directionality of the antenna and the length of time the processor integrates the signal (see Threshold). Because the variation in these parameters is limited, threshold is primarily determined by the total amount of effective receptor pigment. This follows from the fact that the probability of photon capture is directly proportional to the amount of receptor pigment in the cell: the more pigment, the greater the possible operating range. Because of the quantal nature of photons, this lower limit is absolute and cannot be lowered by any amount of processing or amplification. In principle, a photoreceptor could operate up to very high light intensities, but usually it is advantageous to sacrifice performance at high intensity for optimum performance at some intermediate intensity.

Phototaxis also requires that the spectral sen-

sitivity match the color of light the cell can most advantageously use to control its response (see Action Spectra). Both the photoreceptor pigment and the antenna structures that interact with the light must be effective in the same spectral range. Furthermore, the choice (as with photosynthetic pigments) is limited to visible light, the only light appreciably transmitted by water. The photosynthetic pigments, which account for most of the absorption of photosynthetic cells, absorb strongly in the blue and red ranges; there is a range of intermediate wavelengths where their absorption is weaker. In many phototactic algae, at least part of the phototactic range lies at these intermediate wavelengths. This allows the algae to respond to light even when shaded by overlying photosynthetic organisms.

Finally, the problem of rapid and faithful communication of the signal from the antenna to the flagellum is critical. If the receptor were to cover a large portion of the body, then the signal could be spread out in time due to different delays from different parts of the receptor. Such temporal spreading would decrease the directionality of the antenna. The solution to this problem is a small antenna and extremely rapid communication, less than 20 ms in *Chlamydomonas* (see Response). For such rapid communication, large distances must be covered electrically; diffusion can be used only for short distances or where poor performance is tolerated. We discuss below various ways that algae have found to meet this problem (see Antenna Structures, Response).

At the beginning of this introduction we posed the question of how a microorganism solves the formidable problem of detecting light direction. We note that it requires a series of matches between the organism and its environment. The directionality of the antenna matches the spatial light distribution. The rotation frequency of the organism matches a frequency at which the ratio of signal to noise is optimum. The temporal filter of the signal processor matches the temporal variation of the scanning signal. The functional range of the detector matches the range of incident light intensity. The spectral sensitivity of the antenna matches the color of incident light most useful for controlling behavior. The antenna must be integrated with the response mechanism of the cell for rapid communication of the signal and proper phasing of the response. Much of the fascination of phototaxis consists of trying to unravel this complex interplay between the organism and its surroundings.

We discuss colonial algae below (see Antenna Function). Note, however, that instead of a single antenna, colonial algae have an antenna array. The function of the array can be interpreted from an understanding of antenna function in unicellular forms.

We do not discuss one of the most fundamental aspects of phototaxis, namely, the factors that determine whether a cell goes toward the light or away from it. We do not know what design features favor positive or negative phototaxis or how the individual organism regulates which way it goes. We assume that in some way this has already been determined, and we analyze the tracking technique used. The tracking principle is the same for either positive or negative phototaxis.

Finally, we do not consider in detail what the flagellum does when it responds to light or how its response affects the motion of the cell. For a comprehensive review of these subjects, see Jahn and Bovee (126–128). Alteration of flagellar shape by light and its effect on the direction of flagellar response have been described by, among others, Metzner (185), Hand and Schmidt (105), and Diehn et al. (55). Throughout our discussion, we assume that the direction of response is fixed with respect to the cell, and that the timing of the response is critical for tracking.

This introductory discussion of phototaxis has introduced several principles that may be unfamiliar. They should become clearer as we discuss available information on ultrastructure, behavior, and function.

ANTENNA STRUCTURES

In this section we examine the ultrastructure of the antennas of different algae to determine the distribution of light within the structures. In particular we consider how the light distribution varies with the orientation of the cell relative to the light direction. If we know the location of the photoreceptor, we can then ask what the directional sensitivity of the antennas is. In keeping with antenna terminology (41), we use directivity as a measure of the relative sensitivity of the antenna in a particular direction. For a strict definition of directivity, imagine that a test beam of parallel light is shone at the antenna from a particular direction, and that the intensity received by the sensor of the antenna is measured. The directivity is this intensity divided by an isotropic reference, namely, the average intensity received by the sensor when the test beam is moved through all angles of incidence. The directivity is proportional to the ratio of incident to received light intensity in a particular direction. If the antenna had no directional sensitivity, the directivity would be 1.0 in all directions. Normally it is greater than 1.0 in some directions and less than 1.0 in others. For brevity, we say that the direction of the antenna

is the direction of maximum directivity. We frequently use the word directivity simply to refer to the directional properties of the antenna. The antenna ultrastructures we discuss are specializations that achieve a pattern of directivity suitable for phototaxis.

All algal antennas are designed to see primarily in the forward direction. For the most part, their field of view is limited to light beams coming from the front of the antenna. In this respect they are analogous to man-made aperture antennas, and it will be useful in discussing algal antennas to define their effective aperture as the size of the detector normal to the direction of the antenna. It is also useful to define a measure of the angular acceptance of light, the half-beam width. This is the angle between half-intensity points in the main lobe of directivity (angle α in Fig. 9a). All algal antennas are also analogous to so-called screen-reflector antennas, which have an absorbing and reflecting screen behind the sensing element. To evaluate the effectiveness of this screen, we have introduced a measure of the front-to-back contrast, sometimes called the modulation or contrast function, defined as

$$m = (I_{\text{front}} - I_{\text{back}})/(I_{\text{front}} + I_{\text{back}}) \quad (1)$$

Values of m range from 0 for no contrast to 1 for complete contrast. In our case, I_{front} is the directivity in the antenna direction, and I_{back} is the directivity in the opposite direction. The contrast function has been a useful measure in sensory systems and elsewhere (37, 132).

We have said that algal antennas are the same order of size as the wavelength of the light they receive. As is well known, the approximations of geometric optics are strictly valid only for objects that are large relative to the wavelength of light, but this should not discourage the reader from thinking about algal antennas in terms of more familiar optical devices. Even at sizes below about five wavelengths across, for which geometric optics is no longer quantitatively accurate, it gives a qualitative picture that is useful and not grossly misleading (121).

With this general picture of an antenna in mind, we present the different optical principles that apply to understanding algal antennas before we introduce the complicated structures themselves.

Optical Principles

All the optical effects we discuss depend on the interaction of light with matter. Popular accounts are given by Weisskopf (246) and some optical texts (56, 108, 130). Light is an electromagnetic wave, meaning that it has an electric component that exerts a force on any charged particle and a magnetic component that exerts a force proportional to the velocity of the charged particle. However, when light passes through matter, the only effects we need consider are the electric forces on electrons. Light exerts a periodic force on the electrons of every molecule in its path, setting the electrons into oscillation at a frequency equal to that of the light. If this frequency is the natural oscillating frequency of the electrons, a photon of light may be absorbed. Otherwise, the oscillating charges cause light to be emitted in all directions from the molecule. This shows the net velocity of the light wave such that the velocity of propagation v is

$$v = c/n \quad (2)$$

where c is the velocity of light in a vacuum, and n is defined as the refractive index of the material.

In molecules in which the electrons have been raised to a higher energy level by absorption of a photon, the light intensity diminishes during passage through the material. The two effects, reduction in velocity and attenuation of intensity, are described quantitatively by the complex refractive index

$$\hat{n} = n - ki \quad (3)$$

where the real and imaginary indices n and k are both real numbers and $i = \sqrt{-1}$.

At the interface between two media of different composition light is both refracted and reflected. The amounts are a function of n, k, and the angle of incidence. This is important in phototaxis, and much of algal ultrastructure can be understood as ingenious manipulations of interfaces to achieve desirable light distributions.

One fallacy that has caused unnecessary confusion should be disposed of at the outset. It might be argued that achievement of directivity in a light antenna is a trivial task. The argument is as follows. Imagine a thin flat membrane of area A cm^2 containing pigment molecules oriented at random. If light of intensity I photons cm^{-2} s^{-1} is shone on the membrane at normal incidence, IA photons will pass through the membrane per second. If the membrane is tilted, the quantum flux becomes $IA \cdot \cos\theta$ photons per second, where θ is the angle of incidence. Tilting the membrane reduces the number of photons passing through it. From this, one might conclude that the number of photons absorbed by the pigment molecules will also change. This is false. The absorption does not change, because the probability that a molecule will absorb a photon depends only on the intensity of light striking each molecule and the average absorption cross section of each molecule. Neither

quantity changes with angle of incidence provided that the number of photons absorbed is small, in other words, that the pigment molecules do not screen each other. Directivity cannot be achieved merely by putting pigment molecules in a layer. The optical principles discussed below are necessary.

Absorption. Most phototactic algae are also photosynthetic and have a high concentration of photosynthetic pigments. In addition, most have a deeply pigmented organelle, the eyespot. Absorption by the eyespot pigments is an important, but by no means the only, contribution of the eyespot to antenna directivity. For a purely absorbing screen, $I_{back} = I_{front} \times T$, where T is the fraction transmitted, so that the contrast function

$$m = (1 - T)/(1 + T) \quad (4)$$

Absorption of light by a pigmented structure is always accompanied by a certain amount of reflection.

Absorption can be described in several different ways, the most useful description depending on the application. We summarize four descriptions that we will use later.

Lambert's law states that equal paths in the same absorbing medium absorb equal fractions of the light that enters them. From this it follows that

$$T = e^{-\alpha x} \quad (5)$$

where α is the absorption or attenuation coefficient (per centimeter), and x is the distance through an absorbing layer (in centimeters).

For a solution of an absorbing substance, Beer's law states that absorption is directly proportional to the concentration. To the extent that this is true we have, as typically written,

$$T = 10^{-\epsilon c x} \quad (6)$$

where ϵ is the molar extinction coefficient (in liters per mole per centimeter), and c is the concentration of the absorbing compound (in moles per liter). It follows that $\alpha = \ln 10 \cdot \epsilon c$.

For our purposes, the most useful measure of absorption is usually the absorption cross section σ (square centimeters). σ may be assumed to be the area associated with each absorbing molecule, such that if a photon hits the area it will be absorbed, otherwise it will pass through. Stated differently, σ is the probability that one pigment molecule in a thin layer with area 1 cm^2 will be excited by one photon passing through the layer (for example, see Clayton [40] or Blanchard et al. [21]). The absorption coefficient is $\alpha = N_v\sigma$, where N_v (per cubic centimeter) is the number of pigment molecules per unit volume. Because $N_v = N_a c/10^3$ cm^{-3}, where N_a is Avogadro's number, we have $\sigma = 10^3 \ln 10 \cdot \epsilon/N_a = 3.82 \times 10^{-21}\epsilon$.

In calculations involving Maxwell's equations, which describe electromagnetic waves, the complex refractive index (equation 3) is more convenient. For k, the complex term describing absorption, we have

$$k = \alpha\lambda/4\pi \quad (7)$$

where λ is the wavelength of light in vacuum (in centimeters).

Scattering. All cells are optically inhomogeneous and therefore scatter light. Scattering is certain to be a major factor affecting directivity, though the effect of scattering has often been neglected in discussions of phototaxis. For scattering we have the contrast function

$$m = (1 + S - T)/(1 + S + T) \quad (8)$$

where S is the fraction back-scattered, and T is the fraction transmitted. Scattering may also decrease local contrast (as it does in *Phycomyces*) by lighting otherwise dark areas of the cell.

Refraction. It is not known in most instances whether refraction is significantly involved in producing directivity. Cells and colonies of cells are large enough to act as lenses. It is doubtful that the difference in refractive index between the cells and the surrounding water is great enough to cause appreciable focusing at the far side of the cell. Around the equator of the cell or colony a ring of decreased intensity is produced that might have a significant effect. The ocelli of the large Warnowiacean dinoflagellates (96), shown in Fig. 11d, have a lens that does refract the light sufficiently to make the ocellus a directional receptor (84).

Reflection and interference. The reflectivity or reflectance (ratio of reflected energy to incident energy) when light passes from a transparent medium to an absorbing medium at normal incidence is

$$R = [(n_1 - n_2)^2 + k_2^2]/[(n_1 + n_2)^2 + k_2^2] \quad (9)$$

where n_1 is the refractive index of the transparent medium, and n_2 and k_2 are the coefficients of the complex refractive index (equation 3) of the absorbing medium. The corresponding equation for light passing from an absorbing to a transparent medium is

$$R = [(n_1^2 + k_2^2 - n_1 n_2)^2 + (n_2 k_1)^2]/[(n_1^2 + k_1^2 + n_1 n_2)^2 + (n_2 k_1)^2] \quad (10)$$

For reflection without interference, the contrast function is

$$m = (1 + R - T)/(1 + R + T) \quad (11)$$

where R is the fraction reflected, and T is the fraction transmitted.

Wherever the refractive index changes in the path of a light beam, a portion of the light is reflected. Light is an electromagnetic wave. When two waves are present simultaneously, superposition holds, and the resulting amplitude is the sum of the two wave amplitudes. When the crests of two waves coincide, the waves are in phase, and constructive interference occurs. When the two waves are out of phase, they partially cancel each other, the crest of one adding to the trough of the other. It is possible to make structures in which all reflected waves are in phase with the incident wave (Fig. 4b). These devices, known as interference reflectors, have a stack of alternating thin layers of high and low refractive index. We summarize below evidence that layered eyespots in algae are interference reflectors and function as part of the antennas.

In an interference reflector, the greater the difference in refractive index between the layers, the greater the reflection. Absorption in the layers may increase reflection, increase path length, and reduce transmitted light. The amount of reflected light depends on the thickness and refractive index of the layers, the absorption, the angle of incidence, and the wavelength of the light. The complete solution for reflection from a stack of thin layers is a computer problem or a problem for microwave modeling. The optics, assuming parallel layers of infinite extent, is treated by Abelès (1, 2) and Berning (18). A more general treatment is given by Holt for antennas of finite extent (121), by Marcuse for dielectric wave guides (169), and by Wait for curved layers (241).

To understand the principle of an interference reflector, it is helpful to consider two waves of the same amplitude, E_0, but going in opposite directions. Algebraically, the field going to the right is

$$E_r = E_0 \sin(kx - \omega t) \quad (12)$$

where k is the propagation number ($2\pi/\lambda$), x is the distance, kx is in radians, and ω is the frequency (per second). The field is

$$E_l = E_0 \sin(kx + \omega t) \quad (13)$$

Noting that $\sin\alpha + \sin\beta = 2\sin(\alpha + \beta)/2\cos(\alpha - \beta)/2$, we have for the total field

$$E = E_r + E_l = 2E_0 \sin(kx)\cos(\omega t) \quad (14)$$

This is a standing wave. Suppose the reflected wave results from perfect reflection from a metallic mirror, as diagrammed in Fig. 4a. The boundary conditions require that at the mirror

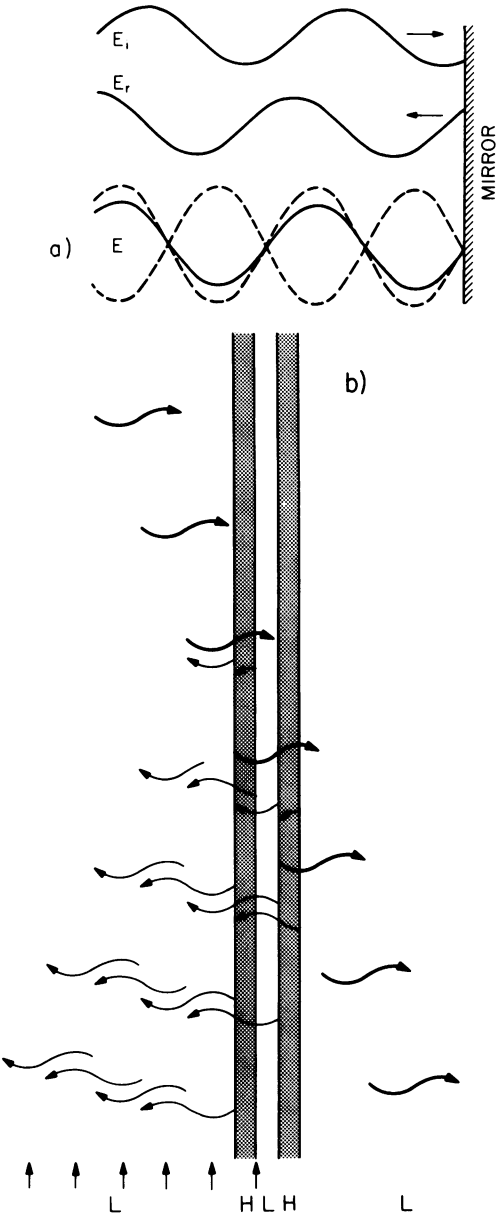

FIG. 4. *Reflection. (a) Perfect mirror. Plot of incident wave, E_i, coming from the left, reflected wave, E_r, going to the left, and the sum $E = E_i + E_r$. The summed wave is a standing wave; the dashed lines show its extrema. (b) Interference reflector. Plot of a segment of a wave one wavelength long at seven successive instants of time. During the time interval between plots the wave advances half a wavelength. The wave is incident on a stack of transparent alternating high (H)- and low (L)-refractive index layers which are one-quarter of a wavelength thick. The first reflections produced by the wave segment at each of the four interfaces are shown. The front of each wave is indicated by an arrow. Vertical arrows indicate the zones of maximum intensity (electric energy density).*

surface the total field, E, equals zero. If we set $x = 0$ at the surface, again equation 14 holds. $E = 0$ not only at $x = 0$, but also at $\lambda/2$, λ, etc., and E oscillates between $2E_0$ and $-2E_0$ at $x = \lambda/4$, $3\lambda/4$, etc.

Now consider light of wavelength λ normally incident on a transparent quarter-wave stack (Fig. 4b). Here the optical distance (thickness times refractive index) of each layer is $\lambda/4$. Light reflected at the low- to high-refractive-index interface changes phase by π radians; light reflected at the high- to low-refractive-index interface does not change phase. In Fig. 4b we have plotted a hypothetical piece of wave one wavelength long at successive times (the time required to advance half a wavelength). All the initial reflections are indicated. Note that constructive interference occurs throughout the structure, forming a partially standing wave to which every reflection contributes. For odd-numbered stacks, the relevant case for our purposes, the reflectivity (25) is

$$R_{2N+1} = \{[1 - (n_2/n_1)(n_2/n_l)(n_2/n_3)^{2N}]/[1 + (n_2/n_1)(n_2/n_l)(n_2/n_3)^{2N}]\}^2 \quad (15)$$

where N is the number of low-refractive-index layers, $N + 1$ is the number of high-refractive-index layers, n_1 is the refractive index outside the stack toward the light, n_2 is the high refractive index, n_3 is the low refractive index, and n_l is the refractive index outside the stack away from the light. The range of wavelengths in which reflection occurs depends primarily on the ratio n_3/n_2 and on the number of layers. In the structures relevant to phototaxis n_3/n_2 is around 0.9. For a large number of layers, the half band width is

$$\Delta\lambda_\infty = \lambda_0 2\Delta g/[1 - (\Delta g)^2] \quad (16)$$

where

$$\Delta g = (2/\pi)\sin^{-1}[(n_2 - n_3)/(n_2 + n_3)] \quad (17)$$

and λ_0 is the center wavelength (156). For smaller N we may use the empirical formula

$$\Delta\lambda_{N+1} = \Delta\lambda_\infty + \lambda_0(N + 1)^{-1.27} \quad (18)$$

where $N \geq 1$.

Interference between the incident and reflected waves produces a standing wave with minimum intensity at the surface of the stack and maximum intensity a quarter of a wavelength out. The intensities are

$$I_{max} = I(1 + \sqrt{R})^2 \quad (19)$$

$$I_{min} = I(1 - \sqrt{R})^2 \quad (20)$$

where I is the incident intensity and R is the reflectivity. The maximum contrast available from interference alone, i.e., between the surface and the quarter-wave position, is

$$m = 2\sqrt{R}/(1 + R) \quad (21)$$

However, this amount of contrast is not available to algal antennas because the receptor measures intensity at only one location. If this location is a quarter-wave in front of the stack, the intensity of light coming from in front is I_{max} as above, but the intensity of light coming from the opposite direction is $I - RI = I(1 + \sqrt{R})(1 - \sqrt{R})$, so that

$$m = \sqrt{R} \quad (22)$$

It is apparent that the contrast is significant even for small R.

Wave guide optics. A dielectric wave guide (Fig. 5) is an optical device that uses refraction and reflection to confine and guide light within a particular structure (169). Many animal photoreceptor organelles use wave guides to increase the efficiency and directivity of reception. For example, the rod cells which contain photoreceptor pigment are long narrow cylinders which are made to point toward the light (67). The diameter of these cylinders is comparable to the receptive wave-length, and their refractive index is greater than that of their surroundings (230). In some algae, the same principle is used, but the geometry is different. The photoreceptor pigment is located in high-refractive-index slabs sandwiched between layers of lower refractive index. In both kinds of receptor, the cylinders or slabs act as wave guides, so that a ray of light incident within a certain angle at the end will be totally internally reflected, increasing the path

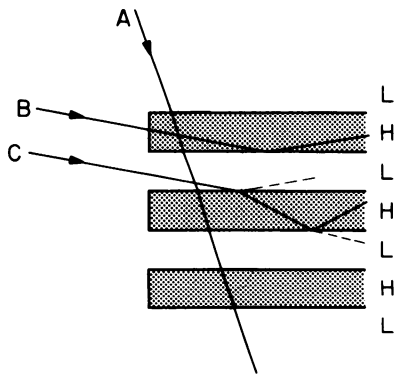

FIG. 5. *Slab wave guide. This optical device consists of a sandwich of alternating high (H)- and low (L)-refractive-index layers, not typically one-quarter of a wavelength thick. Three rays are drawn to indicate the effect. Ray A passes through without getting trapped in layers. Ray B is completely captured in a layer. Ray C is partially trapped in a layer.*

length of the light through the receptor pigment and increasing the probability of receptor excitation. These wave guides also have the advantage that a significant portion of the light falling very near but outside the photoreceptor structure is captured within it. This increases the amount of light within the photoreceptor. The presence of nonabsorbing slabs allows the light to spread out more uniformly through the depth of the structure. The latter effect is significant because the more uniformly a given amount of light is distributed through a receptor, the lower the proportion of inactive to active pigment. Directivity is achieved in the algal structure because light incident end on to the slabs is more strongly absorbed than light entering at higher angles of incidence. A wave guide by itself would be a bipolar antenna. We will see that the unipolarity required for phototaxis is achieved by screening one end of the wave guide.

Dichroism. The preceding mechanisms produce directivity by influencing the amount of light reaching the photoreceptor. Dichroism, on the other hand, causes the fraction of the light absorbed once it reaches the photoreceptor to vary with light direction. This occurs because receptor molecules in dichroic receptors are orientated and consequently have a preferred direction for light absorption. Preferential absorption occurs in both polarized and unpolarized light, but the absorption differences are greater in polarized light.

Absorption by a molecule is proportional to $\cos^2\theta$, where θ is the angle between the electronic transition moment of the molecule and the electric vector of the light (for example, see Dartnall [48]). In effect, dichroism changes the absorption cross section of the receptor molecule, which is σ for unoriented molecules. In unpolarized light, the theoretical maximum for absorption is 1.5σ, and the theoretical minimum is zero, depending on the orientation of the molecule to the light. In polarized light, the theoretical maximum is 3σ, and the theoretical minimum is zero.

Dichroism based on a three-dimensional crystalline array of receptor molecules occurs in *Euglena* (see Polarized Light).

Dichroism also occurs in the rhodopsin membranes of vertebrate photoreceptors and contributes significantly to their absorption. In these membranes, the transition moments of the rhodopsin molecules lie approximately parallel to the plane of the membrane and are randomly oriented within the plane (48).

It is probable that some algae have rhodopsin photoreceptors. By analogy with vertebrate receptors, we can estimate the magnitude of the dichroic effect in such receptors. In unpolarized light, the receptor molecules should have an absorption cross section of about 1.5σ for a ray of light normal to the membrane and 0.75σ for one parallel to the membrane. In polarized light at normal incidence, the absorption cross section should be 1.5σ, whatever the orientation of the plane of polarization. In polarized light rays incident parallel to the membrane, the cross section should be 1.5σ when the plane of polarization is parallel to the membrane and zero when it is perpendicular. The directional properties of such a membrane in unpolarized light are shown in Fig. 9a.

Tracking Antenna Designs

In this section we discuss organisms for which electron microscopic or behavioral studies are available to illustrate antenna theory. We have not attempted to include all the algae that have antennas or all the kinds of antennas that algae have. Besides the groups that lack flagellated forms, we omit the Bacillariophyceae and Chloromonadophyceae because we lack information about their antennas and in most cases do not even know whether they are phototactic. We recognize that much information on phototaxis in diverse algae exists in papers on natural history and taxonomy and in other papers not specifically concerned with phototaxis. We would welcome identification of more of these references.

Chlorophyceae: multilayer quarter-wave stack antennas. The most common form of eyespot in green algae is a single layer of pigmented granules, but the eyespots of many green algae consist of stacked layers of pigmented granules. In these eyespots two layers are most common, but some algae have as many as nine. The spacing of the layers suggests that they act as quarter-wave reflectors, and observation shows that multilayered eyespots are indeed strongly reflective. Quarter-wave reflection is a principle widely used in nature to produce either reflection or color (139, 140, 187). Well-known examples are the tapeta of the eyes of nocturnal and marine animals, the silvery scales of fish, and the structural colors (not the pigment colors) of bird feathers, butterfly wings, and insect cuticle. In these cases the reflected light is sensed at a distance. We will show that the algae probably use quarter-wave reflection for a different purpose, namely, to produce a directional antenna with its receptor located at one of the interference surfaces.

Eyespot reflection has a curious history. Over a period of thirty years, Mast described the phenomenon and emphasized its importance in phototaxis. In 1911 he wrote of *Pandorina* and *Eudorina*, "In direct sunlight they become luminous, giving off a greenish blue light, and as

the colonies rotate they sparkle and glitter, presenting a wonderfully beautiful spectacle" (172). He soon abandoned the notion that the cells are self-luminous and in 1927 stated the following facts about eyespot reflection (175). (i) The phenomenon is not visible when the organism is viewed through a transmission light microscope because reflected light does not reach the eye. (ii) The more anterior eyespots of colonial algae reflect more light than the more posterior ones. We now know from electron microscopy that the anterior eyespots have more layers than those farther back (118, 141). (iii) The eyespots of euglenoid algae are not reflective. Electron microscopy shows that these structures are not layered, but contain irregularly spaced pigment granules of different sizes (243). (iv) The integrity of eyespot structure is essential. In disintegrating cells, Mast observed that reflection disappeared before other signs of alteration became visible. (v) The amount of reflected light varies with the angle of incidence. (vi) Probably related to this, in colonial algae only part of the colony is seen to reflect light at any particular instant. (vii) Only blue or green light is reflected. The foregoing observations, fundamental to phototaxis, have been largely ignored. There are probably two reasons. In the first place, microscopic algae are usually viewed by transmitted light. With epi-illumination, eyespot reflection in *Chlamydomonas* and *Volvox* is impressive (Fig. 6). The second reason is that Mast's physical interpretation seemed implausible. He believed that focusing by a lens was necessary to account for the reflection. No lens has been observed by electron microscopy, nor is it required to interpret any of Mast's observations on phototaxis.

The foregoing observations are all consistent with reflection from an interference reflector. In reflecting eyespots, layers of pigmented globules alternate with unpigmented layers. Within the layers the pigmented globules are arranged in a hexagonal array 75 to 100 nm center to center (29, 193). Absorption in the pigmented layer may increase the reflection of that layer. How closely does the eyespot resemble a quarter-wave stack, and how much reflection would we predict? We have estimated some of the parameters from an electron micrograph kindly made available to us by Andrew Staehelin (Fig. 7). The photograph shows a thin section, prepared by a method that gives excellent preservation of structure (148), through a *Chlamydomonas* eyespot. The eyespot contains four layers of pigmented droplets. The unpigmented layers average 77.7 nm in thickness; the pigmented layers average 69.0 nm. A double membrane (average thickness, 15.4 nm) lies at the inner surface of each pigmented layer. To calculate the reflectivity, we must estimate the refractive indexes of the layers and the absorption of the pigmented layer. We assume that the refractive index of the unpigmented layer is 1.35, slightly greater than the refractive index of water. We assume that the refractive indexes of the pigmented layer, which consists mostly of β-carotene (202), and of the membranes are both 1.5. (The refractive index of oil droplets from natural sources varies between about 1.45 and 1.52. We chose 1.50, toward the high end, on the supposition that a high refractive index would be advantageous to the algae and therefore selected.) We assume that 10% of the total carotenoid of the cell (201) is in the pigmented layers, giving a concentration of 0.14 M. (This gives $k \simeq 0.05$ at 450 nm.) The path length in the low-refractive layer is 1.35×77.7 nm, one-fourth of 420 nm; the path length in the high-refractive layer, neglecting absorption, is 1.5×84.4 nm, one-fourth of 506 nm. Because the eyespot is not exactly a quarter-wave stack and has absorbing layers, we made a computer calculation (based on Maxwell's equations) of the reflectivity at normal incidence as a function of wavelength by using the computational method of Berning (18). This gave

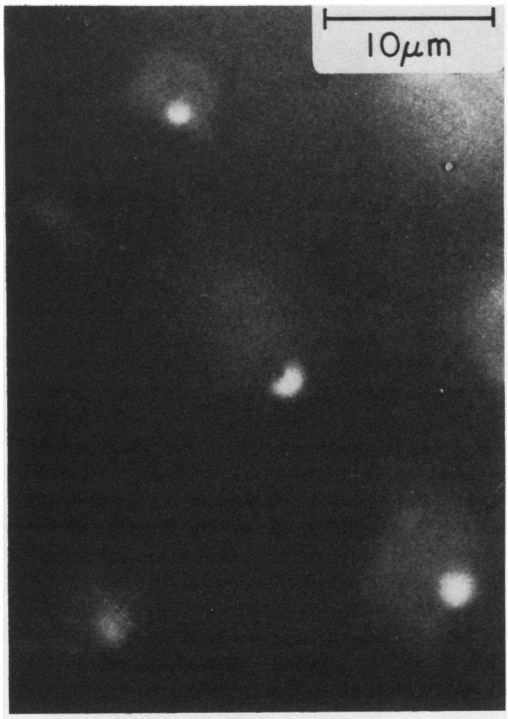

FIG. 6. *Photograph of light reflected from the anterior surface of a colony of Volvox carteri f. weismannia taken with an epi-illuminated microscope. The bright spots (about 2.5 μm across) are reflections from the eyespots. Each cell is visible by chloroplast fluorescence. (Photo by K. Foster and R. Birchem.)*

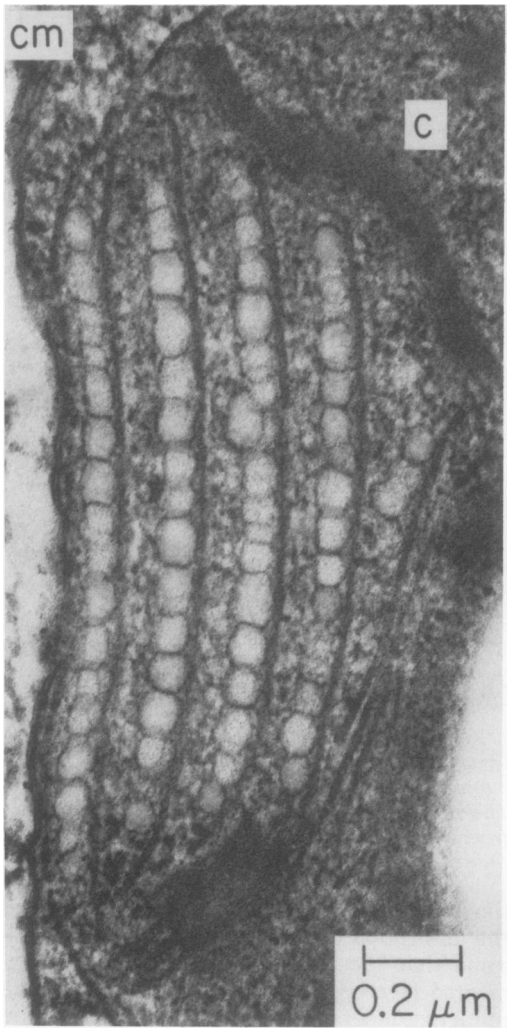

FIG. 7. *Section through the eyespot of the chlorophycean Chlamydomonas reinhardtii showing the four layers of pigment globules making up the eyespot; each layer is covered on its inner face by a thylakoid double membrane. Abbreviations: cm, cell membrane; c, chloroplast. (Electron micrograph by L. Andrew Staehelin using a spray freezing technique [148].)*

maximum reflectivity of 0.14 at 450 nm and a band width at half maximum of 113 nm. The result is rather insensitive to the amount of absorption assumed. We conclude, therefore, that the observed reflection can be explained on the basis of interference reflection from the eyespot layers. When the values 1.5 and 1.35 for refractive index are substituted into equation 15 with $N = 3$ for an exact quarter-wave stack, we obtain 0.16 for the reflectivity; from equation 18 we obtain a half band width of 108 nm. The reflective properties are very close to those of a quarter-wave stack.

Most published electron micrographs do not permit accurate measurement of the thickness of single layers, but many permit measurement of the combined thickness of one pigmented layer plus one unpigmented layer. By measuring transverse sections in published photographs of *Chlamydomonas reinhardtii* (98, 203, 220), *Volvulina pringsheimii* (141), *Platydorina caudata* (141), *Volvox aureus* (63), *Pteromonas tenuis* (11), *Volvox tertius* (213), *Pyramimonas montana* (157), and *Eudorina illinoiensis* (118), we obtained values for the double thickness almost exclusively in the range 160 to 180 nm. Part of the variation probably is caused by deviation from the normal of the plane of section, and part is caused by different amounts of shrinkage and swelling during preparation. It seems probable that these eyespots are all designed as quarter-wave stacks with reflecting properties similar to those of *Chlamydomonas*.

Reflection might appear to be an effective method of making a directional antenna. In green algae the eyespots are asymmetrically placed, lying in the chloroplast near one surface of the cell. If we assume that the photoreceptor pigment is located between the eyespot and the adjacent cell surface, then light shining on this surface would produce an intensity at the receptor equal to the sum of the incident and reflected intensities. On the other hand, light shining from the opposite side would be attenuated by absorption within the cell, absorption within the eyespot, and reflection from the eyespot. This scheme clearly would modulate the light to produce a directional antenna. In fact, it constitutes the essential part of Mast's theory. Equation 11, however, shows that the amount of modulation achievable in this way is modest. Approximately the same degree of directivity could be obtained by putting pigment in the unpigmented layers and not using reflection at all. Consideration of only the total reflection gives a misleading idea of the light intensity close to the eyespot, where the receptor pigment presumably is located. Within the eyespot and near its surface, interference occurs between the incident and reflected waves. The pattern of interference is shown in Fig. 8, calculated for light of 480 nm on the basis of the assumptions used above to calculate the reflectivity. Light striking the outer surface of the eyespot (Fig. 8a) produces a series of intensity maxima, one approximately a quarter wavelength out from the eyespot and one at the inner surface of each of the pigmented layers. Light striking the eyespot from the opposite side (Fig. 8b) produces a series of minima at the same positions within the eyespot, thereby producing maximum contrast at these locations. It is possibly significant that the plasma membrane and

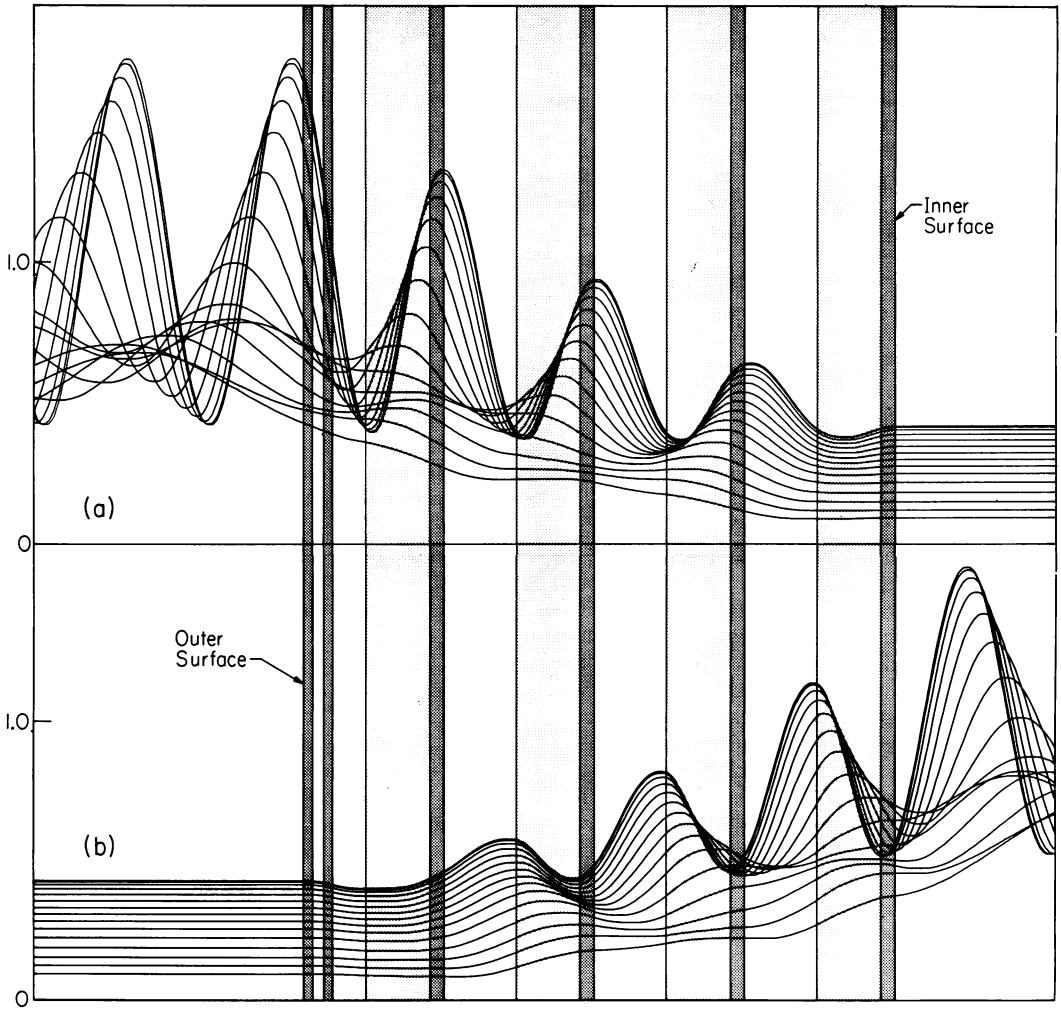

FIG. 8. *Pattern of light intensity within and near eyespot at different angles of incidence for (a) light incident on outer surface of eyespot from the left and (b) ligh: incident on inner surface of eyespot from the right. (Data have not been corrected for the absorption of light within the cell before it reaches the eyespot.) Dimensions are taken from the eyespot section in Fig. 7. Dark areas: plasma membrane outermost, chloroplast double membrane adjacent, four double membranes inside eyespot. Gray areas: pigmented lipid droplets. Assumed refractive indexes: membranes, $\hat{n} = 1.5 + 0.0\,i$; pigmented layers, $\hat{n} = 1.5 + 0.1\,i$; unpigmented layers, $\hat{n} = 1.35 + 0.0\,i$. Wavelength, 480 nm. A more precise estimate of the pertinent field would require correction for the spectral irradiance at the appropriate depth in the water (155) and the wavelength dependence of the photoreceptor sensitivity. $\bar{E}^2$ is the tangential component of the time averaged electric energy density scaled to 1.0 for the incident light. (We assume that the receptor chromophore does not absorb the electric component normal to the eyespot layers, as would be approximately true for rhodopsin.) Curves are drawn for different angles of incidence at 5° intervals from normal incidence (upper curve) to 70° (lowest curve). Computed by the method of Berning (18). The method solves Maxwell's equations for the case in which both the parallel layers and the incident beam are of infinite extent. The assumptions are justified for these angles of incidence because the eyespot has a width of about four wavelengths (121), but sidebands caused by diffraction at high angles of incidence are probably underrepresented.*

the internal membranes of the eyespot are located at precisely these positions. These membranes are therefore the most likely locations of the photoreceptor pigment. This agrees in part with the suggestion of Arnott and Brown (4) and Walne and Arnott (243) that the receptor is located in the plasma membrane over the eyespot. As these authors point out, this location provides a plausible means of communication with the flagella, since the plasma membrane is continuous with the flagellar membrane. Close communication with the exterior of the cell must

occur because light-induced changes in ion flow exterior to the cell are seen in less than 1 ms (151). It is less obvious how the internal membranes could communicate with the flagella. The internal membranes come together in a ring around the eyespot (well shown in Maiwald's Fig. 6b [157]), which may relate to their function. The hypothesis suggested by the interference pattern is that layering in eyespots creates zones of interference contrast where receptor pigment can effectively be placed. (The internal membranes, though of thylakoid origin, contain no chlorophyll [P. Siekevitz, private communication].) Use of internal layers as well as the plasma membrane would increase the area available for photoreception.

Layered eyespots range in aperture from about 1 wavelength up to 10 wavelengths in the largest curved eyespots of colonial algae. The distribution of light within the layers is therefore dominated by interference and diffraction. The design provides appropriate directivity and proper location. Directivity increases with the number of layers. The interference maximum that forms a curtain at a quarter wavelength from the front surface when the light is of the design wavelength moves outward as the angle of incidence is increased. The distance increases as $1/\cos\theta$, where θ is the angle of incidence (angle from the normal) (25, 64, 130, 139). At a sufficient angle of incidence, reflection from a lower layer interferes at the receptor layer, producing a significant side band or maximum in absorbed intensity. The antenna seems designed to suppress side bands. Light at a high angle of incidence or end on is trapped within the high refractive layer, and the amount of trapped light is increased by the curvature of the eyespot, which is concave outward. The pigment in the high refractive layer can thereby absorb a significant fraction of the trapped light. Curvature of the eyespot also broadens the main beam, because some oblique rays encounter a surface normal to each ray. At wavelengths shorter than the design wavelength, the maximum intensity occurs closer to the eyespot and at a slightly oblique angle of incidence. This probably explains the fact that the plasma membrane appears to be somewhat closer to the eyespot than the quarter of a wavelength the layers are designed for, the idea being that this position of the receptor causes the sensed intensity of light of the spectral composition occurring naturally to be maximum at normal incidence. Orientation of the receptor molecules in the receptor plane probably adds to the directivity. Reflection from the cell wall reduces obliquely incident light. All of the features discussed in this paragraph seem designed to shape the intensity at the receptor so that the directivity of the antenna decreases smoothly with increasing angle of incidence from a maximum at normal incidence. Note also that the directivity depends strongly on the polarization of the incident light.

Man-made antennas sometimes focus radiation into a small area. This would be disadvantageous in the algal antennas we are considering, because the light must excite a sufficient amount of pigment to allow a range of sensitivity. The pigment must also be located so as to facilitate communication with the responder. Use of the full interference curtain seems to be the best solution and agrees with our estimate of the photoreceptor pigment content in *Chlamydomonas* (see Threshold).

Curvature of the eyespot probably accounts for two observations of Mast (175), the focusing of the reflected light and the focusing of yellow light at the back of the eyespot opposite the incident beam. Geometrical optics provides a qualitative interpretation of both observations, the first being simply focusing by a concave mirror. The yellow spot is undoubtedly formed from light that cannot be absorbed by the eyespot pigment and can therefore undergo multiple reflection within the eyespot. Successive reflections from a posterior concave mirror and an anterior convex mirror directs the light toward a point aligned with the beam direction, in the manner of a Cassegrain telescope.

The marked directivity of quarter-wave stack antennas (Fig. 9b) implies that their position and orientation in the cell is critical to their role of providing accurate phasing of the response. In *Chlamydomonas*, at least, they are precisely located (Fig. 2). Because the cell rotates consistently in the left-hand sense, the antenna can provide accurate information about the direction of the light.

Chlorophyceae: variations in design. In all of the chlorophycean algae we have discussed so far, the layered eyespot contains one internal thylakoid double membrane at the inner face of each lipid droplet layer (Fig. 10a). The organisms are all in the order Volvocales. For brevity we refer to this as the volvocalian design.

We do not know whether the volvocalian design is found in other orders, but at least three other designs of layered eyespots are found in other chlorophyceans and forms related to them. The phylogeny of the Chlorophyceae is in a state of flux, some forms, for example, being placed in the new class Prasinophyceae. For convenience here we refer to all of these organisms as chlorophyceans.

In another design, a double thylakoid membrane lies between each lipid droplet layer, as in the volvocalian design, but the thylakoid mem-

branes are smoother and separated so that one membrane is adjacent to the lipid droplet layer in front, and the other is adjacent to the lipid droplet layer behind (Fig. 10c). In most cases, the two membranes form a sac between the lipid layers. This design is found in *Platymonas suecica* (165), *Platymonas convolutae* (208), *Platymonas impellucida* (179), *Platymonas* sp. (58, 59), *Tetraselmis cordiformis* (182), and *Prasinocladus marinus* (207). Unless there are other criteria for separating them, the similarity of eyespots suggests that these organisms belong in the same order. It should be noted that gametes of *Acetabularia mediterranea* (order Dasycladales) also show this design (43, 44), as do the zoospores of *Schizomeris leibleinii* (order Chaetophorales or Ulvales) (20). The structure has also been seen in several presumed Volvocales: an unusual marine chlamydomonad *Chlamydomonas reginae* (71), *Carteria turfosa* (134), and *Carteria crucifera* (145). In these Volvocales, some of the pigmented droplet layers appear to lie inside a sac, with a clear layer between the two sacs (Fig. 10d). It will be necessary to determine the inside and outside of the thylakoid sacs to be sure of the exact relationship. Measurement of the photographs of these eyespots gives thicknesses of the double layer (lipid droplet layer plus cytoplasmic layer) in the range 150 to 220 nm. Some of the variation is probably caused by collapsing or swelling of the thylakoid sac during preparation for electron microscopy. The measurements show that the thylakoid sac produces a quarter-wave spacing between the layers.

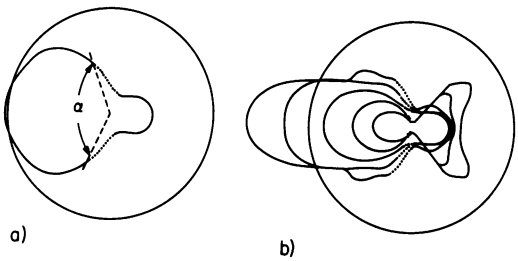

FIG. 9. *Directivity of antennas. Polar plot of $\bar{E}^2$, the tangential electric energy density at a particular membrane layer(s) as a function of angle of incidence. Circle represents what $\bar{E}^2$ would be if the receptor was not oriented and there was no refractile and absorbing structure. (a) A hypothetical antenna in which a single membrane layer containing photoreceptor pigment lies 62 nm in front of a single 338-nm-thick layer with $\hat{n} = 1.5 + 0.1\,i$. In such an antenna, directivity in unpolarized light is produced primarily by absorption and orientation of the receptor chromophore in the plane of the membrane (dichroism). The angle α indicates the half-beam width, in this case α = 133°. (b) A quarter-wave-spaced layered structure with the dimensions of the Chlamydomonas eyespot made by using the method and assumptions described in the legend to Fig. 8. Note that the different curves correspond to each membrane layer, with the outermost curve on the left side being that calculated for the outermost layer. α for the plasma membrane (the outermost layer) is 60°.*

Melkonian and Robenek (182) have made a detailed study of the eyespot in *Tetraselmis cordiformis* which reveals specialized associations between the eyespot and the overlying plasmalemma. Transverse sections show that about a dozen pinlike projections approximately 100 nm long connect the plasmalemma and the overlying theca. Chloroplast membranes extend into these pins. The plasmalemma lies at a uniform distance of 60 to 65 nm in front of the first layer of lipid globules. Tangential sections show that the lipid globules are hexagonally close packed and about 90 nm in diameter. Freeze fracture through the chloroplast membrane shows that it is specialized in the region of the eyespot. The protoplasmic fracture face contains more particles and a different particle size distribution in this region than elsewhere. Melkonian and Robenek interpret the extra 6- to 8-nm particles found in the chloroplast membrane over the eyespot as photoreceptor molecules. The density of these particles is low compared

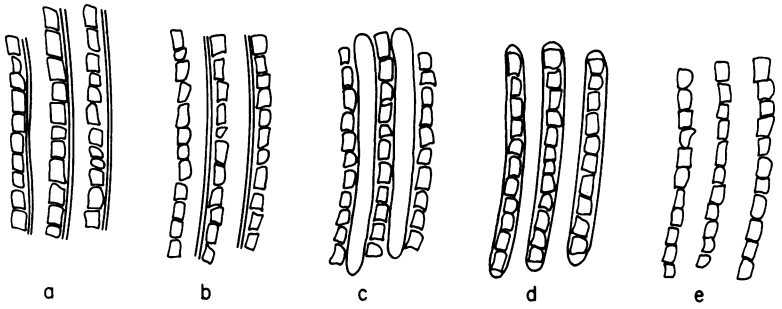

FIG. 10. *Different types of quarter-wave stack antenna construction showing possible associations between the thylakoid membranes and the pigmented droplet layers. Each antenna is directed toward the left. All but design (b) have been observed (see text).*

with the density in rhodopsin membranes (112, 136). For this reason and because the plasmalemma lies closer to the zone of maximum interference contrast than does the chloroplast membrane, it seems more likely to us that the photoreceptor molecules are in the plasmalemma, and that the 6- to 8-nm particles have some other function. We agree completely with these authors that the eyespot is closely associated with the photoreceptor.

A third design of the quarter-wave stack is seen in the true *Pyramimonas* species *P. parkeae* (197) and *P. orientalis* (190). In this design there are no thylakoid membranes between the lipid droplet layers (Fig. 10e). In *P. parkeae* a fibrillar hexagonal matrix in the lipid layer appears to hold the droplets together. Spacing of the layers is similar to the spacing in other chlorophycean eyespots. *P. orientalis* differs from the other forms we have discussed in having two double-layered eyespots in two separate chloroplast lobes. The eyespots lie adjacent to each other, forming a single antenna. *Pyramimonas obovata* apparently has two separate antennas not even fixed with respect to other cell features (36), but we do not know of any behavioral studies on these forms.

The eyespots of most chlorophycean algae have only a single layer, formed as a specialization of the chloroplast, which is closely apposed to the plasmalemma at only this point. These eyespots presumably function by absorption and by quarter-wave interference of the light reflected from their front and back surfaces. In some, the reflection is increased by other structures. In the uniflagellate *Pedinomonas minor*, for example, the strongly refractive pyrenoid is located immediately behind the eyespot. The reflective surface of the pyrenoid lies three-quarters of a wavelength behind the rear surface of the lipid layer of the eyespot, strengthening the constructive interference at the plasmalemma. This is particularly important because the organism is only 2.5 to 7.0 μm long by 1.8 to 4.4 μm wide by 1.0 to 2.2 μm (68, 69, 160, 161, 214). The small size reduces the amount of screening by the cell body. *Mantoniella squamata* (formerly *Micromonas squamata*) is another small phototactic alga with a small single-layered eyespot (52, 164, 209, 223). *Heteromastix* (166, 176) and *Monomastix minor* (162) are small biflagellated green algae with single-layered eyespots.

Single-layered eyespots are not restricted to small organisms. For example, they are found in Volvocales, *Chlamydomonas eugametos* (243) and *Chlamydomonas dysosmos* (229); in Tetrasporales, *Gloeococcus bavericus* (113); in Chlorosarcinales, zoospores of *Chlorosarcinopsis minor* and *C. dissociata* (181); in Caulerpales, female gametes of *Bryopsis hypnoides* (34); in Chlorococcales, gametes of *Hydrodictyon reticulatum* (167); in Ulvales, zoospores of *Entermorpha intestinalis* (72), gametes of *Ulva lactuca* (186), zoospores of *Ulva mitabilis* (28), and gametes of *Ulvopsis* (*Monostroma*) *grevillei* (189); in Ulotrichales, zoospores of *Cylindrocapsa geminella* (119); in Oedogoniales, zoospores of *Bulbochaete hiloensis* (217) and zoospores of *Oedogonium cardiacum* (120); and in Chaetophorales, zoospores of *Microthamnion kuetzingianum* (245), zoospores of *Fritschiella tuberosa* (180), and zoospores of *Stigeoclonium* (70, 159). In most photographs these eyespots are in their characteristic position adjacent to two chloroplast membranes and the plasmalemma at the cell wall.

In most chlorophycean algae it is probable that only the plasmalemma contains receptor pigment. In this location the receptor could communicate to the site of response by gating or pumping ions, causing a change in membrane potential that would propagate rapidly to the flagella. The volvocalian design may represent an evolutionary advance over these simpler receptors. As mentioned above, these organisms may have taken advantage of the internal zones of interference maximum by placing receptor membranes there and developing some means of signal communication to the flagella. At least one case is known, *Cryptomonas* (see below), in which a receptor in the interior of the chloroplast is able to function.

Dinophyceae: quarter-wave stack antennas and lens antennas. The dinoflagellates, a diverse group with respect to habitat, nutrition, and morphology, are also diverse with respect to their antennas. They have traditionally been separated into two main groups, the Dinophyceae and the Desmophyceae (23). The limited information available (77–79, 101, 102) suggests that these two groups may use different photoreceptor pigments for phototaxis. Some desmophyceans are known to be phototactic, although they seem not to have eyespots (61, 62, 101). No structural information is available about antennas or photoreceptors in this group.

The motile dinophyceans have a unique flagellar form. They have two flagella, one lying in a transversely aligned groove, the other in a longitudinally aligned groove. The eyespot, when present, is posterior in the cell and underneath the groove of the longitudinal flagellum (Fig. 11b). Some unarmored marine forms and some fresh-water species have eyespots; many phototactic species have no clearly visible eyespot, for example, *Peridinium trochoideum* (101), *Goniaulax catenella* (101), and *Ceratium* (185, 196). Metzner (185) says that the photosen-

sitive spot in *Ceratium cornutum* is located near the point where the two grooves meet. Halldal (101) reports that the dinoflagellates without eyespots track poorly compared with other algae.

Peridinium (184) and *Gymnodinium* (228) have the simplest eyespots described for this group. The antenna resembles that of some chlorophyceans (for example, *Platymonas* and *Tetracystis*) and probably functions similarly. A single pigmented layer with quarter-wave spacing lies adjacent to the sulcus membrane. Its closeness to the membrane and the bases of the flagella should facilitate rapid communication of the signal. These eyespots lie within a chloroplast with a triple membrane. Several thylakoid membranes lying about a quarter wave behind the lipid droplet layer probably contribute to antenna function.

Eyespots of *Woloszynskia tenuissimum* (42) are sometimes multilayered, just as in the chlorophycean quarter-wave stack. Sometimes these quarter-wave layers are wrapped in triple membranes (suggestive of dinoflagellate chloroplast origin) with loss of chloroplast function. An example is *Peridinium balticum* (238; D. Tippet, private communication), shown in Fig. 11a. The dimensions are precisely as expected for a quarter-wave stack, and the structure is located adjacent to the sulcus membrane. The chloroplasts used for photosynthesis in this organism appear to be of separate chrysophyte origin (129). The design of the eyespot is like that of *Pyramimonas* in which there are no thylakoid membranes between the multiple layers (Fig. 10e), but the quarter-wave stack probably originated independently in the two groups. The origin of the dinophycean chloroplast, which contains chlorophyll *c*, is thought to be distinct from the origin of the chlorophycean chloroplast, which contains chlorophyll *b*.

Some algae in the family Warnowiaceae have a specialized antenna with an elaborate ocellus (Fig. 11d) or refractive lens. Francis (84) estimates the index of refraction to be 1.52. The lens focuses light on a crystalline lamellar body which is sometimes backed by a quarter-wave reflecting layer (for example, *Erythropis pavillardi* [94]). Though large by algal standards, these lenses are less than 30 wavelengths wide

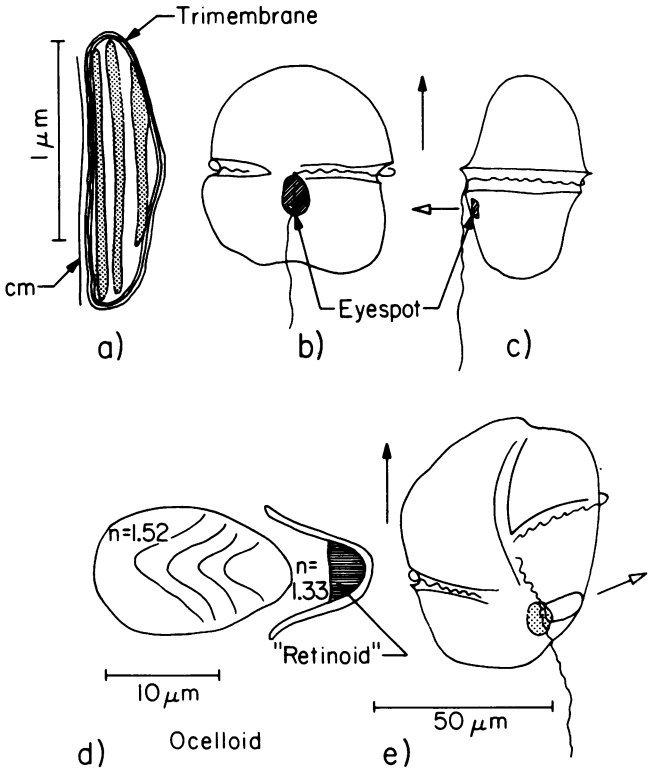

FIG. 11. *Dinoflagellates. Peridinium: (a) section through eyespot, showing layers of pigmented droplets (after reference 238, which had 8 rather than 3 pigmented layers); cm, cell membrane; (b and c) two side views showing the location of eyespot and flagellum (after reference 185). Nematodinium: (d) ocelloid (after reference 84); (e) location of ocelloid and flagella in cell. Closed arrows show swimming direction, and open arrows show presumed direction of antenna (97).*

and can be considered antennas. Like man-made lens antennas, they use refraction to increase directivity. Francis estimates the field of view as 30°. Because the structure protrudes from the body, it is not restricted to being directed normal to the body surface (96, 101); in many forms it points more forward. This may imply that the latter forms use the antenna for some other function in addition to phototaxis (see Prospects and Conclusions). Greuet (95) reports that *Leucopsis* has an array of 15 or so antennas directed forward. Such an antenna array could be connected to process an image, as our own retina does.

Cryptophyceae: dielectric slab wave guide antennas. The antennas in *Chroomonas mesostigmatica* (57, 58) and *Cryptomonas rostrella* (152) resemble the antennas already discussed in originating as a specialized part of the chloroplast, but they lie in the middle of the cell rather than at the cell surface (Fig. 12). This type of antenna is a spur of the chloroplast about 1 μm on a side. On one of its longitudinal faces there are about 35 pigment granules ranging up to 260 nm in diameter. This pigmented layer absorbs most strongly when the light is perpendicular to the swimming axis of the cell. The remainder of the structure contains thylakoid disks perpendicular to both the plane of the pigment granules and the long axis of the cell. Phycoerythrin, the pigment implicated by the action spectum as the receptor for phototaxis (244), presumably lies in the intrathylakoid spaces (86). These chloroplast disks undoubtedly contain lipid and protein, which give them a high refractive index. This makes them act as wave guides, especially for light that strikes them end on. The absorbing stop (pigmented layer) lies at one end of the disks, causing the system to function as a directional antenna. The antenna lies about 1 μm from the bases of the flagella, a distance short enough that diffusion could effectively communicate the signal to the flagella.

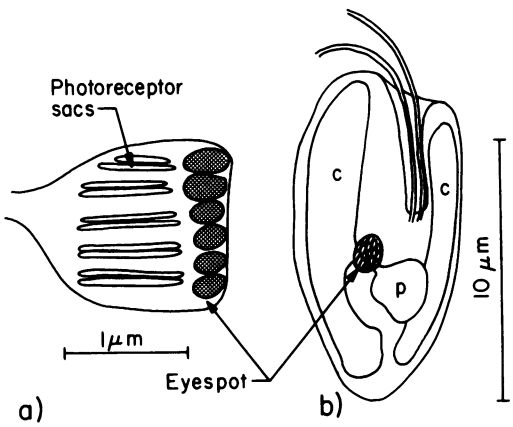

FIG. 12. *(a) Eyespot of Chroomonas (after reference 58). The antenna is directed leftward, with the photoreceptor sacs in front of a layer of large pigmented droplets. (b) Whole cell of Chroomonas (after reference 57). The antenna is a pinched-off part of the chloroplast (c). (The pyrenoid [p] is also part of the chloroplast.) In the antenna, but not in the rest of the chloroplast, the thylakoid membranes are oriented perpendicular to the long axis of the cell.*

Euglenophyceae: absorbing screens and dichroic crystal detectors. *Euglena gracilis* is a unicellular organism about 50 μm long and 10 μm in diameter with a single anterior flagellum (Fig. 13b)(32, 144). It is not closely related to the algae whose antennas we have already discussed. Phototaxis in *Euglena* and its near relatives appears to have originated independently and employs structures not of chloroplast origin. Action spectra for phototaxis in *Euglena* suggest that the photoreceptor pigment is a flavoprotein (38, 53), not rhodopsin or a carotenoprotein as is likely in the green algae. Structures corresponding to both the photoreceptor and the screen can be identified (Fig. 13a). The presumed photoreceptor is the paraflagellar body, a swelling of the flagellum at its base that is essential for phototaxis (144) and lies at the front of the antenna. As determined by absorption spectra (248) and fluorescence (14, 15), it contains a flavoprotein. The size of the paraflagellar body is consistent with our estimate of the amount of pigment it contains (see Threshold). The screen at the back of the antenna is the stigma, a pigmented mass 3 to 7 μm in diameter lying in the cytoplasm on one side of the paraflagellar body. It contains predominantly carotenoid pigments (7, 8, 110, 137) contained in an irregular assortment of granules with no stacked layers (243). The stigma is so located that in most orientations of the cell it must modulate the light that reaches the paraflagellar body during the rotation of the cell.

In *Euglena* the photoreceptor is a dichroic crystal. Structural evidence shows that the molecules in the paraflagellar body are oriented in a crystal of fixed orientation with respect to the antenna (135, 211, 248). The *c* axis of each unit cell lies nearly parallel to the axoneme, and the *a* axis points toward it (211). This has important implications for the directivity of the antenna for polarized and unpolarized light and the mechanism of communication with the flagellum. Electron-dense spots, adjacent to the crystal and lying next to the paraflagellar rod (211), and the paraflagellar rod itself may play a role in the control of flagellar function. Since re-

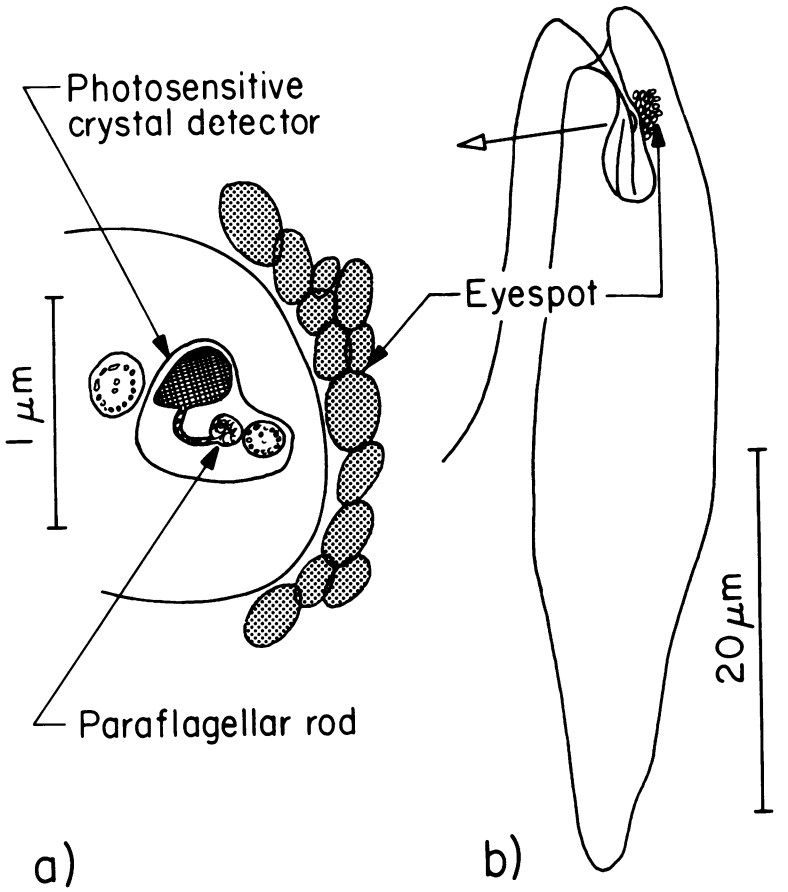

FIG. 13. *Euglena. (a) Cross section (viewed from the anterior end of the cell) through the antenna parts (after reference 135). The crystal detector (paraflagellar body) is connected to the paraflagellar rod and lies within the membrane of the emergent flagellum in front of a large screen of pigmented droplets. (The second, nonemergent flagellum is also shown.) (b) Whole cell showing location of antenna (paraflagellar swelling and eyespot) and flagella (after reference 144). Open arrow indicates the antenna direction. Euglena, as drawn, would swim upward.*

sponse takes as long as 150 ms (55), there is probably a diffusion step between these closely adjoined parts. Presumably, too, there is transfer from the site of photon excitation preferentially across the crystal to where the signal is captured. It is not surprising that polarized light has a strong effect on the behavior of *Euglena* (27, 45, 53, 54)(see below).

The stigma, on the other hand, is probably not dichroic, since its granules show spherite birefringence, characteristic of a radial rather than linear array of molecules (243). In fact, the stigma partially depolarizes incident light. The net directivity is caused by a combination of an oriented, and therefore dichroic, receptor and an effective absorbing screen.

Antennas of the same design are found in *Phacus pleuronectes* (65), *Trachelomonas volvocina* (60), and *Eutreptiella gymnastica* (236), but they have been less well studied.

Chrysophyceae, Xanthophyceae, and Phaeophyceae: absorbing screens and paraflagellar swelling. Although the antennas of the Chrysophyceae, Xanthophyceae, and Phaeophyceae have the same design principles as those of the Euglenophyceae and Eustigmatophyceae, namely, a detector abutting a shading device (Fig. 14), their antenna structures differ in several fundamental respects. First, the eyespot consists of droplets formed within rather than outside the chloroplast. Second, the eyespot and paraflagellar swelling are always associated with a short smooth secondary flagellum rather than with the primary one. Third, the flagellar swelling is not crystalloid as in Euglenophyceae. The motile cells of the classes of this section share a number of common structural features (114). Most important to us, the struc-

ture and position of the flagellar swelling are similar in all of them. The swelling is presumed to be part of a photoreceptor apparatus, although there are no detailed reports on phototactic behavior. The eyespot typically consists of a single sheet of droplets 200 to 500 nm in diameter. They are larger and much more variable in size than the droplets in chlorophycean eyespots. Typically, the eyespot is as large as 1 μm in *Uroglena* and *Dinobryon* and forms a depression into which is pressed the flagellar swelling, which typically contains amorphous dense homogeneous material. In *Dinobryon* there are layers in the swelling.

The secondary inactive flagellum can be quite small; in *Chrysococcus rufescens* (114) it is only 75 nm long complete with its swelling. In *Chromulina psammobia* (114) the stubby flagellum is completely enclosed in a pocket. In *Chromulina placentula* (10) and *Phaeaster pascheri* (12) it is embedded in the cell surface. In each case the secondary flagellum appears to have been specialized for photosensory function.

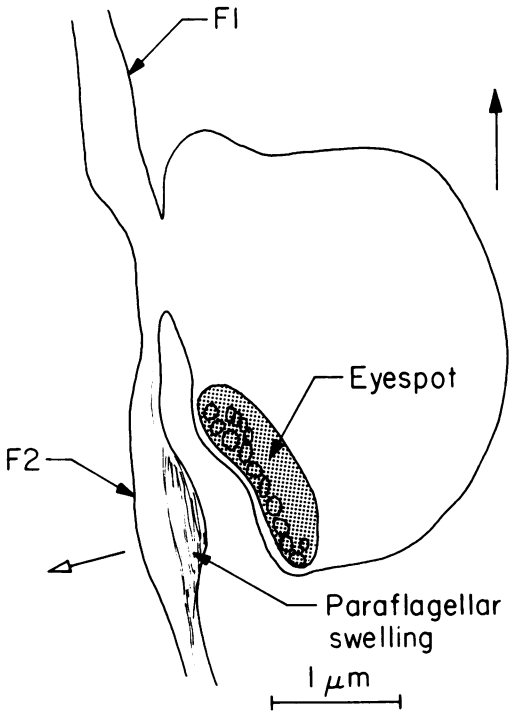

FIG. 14. *Fucus spermatozoid. Section through primary flagellum (F1) and secondary flagellum (F2), showing paraflagellar swelling on F2 and adjacent pigment droplets (after reference 58). This antenna design is found, with variations, among the Chrysophyceae, Xanthophyceae, and Phaeophyceae. Closed arrow indicates the swimming direction. Open arrow indicates the antenna direction.*

Some advantage of this specialization must overcome the problem of communication from the sensory flagellum to the one that is controlled. In cases such as *Ochromonas tuberculatus* and *Anthophysa vegetans* (13) there is a dense paraflagellar rod similar to the one in *Euglena* on the side of the axoneme opposite the flagellar swelling. Whether this is used for communication or in some other way is not known.

In other species some of the components appear to be missing. If antennas function in these organisms, some must do so without an eyespot, and others must function without a paraflagellar body. For example, *Poterioochromonas malhamensis* (114) is a chrysophycean with a small paraflagellar swelling adjacent to a dense region of plasmalemma. *Mallomonas papillosa* and *Chrysamoeba radians* (114) also have a paraflagellar body adjacent to the cell surface, but no eyespot. Bouck (26) suggests that a modified plasmalemma may sometimes be the receptor. Without behavioral data on these organisms we have no way of knowing whether the structures found are functional or merely vestigial. *Rhizochromulina marina* appears to be unique among the chrysophyceans in having lost all components of the antenna (116).

We presume that as with other algae the antennas of these forms point normal to the swimming path of the cell. This is not necessarily obvious from cell structure itself. Apparently, *Chromulina placentula* swims with its flagellum leading and its concave surface inclined 45° to its swimming direction (10). This causes the antenna to point approximately normal to the swimming path. In *Ochromonas*, also, the antenna appears to be fairly normal to the swimming path (114). It is premature to say whether this is true for other species.

Eustigmatophyceae: absorbing screens and paraflagellar buttons. As the name implies, organisms of this class have conspicuous eyespots (Fig. 15b) (117). The principles of antenna design appear to be similar to those used by the Euglenophyceae, Xanthophyceae, Phaeophyceae, and Chrysophyceae, although the Eustigmatophyceae are probably phylogenically remote from these groups. In these groups an extension of the flagellum abuts an aggregation of pigment droplets. In the Eustigmatophyceae the extension is button shaped, 1 to 1.5 μm in diameter, and T shaped in cross section. It abuts the eyespot, which is 1 to 2 μm in diameter and has an irregular shape. The eyespot is an aggregation of droplets of variable size lying outside the chloroplast in the main body of the cell. It acts as a shade and presumably as a reflector (Fig. 15a). Unlike the other classes, there is no

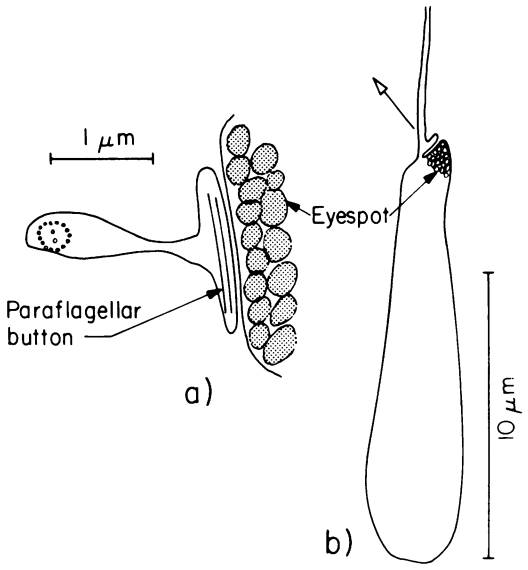

FIG. 15. *Eustigmatophyceae. (a) Cross section through the paraflagellar button in Polyedriella (after reference 117), showing the single flagellum and the adjacent pigment droplets. The droplets are irregularly shaped and lie outside the chloroplast. (b) Diagram of cell showing the location of the flagellum, pigmented droplets, and paraflagellar button. Open arrow indicates the antenna direction.*

evidence of a second flagellum or a paraflagellar rod. In *Polyedriella helvetica* the paraflagellar button contains layered material. The only information about behavior is that the cells stop in bright light. We do not know whether the receptor pigments are similar to those of other classes, nor do we know the threshold for phototaxis. We do not know the exact location of the photoreceptor, how it communicates to the flagellum, or how the flagellum responds. Presumably, the receptor is some part of the paraflagellar button and, thus, lies so close to the flagellum that communication would be rapid even by diffusion.

Prymnesiophyceae (Haptophyceae). Unfortunately, we know little about the behavior of this class of organisms. Mjaaland (188) reports that the motile stage of the coccolithophorid *Coccolithus huxleyi*, which lacks an eyespot, is phototactic and accumulates toward diffuse and parallel light. Also, a few species of the order Pavlovales (for example, *Diacronema vlkianum* [92] and *Pavlova lutheri* [91]) have an eyespot of the chrysophycean type associated with a paraflagellar swelling of the posterior flagellum. The swelling (92) appears to be long and complex and to have a different phylogenetic origin from the flagellar swelling of the Chrysophyceae; furthermore, the cells in this study were not phototactic. Although the eyespots are not associated with either flagellum in *P. granifera* (90) and *P. gyrans* (93), they do border a pit which runs beneath the flagellar basal bodies. Probably, a layer of the pit surface or something that could fit into the pit forms the rest of the antenna. The haptonema, a coiled process extending from the cell near the base of the flagella, has a basal swelling that may be part of the antenna (142, 163, 206).

Discussion

Because antenna function requires precise geometrical structures and precise relationships among component parts, electron microscopy will continue to be the primary source of information about antennas. The ubiquity of antennas among flagellated algae makes it certain that more antennas remain to be discovered and probable that there are more antenna principles than we have discussed. The value of electron microscopy observations could be enormously increased if behavioral information were available on the same material. In general, it is not feasible for a single laboratory to undertake both elaborate electron microscopy investigations and elaborate experiments on phototaxis, but there are a few simple physiological observations that could conveniently be made on the same cultures used for electron microscopy. We emphasize especially the value of threshold measurement. An approximate estimate of threshold requires, besides a source of monochromatic light of known intensity, only a microscope, a clock, and a certain amount of patience. In the next section we discuss in detail the use of threshold measurements for estimating the amount of photoreceptor pigment and the size of photoreceptor structures.

Algal antennas require a precise structure and must occupy a precise location within the cell. They exert a dramatic effect on behavior without being essential to the life of the cell under laboratory conditions. Moreover, the eyespot can be seen in the light microscope. For all of these reasons the antennas provide a promising model system for investigating the genetic control of cell architecture. This is especially true of the quarter-wave stacks, with their tight spatial requirements. The availability of well-developed genetic systems (147) as well as microbiological, biochemical, and biophysical tools should make such studies of microscopic algae both efficient and rewarding.

From our discussion of structure it is clear that antennas, when present in motile stages, are a useful phylogenetic character. This character has been used by several authors (58, 115),

and we expect that it will become even more prominent in phylogenetic studies.

ANTENNA PROPERTIES DETERMINED FROM BEHAVIOR

Threshold: Receptor Pigment Concentration

Threshold is defined as the lowest light intensity at which response occurs. It is important because it can be used to estimate the minimum amount of receptor pigment a receptor contains. In fact, until chemical estimates become available, it provides the only information we have about receptor pigment content. The methodological details are important for interpreting threshold measurements. Three different criteria of threshold have been reported in the phototaxis literature: (i) the lowest light intensity that produces visible orientation of individual cells, (ii) the lowest light intensity that produces visible aggregation, and (iii) the extrapolation of the log intensity-response curve to zero response. The interpretation of results obtained by these different methods is discussed below. It is also shown that the interpretation is different for colonial and for unicellular algae.

To analyze threshold, we assume that the sensor acts as a photon counter. This assumption is justified because visible light is the stimulus for phototaxis. One photon of visible light contains much more energy than thermal motion alone can impart to one molecule at biological temperature. Hence, after the pigment molecule has been excited by absorption of a photon, it can activate some detection process that is unlikely to be activated by thermal motion alone. Therefore, a cell can detect single photons, and, as far as it is known, all biological photoreceptors are photon counters (39, 99, 109).

Time must always be considered when analyzing threshold because the probability of a response depends on the time available to sense a stimulus. Up to a limit, the longer one waits the greater the chance of response. We show below when we discuss signal processing that the memory time must be of the order of the rotation period of the organism. This enables the organism to filter its past experience in such a way that it can determine the phase of the rotation cycle. For analyzing threshold, certain simplifications are possible, particularly since we use threshold to calculate only a lower limit to the receptor pigment content. We consider only two light intensities at the photoreceptor: the maximum of the modulation cycle, assumed equal to the incident intensity, and the minimum of the cycle. We refer to whatever reduces the light intensity at the receptor as the screen, and we refer to the magnitude of its effect as the screen extinction. We assume that the photoreceptor acts as the equivalent of a quantum difference counter: it first counts the number of photons at the higher light intensity and then counts the number at the lower intensity, compares the two counts, and produces a response whenever it detects a significant difference. The photoreceptor does not count every photon absorbed by the photoreceptor pigment. The ratio of photons counted to photons absorbed is the quantum efficiency ϕ_r of the photoreceptor.

As explained above, we use the absorption cross section σ as a measure of absorption (see Optical Principles). We assume that the photoreceptor pigment is sufficiently dilute that the number of excitations per photon per second is equal to $\phi_r\sigma_r$ times the number of pigment molecules in the light path.

The smallest signal that can be measured reliably in one rotation cycle occurs at the light intensity at which the quantum difference equals its standard deviation; that is, where

$$e_0 - e_1 = s_{e_0 - e_1} \tag{23}$$

Here e_0 is the mean number of receptor pigment excitations during the unscreened phase, e_1 is the mean number of excitations during the screened phase, and $s_{e_0 - e_1}$ is the standard deviation of the difference $e_0 - e_1$. We know from propagation of error theory (for example, see Parratt [210]) that

$$s^2_{e_0 - e_1} = s^2_{e_0} + s^2_{e_1} \tag{24}$$

where s is the standard deviation. To calculate $s^2_{e_0}$ and $s^2_{e_1}$, we note that at threshold the number of pigment molecules in the photoreceptor is large relative to the number of excitations during the modulation cycle. Therefore, e_0 and e_1 are Poisson distributed, and their variances are equal to their means. It follows that at threshold

$$e_0 - e_1 = (e_0 + e_1)^{1/2} \tag{25}$$

Replacing e_1 by Te_0, where T is the transmission of the screen, and rearranging, we have

$$e_0 = (1 + T)/(1 - T)^2 \tag{26}$$

This is the minimum number of excitations that must occur during the unscreened phase.

Equation 26 provides a conservative criterion of threshold, since it gives the excitation level at which a single receptor can reliably measure an intensity difference in a single modulation cycle. In many threshold experiments more than one receptor or more than one cycle is involved. For example, colonial algae may have hundreds of receptors in a single organism, and the organism

as a whole can go toward the light even when the intensity is so low that an individual receptor cannot detect the intensity modulation. Likewise, in experiments where the presence or absence of aggregation within a certain period of time is determined, each organism makes many measurements of the intensity difference during the observation period and can drift toward the light even if it gives the wrong response during some cycles. We therefore derive expressions that take these effects into account.

In a colony, the signal is averaged over many receptors, and intrinsic noise, rather than quantum noise, is likely to be limiting. Our reasoning is as follows. Suppose that in addition to the photon excitations there is intrinsic random noise that gives in effect i random counts to the sensor during the memory time of the cell. For one cell the variance is $e_0 + e_1 + i$, instead of $e_0 + e_1$. For N effective cells in a colony, the mean is still $e_0 - e_1$, but the variance is $(e_0 + e_1 + i)/N$. Assuming as before that at threshold the signal equals its standard deviation and replacing e_1 by e_0T, we have for the number of quanta required at threshold $e_0 = [1 + T + \sqrt{(1 + T)^2 + 4(1 - T)^2Ni}]/(1 - T)^2N$. For large Ni,

$$e_0 \simeq 2\sqrt{i/N}/(1 - T) \tag{27}$$

Note the dependence on $1/\sqrt{N}$; e_0 would depend on $1/N$ if intrinsic noise were not considered. From equation 26 the quantum noise at the threshold of a single cell, $e_0 + e_1$, is $e_0(1 + T) = (1 + T)^2/(1 - T)^2$. We make the plausible assumption that the intrinsic noise is smaller but of comparable magnitude, and assume that $i = (1 + T)^2/4(1 - T)^2$. Substituting into equation 27, we have

$$e_0 = (1 + T)/(1 - T)^2\sqrt{N} \tag{28}$$

Note that, strictly speaking, equation 26 is not the same as equation 28 with $N = 1$, because the two equations were derived from different assumptions.

Aggregation in a light beam is a complicated process whose analysis requires knowledge of the rotational and translational diffusion constants of the organism, the concentration of organisms in different regions of the suspension, and the boundary conditions imposed by the geometry of the beam and chamber. This information is not available from reported experiments, so a detailed analysis is not possible. As we have already seen, threshold calculated on the assumption that the receptor accurately measures an intensity difference every cycle is clearly too high. We can set a lower limit by assuming that every cell in the light path must accurately measure the mean intensity difference during the period of observation. If we assume that the organism makes an independent estimate of the intensity difference during each rotation, the variance of the mean count difference is

$$s^2_{e_0 - e_1} = (e_0 + e_1)/N_{\text{rot}} \tag{29}$$

where N_{rot} is the average number of rotations during the observation period. If, as before, we set the mean count difference equal to the standard deviation of the difference, we have for unicellular organisms

$$e_0 = (1 + T)/(1 - T)^2\sqrt{N_{\text{rot}}} \tag{30}$$

and for colonial algae

$$e_0 = (1 + T)/(1 - T)^2\sqrt{NN_{\text{rot}}} \tag{31}$$

The third method of measuring threshold requires its estimation from a plot of response versus log intensity. We assume that in the linear portion of the curve the organisms track the light beam and therefore respond during every rotation. In this case, equations 26 and 28 are applicable. We estimate threshold by extrapolating the linear portion of the curve to zero response.

We can use the preceding equations to estimate the minimum number of molecules of receptor pigment per receptor. Note that for colonial algae this is the number of molecules per sensitive cell, not the number per colony. From our assumption that the pigment is dilute, it follows that the number of excitations e_0 in time τ is

$$e_0 = In_r\phi_r\sigma_r\tau \tag{32}$$

where I is the light intensity (in quanta per square centimeter per second), n_r is the number of receptor molecules per receptor, ϕ_r is the quantum efficiency of the photoreceptor pigment, σ_r is the absorption cross section of the photoreceptor pigment (in square centimeters), and τ is the duration of the unscreened phase (assumed to be equal to the duration of the screened phase) (in seconds). We write equations 26, 28, 30, and 31 as a single equation

$$e_0 = (1 + T)/(1 - T)^2K \tag{33}$$

where $K = 1$ for unicellular algae responding during every rotation cycle, $K = \sqrt{N}$ for colonial algae with N receptors responding continuously, $K = \sqrt{N_{\text{rot}}}$ for unicellular algae responding during N_{rot} rotation cycles, and $K = \sqrt{NN_{\text{rot}}}$ for colonial algae with N receptors responding during N_{rot} rotation cycles. Substituting for e_0 in equation 32 and rearranging, we have for the

number of receptor molecules in the receptor

$$n_r = [(1 + T)/(1 - T)^2K][1/(I_{min}\phi_r\sigma_r\tau)] \quad (34)$$

where I_{min} is the threshold light intensity.

Receptor pigment content of various algae. Equation 34 provides a method of calculating the amount of photoreceptor pigment from the threshold light intensity. Because the amount of receptor pigment has not been measured in any alga, we have not been able to test the validity of this equation directly. Instead, we have collected threshold values from the literature, estimated the other parameters, calculated minimum estimates of n_r, and then compared these to the space available in the assumed structures. The n_r values are listed in Table 1. Because of the uncertainty of the estimated parameters and because the original experiments were not, in most cases, specifically designed to measure threshold, the values of n_r are at best good to only an order of magnitude.

For all algae except *Euglena*, we took the extinction coefficient (40,000 liters mol^{-1} cm^{-1}) and quantum efficiency (0.67) for vertebrate vision (48) as a practical upper limit to the effective absorption of a biological photoreceptor. This gave $\phi_r\sigma_r = 0.67 \times 40{,}000 \times 3.82 \times 10^{-21} = 1.0 \times 10^{-16}$ cm^2. For *Euglena* we assumed that the receptor is a flavoprotein with a maximum extinction coefficient of 10,000 liters mol^{-1} cm^{-1} and a σ_r of 3.8×10^{-17} cm^2. The effective absorption is probably increased in *Euglena* by dichroism and decreased by the usually low (10 to 20%) quantum efficiency of solid-state photodetectors. We estimated that the combined effect reduced the unscreened absorption by 0.3 in polarized light and by 0.15 in unpolarized light. Only one experimental value for the transmission of the screen is available, namely, 0.3 for the in vivo transmission of the stigma in *Euglena* (248). Taking this as a reasonable lower limit to the transmission of the screen in other algae, we used $(1 + T)/(1 - T)^2 = 2.65$. Measured values of rotation rate for unicellular algae are about 1 to 2 rotations per s (*Euglena* [5]; *Gyrodinium* [105]; *Chlamydomonas*, Smyth and Berg, in preparation). For *Volvox*, Gerisch (87) found 0.23 rps, and Schletz (226) found 0.27 rps, whereas Sakaguchi and Iwasa (221) found 0.15 to 0.6 rps, depending on temperature. Assuming that the memory time is equal to half the rotation period, we used $\tau = 0.5$ s in the unicellular algae, and $\tau = 2$ s in the colonial algae. In *Volvox*, only the cells in the front half of the colony respond to light, and they are not equally responsive. Because the species reported have small colonies, we estimated that $N = 400$ receptors per colony. In experiments based on the observation of visible accumulation, most authors report that they waited until aggregation had stopped. In these experiments we assume that aggregation was actually visible sooner, and use N_{rot} equal to the estimated number of rotations in one-half of the reported observation time. Other assumptions are stated in the footnotes to Table 1.

A more conservative estimate of photoreceptor pigment content could be obtained by assuming that the screen is opaque, the quantum efficiency is 1, and the photoreceptor extinction coefficient is 100,000 liters mol^{-1} cm^{-1}. Our assumptions give n_r values 1 order of magnitude higher and seem more realistic. The largest error is probably in the estimation of the screen. We do not have experimental values for T in any alga except *Euglena*, and n_r becomes large as the transmission increases. Moreover, we have not attempted to take the details of reflection and directivity of receptors into account. The latter design mechanisms may raise the maximum intensity at the photoreceptor, making the true value of n_r smaller than our estimate.

The estimates of photoreceptor pigment listed in Table 1 cover about 3 orders of magnitude from 560 to 980,000 molecules per receptor. The geometric mean is 3.4×10^4 molecules. Are these values compatible with the suggested structures? We know the size of the receptor in *Euglena*. The photoreceptor is presumed on good evidence to be the paraflagellar body. Kivic and Vesk (135) give dimensions 0.4 by 0.3 by 1.2 μm for the paraflagellar body. The body is crystalline, with a unit cell of 8.9 by 7.7 by 8.3 nm, and $\beta = 110°$ (211). The paraflagellar body contains about 2.5×10^5 unit cells, and our estimates would give two to four photoreceptor molecules per unit cell. We can compare this number with the pigment concentration in the purple membrane of *Halobacterium*. This is also a biological crystalline photoreceptor, a two-dimensional crystalline array of bacteriorhodopsin (112). The purple membrane has 1.8×10^7 chromophores/μm^3, so a volume the size of the paraflagellar body would contain 2.6×10^6 molecules. Our estimates for *Euglena* give 0.5×10^6 to 1.0×10^6 chromophores per receptor. These numbers are close enough to suggest that our value is at least physically plausible. Another check on our estimate is the maximum molecular weight derived from the weight of the paraflagellar body per molecule. Assuming a density of 1.0, we obtain values of 88,000 and 170,000, which is in the range of protein molecular weights and seems plausible. Still another check is to estimate the pigment content from Wolken's in vivo extinction spectrum of the paraflagellar body (248).

Assuming this spectrum was taken laterally through the paraflagellar body, and correcting it for scattering by assuming that the absorption at 410 nm is 0.58 times the absorption at 450 nm, as in flavoprotein, we obtain an estimate of 3.6 $\times 10^7$ flavin molecules in the paraflagellar body. This is 1 to 2 orders of magnitude greater than our values and seems implausibly high. Most of

TABLE 1. *Minimum number of receptor pigment molecules per cell calculated from threshold light intensity*

Organism	Wavelength (nm)	Threshold intensity (quanta cm^{-2} s^{-1})	Minimum no. of molecules per cell[a]
Dunaliella salina (red form)	483–508	7.9×10^{12}[b]	5.6×10^2
Cryptomonas sp.	570	1.8×10^{13}[c]	3.0×10^3
Dunaliella salina (green form)	483–508	1.4×10^{12}[b]	3.1×10^3
Gymnodinium splendens	453	1.5×10^{13}[d]	3.6×10^3
Volvox minor	492	2.0×10^{10}[e]	5.4×10^3
Pyramimonas reticulata	(white)	6.7×10^{12}[f]	7.9×10^3
Ulva lactuca (gametes)	(white)	4.8×10^{12}[g]	1.0×10^4
Chlamydomonas reinhardtii [strain 137c (+)]	465–570	4.4×10^{12}[h]	1.9×10^4
Chlamydomonas reinhardtii [Gottingen strain 11-32(+)]	503	1.8×10^{12}[i]	2.9×10^4
Eudorina elegans	492	1.2×10^{10}[e]	3.2×10^4
Platymonas subcordiformis (negative phototaxis)	500	7.3×10^{10}[j]	6.6×10^4
Volvox aureus	491	5.0×10^{9}[k]	1.3×10^5
Chlamydomonas reinhardtii [strain 137c (+)]	465–570	3.7×10^{11}[h]	2.3×10^5
Chlamydomonas reinhardtii [strain 137c (+)]	503	1.8×10^{11}[i]	2.9×10^5
Chlamydomonas sp.	492	1.5×10^{10}[e]	2.9×10^5
Platymonas subcordiformis (positive phototaxis)	500	1.2×10^{10}[j]	4.0×10^5
Euglena gracilis (without chloroplasts)	410	1.6×10^{11}[l]	5.2×10^5
Euglena gracilis	472	4.7×10^{11}[m]	9.8×10^5

[a] Calculated from equation 34. Estimated parameters: screen transmission $T = 0.3$; quantum efficiency of photoreceptor pigment $\phi_r = 0.67$ (except for *Euglena*); absorption cross section of photoreceptor pigment σ_r(472 nm) = 3.8×10^{-17} cm^2 (*Euglena*), $\sigma_r = 1.5 \times 10^{-16}$ cm^2 (others); integration time $\pi = 2.0$ s (*Volvox* and *Eudorina*), $\tau = 0.5$ (others); number of photoreceptors $N = 400$ (*Volvox*), $N = 32$ (*Eudorina*). These assumptions are discussed in the text. In two experiments in which I_{min} was given in lux, 1 lux = 4.5×10^{11} effective quanta cm^{-2} s^{-1} was assumed, because the spectral sensitivity of the algae roughly matches the spectral sensitivity of the human eye.

[b] Blum and Fox (22). Threshold for visible accumulation (positive) in 5 min, $N_{rot} = 150$. The authors give nominal voltage and wattage of the lamp, its efficiency and color temperature at the operating voltage, and filter transmissions. For absolute intensities we estimated lamp output from the conversion formulas of Carlson and Clark (35), converted to quantum flux assuming black body radiation and using tabulated lumens per watt, and assumed that intensity varies as $1/\pi^2 d^2$, where d is distance from the lamp (35). Wavelength range is one-half band width.

[c] Watanabe and Furuya (244). Extrapolation of the log intensity-response curve for positive phototaxis to zero response.

[d] Forward (79). Extrapolation of log intensity-response curve for positive phototaxis to zero response.

[e] Luntz (154). Threshold for visible accumulation (positive) in 5 min, $N_{rot} = 40$ (*Volvox*, *Eudorina*), $N_{rot} = 150$ (*Chlamydomonas*).

[f] Belcher (9). Threshold for oriented swimming (positive phototaxis) of individual cells observed in microscope; $I_{min} = 15$ lx; assumed $N_{rot} = 1$.

[g] Haxo and Clendenning (107). Extrapolation of log intensity-response curve for positive phototaxis to zero response. $I_{min} = 1$ footcandle (10.8 lx).

[h] Feinleib and Curry (76). Extrapolation of log intensity-response curve for positive phototaxis to zero response; two separate experiments. Spectral composition of light estimated from filter transmission, assuming black body radiation at color temperature 2,700°K. Maximum at 530 nm; half band width, 465 to 570 nm. Quantum absorption estimated from absorption spectrum of bovine rhodopsin (242).

[i] Nultsch (198). Extrapolation of log intensity-response curve for positive phototaxis to zero response.

[j] Halldal (103). Threshold for visible gradient of cell concentration in 2 min. Because he did not wait for aggregation to stop, we assume $N_{rot} = 120$. I_{min} at 405 nm reported as 0.15 erg cm^{-2} s^{-1} (positive phototaxis) and 0.80 erg cm^{-2} s^{-1} (negative phototaxis). These values were converted to I_{min} at 500 nm by using the action spectra of Halldal (102). The absolute values of I_{min} (102) seem inconsistent with Halldal (101, 103).

[k] Schletz (226). Extrapolation of intensity-response curve for positive phototaxis to zero response.

[l] Gössel (88). Threshold for visible accumulation (negative) in 6 min, $N_{rot} = 180$. Assumes σ_r(410 nm) = 0.8 σ_r(472 nm); $\phi_r \times$ dichroism = 0.15.

[m] Creutz and Diehn (45). Threshold for orientation to polarized light. Cells positively phototactic. Assumes $\phi_r \times$ dichroism = 0.3, $N_{rot} = 1$.

the discrepancy is probably caused by the inaccuracies in this method of estimating the absorption of the paraflagellar body.

We can also make a rough estimate of the amount of photoreceptor pigment in *Chlamydomonas* from the size of the eyespot. We assume that the receptor pigment is rhodopsin, that the pigment lies in a single membrane with the same area as the eyespot, and that the eyespot has a diameter of 1.5 μm. We take as an upper limit to the rhodopsin concentration 8.7 $\times 10^4$ molecules per μm^2 (*Halobacterium* purple membrane [112]) and as a lower limit 2×10^4 molecules per μm^2 (bovine rod [136]); this gives values for the *Chlamydomonas* of 1.5×10^5 and 3.5×10^4 molecules per receptor, respectively. This is within the range of our estimates, although on the low side. If the internal membranes of the eyespot contain receptor pigment, the total amount could be greater by a factor of 10 than the amount in the plasmalemma alone.

Cryptomonas is exceptional in that its action spectrum for phototaxis, maximum at 560 nm, coincides with the absorption peak for phycoerythrin clearly visible in the absorption spectrum of the extracted pigments. Here the eyespot is a small region of the chloroplast almost completely separated from the rest of the chloroplast. We estimate that the thylakoid membranes in the eyespot have a total area of 1 to 2 μm^2, large enough to accommodate the estimated amount of photoreceptor pigment (phycobiliprotein) in the intrathylakoid spaces (85, 86).

In most algae there is no peak in the absorption spectrum of the extracted pigments that can be identified with the photoreceptor pigment, implying that the amount of photoreceptor pigment is at least 10 to 100 times less. This observation is particularly significant for the green algae, for which the peak absorption of the bulk pigments is clearly separated from the peak absorption of the photoreceptor pigment. Nultsch et al. (201) report the content of chlorophyll and carotenoids, the main bulk pigments, in *Chlamydomonas*. From these values we estimate that the cells contain about 7×10^8 molecules of chlorophyll and 4×10^8 molecules of carotenoid per cell, almost 4 orders of magnitude greater than our estimate of photoreceptor pigment. This sets an upper limit to the photoreceptor pigment content in *Chlamydomonas* that is about 100 times our minimum estimate.

The foregoing comparisons suggest that our estimates of receptor pigment content are of the right order of magnitude. From them we can judge the scale of operation required to isolate the photoreceptor pigment. The results are encouraging. Compared with many biologically active compounds, the concentration of photoreceptor pigment is not particularly low. If, for example, *Chlamydomonas* contains 1.5×10^5 photoreceptor molecules with $\epsilon = 40{,}000$ liters mol^{-1} cm^{-1}, then the pigment extracted from 20 liters of cells grown to 6.5×10^6 cells per ml and dissolved in a volume of 1 ml would have an optical density of 1.3 and be readily detectable. Quantities sufficient for chemical characterization should be obtainable. Moreover, given knowledge of the location of the receptors, estimation of receptor pigment content in cultures by biochemical assay should be straightforward. Accurate experimental values of photoreceptor pigment content should clarify the relationships among the other quantities that determine threshold. This is important for understanding both the physiology and the biological role of phototaxis.

Action Spectra: Identity of Photoreceptor Pigment and Mechanisms of Producing Directivity

Usually the purpose of measuring an action spectrum (response versus wavelength) is the identification of a photopigment by correlating its absorption spectrum with the action spectrum. Action spectra are particularly useful for studying receptor pigments in photobiological processes like phototaxis, for which the receptor has not been analyzed biochemically. Considerable information is already available about the different receptor pigments in algal phototaxis, and we believe that their chemical structure will soon be known. In the following discussion, therefore, we emphasize the potential value of action spectra for analyzing how light that reaches the receptor is modulated by the antenna, or, in other words, the details of the wavelength dependence of antenna directivity. In the Appendix we describe a method for analyzing action spectra based on the intensity-response curve (fluence-response curve). This seems to be the most satisfactory approach available, but few of the action spectra reported for phototaxis are based on the intensity-response curve. Therefore, we introduce formulas relevant to the different kinds of action spectra that have been measured and discuss what can be learned from them about both the receptor pigment and the modulation system.

Threshold action spectrum. The threshold action spectrum is obtained by plotting the reciprocal of the threshold light intensity against wavelength. It is a composite of the absorption spectrum of the photoreceptor pigment and the extinction spectrum of the screen. This action

spectrum can be derived from equation 34. Substituting $T = 1 - A$ and omitting terms assumed independent of wavelength, we have

$$1/I_{min}(\lambda) \propto \sigma_r(\lambda)A(\lambda)^2/[2 - A(\lambda)] \quad (35)$$

If $A(\lambda)$ is small, it can be omitted from the term $2 - A(\lambda)$. Even if $A(\lambda)$ is not small, the term $2 - A(\lambda)$ has only a small effect on the shape of the action spectrum. Therefore, we have

$$1/I_{min}(\lambda) \propto \sigma_r(\lambda)A(\lambda)^2 \quad (36)$$

where $I_{min}(\lambda)$ is the threshold light intensity at wavelength λ (in quanta per square centimeter per second), $\sigma_r(\lambda)$ is the absorption cross section of the photoreceptor pigment at λ (in square centimeters), and $A(\lambda)$ is the fractional absorption of the screen at λ. Note that $A = 1 - T = 1 - e^{-\alpha x}$ (see Absorption). If αx or A is small, $A \propto \alpha x$. Therefore, A is roughly proportional to the extinction of the absorber.

Finite-response action spectra. Action spectra have often been determined by measuring the light intensities at different wavelengths that produce equivalent responses, by measuring the response at a constant intensity, or by a combination of the two. For phototaxis this procedure has serious disadvantages. As with the threshold action spectrum, the shape of such action spectra is complicated, because the extinctions of both the screen and the photoreceptor pigment contribute to them. Also, the shape varies depending on the particular magnitude of response or intensity that is chosen as the standard of comparison. Furthermore, there is no theoretical justification for assuming that these action spectra bear any simple relationship to the extinction spectra of the screen or the photoreceptor. (Indeed, equation A5 in the Appendix implies that the light intensities that produce equivalent responses are a quadratic function of the screen and receptor extinctions.) For all of these reasons, finite-response action spectra are difficult to interpret, and action spectra determined from the intensity-response curve are clearly preferable (see Appendix).

To derive equations for the finite response action spectrum, we assume that the response is proportional to the difference in the number of excitations in the screened and unscreened phases. This gives $R = C(e_0 - e_1) = Ce_0(1 - T)$, where C is a constant independent of wavelength. Replacing e_0 by the value from equation 32 and remembering that $1 - T = A$, we have for the magnitude of the response $R = Cn_r\phi_r\sigma_r I\tau A$. If the action spectrum is constructed by measuring the intensity that gives some fixed response at different wavelengths, we have the equal-response action spectrum

$$1/I(\lambda) \propto \sigma_r(\lambda)A(\lambda) \quad (37)$$

If the stimulus light contains equal numbers of quanta at each wavelength, we have the equal-stimulus action spectrum. $I(\lambda)$ is constant, so that

$$R \propto \sigma_r(\lambda)A(\lambda) \quad (38)$$

If both intensity and response are allowed to vary, we obtain the response-per-intensity action spectrum

$$R/I(\lambda) \propto \sigma_r(\lambda)A(\lambda) \quad (39)$$

The equal-response, equal-stimulus, and response-per-intensity action spectra have the same form, all being proportional to the product of the receptor and screen extinctions.

Algae with layered eyespots. (i) *Volvox.* Schletz (226) made a detailed study of screening in *Volvox*, a colonial green alga. This organism contains from one thousand to several thousand cells arranged in a single layer on the surface of a hollow sphere up to 1 mm in diameter. Each cell has two flagella, directed outward. The colony rotates about a fixed axis, and translates in a direction nearly parallel to the rotation axis. The stop response given by individual cells, a cessation of flagellar movement when illumination on the cell increases, is used for phototaxis. When a colony deviates from the light direction, rotation of the colony causes some cells to pass from the shaded to the lit side, whereupon their flagella stop beating. Continued activity of the other flagella steers the colony toward the light (87, 104, 123, 222).

Schletz measured the action spectrum of the stop response, finding a single peak at about 490 nm (Fig. 16b). Because the stop response does not require modulation by the screen, the action spectrum should correspond to the absorption spectrum of the photoreceptor pigment. (In some orientations of the cell the bulk pigment screens out some of the light before it reaches the photoreceptor, but the effect on the action spectrum is small.) On the basis of the action spectrum, Schletz concluded that the photoreceptor pigment is a carotenoprotein. As shown in Fig. 16b, the action spectrum is close to the absorption spectrum of vertebrate rhodopsin.

The threshold action spectrum for phototaxis is reproduced in Fig. 16a. The spectrum has a maximum at 490 nm, corresponding to the absorption maximum of the photoreceptor pigment, and a shoulder at 430 nm. A measure of the wavelength dependence of the screen can be obtained by applying equation 36 to the action spectrum. Rearranging and taking the square root, we have for the fractional absorption of the

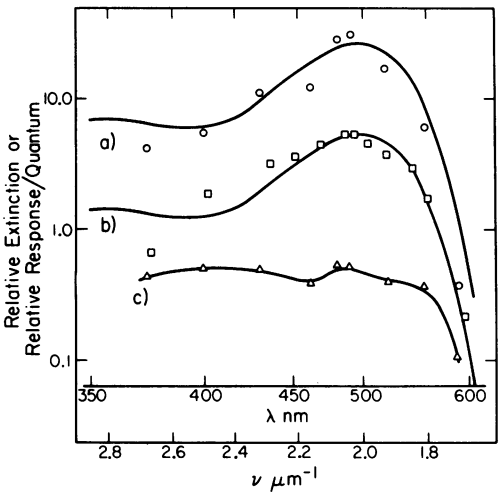

FIG. 16. *Volvox spectra. (a) Threshold action spectrum for oriented swimming. (b) Action spectrum for stop response. Solid lines (a) and (b) are the absorption spectra of cattle rhodopsin (242). (c) Estimated extinction of screen calculated from (a) and absorption spectrum of rhodopsin by using equation 40. Volvox data are from Schletz (226). Note that in all spectral plots the ordinate is a logarithmic plot of extinction or response per number of photons and the abscissa is linear with respect to wave numbers (energy). In this plot Gaussian absorption bands are symmetrical and have linear tails. Shape is not altered by position on the ordinate, and absorption bands throughout the ultraviolet and visible spectra have about the same widths.*

screen

$$A(\lambda) \propto [I_{min}(\lambda)\sigma_r(\lambda)]^{-0.5} \quad (40)$$

Because of the similarity between the stop response action spectrum and the absorption spectrum of rhodopsin, we estimate $\sigma_r(\lambda)$ from the absorption spectrum of cattle rhodopsin (24, 242). The calculated values of $A(\lambda)$ are plotted in Fig. 16c. These values suggest that the screen is a combination of absorption (primarily by the chloroplast), scattering, and, in the region from 475 to 550 nm, reflection and interference in the eyespot. The quarter-wave properties of the eyespot extend the usefulness of the screen to these nonabsorbing wavelengths.

(ii) *Chlamydomonas.* The equal-response action spectrum is one of the most common types in sensory physiology, but in phototaxis it is represented only by the action spectrum of Nultsch et al. (201) for *Chlamydomonas*. Their data are reanalyzed and discussed below (see Intensity-Response Curve). The action spectrum and the extinction spectrum of the screen calculated from this analysis are shown in Fig. 17.

(iii) *Platymonas.* Halldal (102) measured the threshold action spectrum for phototaxis in *Platymonas* over the range of 220 to 560 nm. This spectrum and the computed extinction spectrum of the screen are shown in Fig. 18. As Halldal points out, the action spectrum suggests a carotenoprotein, the absence of a peak around 370 nm excluding a flavin receptor.

The screens in *Volvox*, *Chlamydomonas*, and *Platymonas* all have appreciable extinction in the range of 475 to 550 nm, at which the receptor has maximum absorption and at which absorption by bulk pigments is low (Fig. 16, 17, and 18). This extinction is probably caused by reflection and interference in the eyespot and is greatest in *Volvox*, which has the largest number of layers. It is least in *Platymonas*, which has the smallest number of layers. In *Platymonas* the effect of reflection and interference is probably small compared with the effect of absorption.

Dinoflagellates. Action spectra for phototaxis have been obtained for species of *Gyrodinium* (77, 78), *Gymnodinium* (79), *Peridinium*

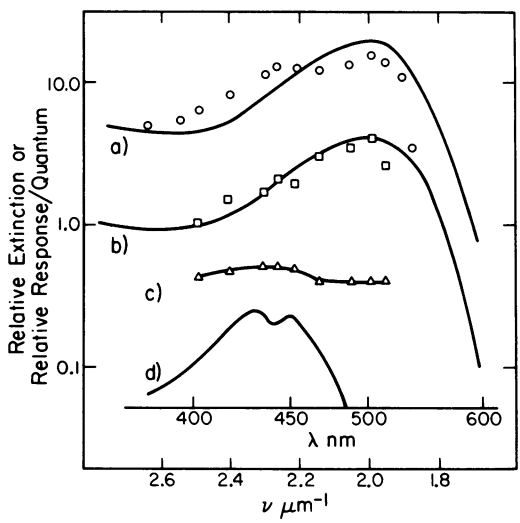

FIG. 17. *Chlamydomonas spectra. (a) Action spectrum for phototactic aggregation. (b) Reciprocals of intercept intensities from linear plots of response versus log intensity. By theory these intercepts should be proportional to the absorption of the photoreceptor pigment. Solid lines (a) and (b) are absorption spectra of cattle rhodopsin (242). (c) Slope of lines obtained by plotting response versus log intensity at each wavelength. By theory the slopes should be proportional to the extinction spectrum of the screen. (d) Absorption spectrum of bulk pigments calculated from absorption spectra of chlorophyll a and b (216) and β-carotene (240) and concentrations in cell (201). The maximum of (c) coincides with the peak absorption of the bulk pigments in (d). Chlamydomonas data are from Nultsch et al. (201).*

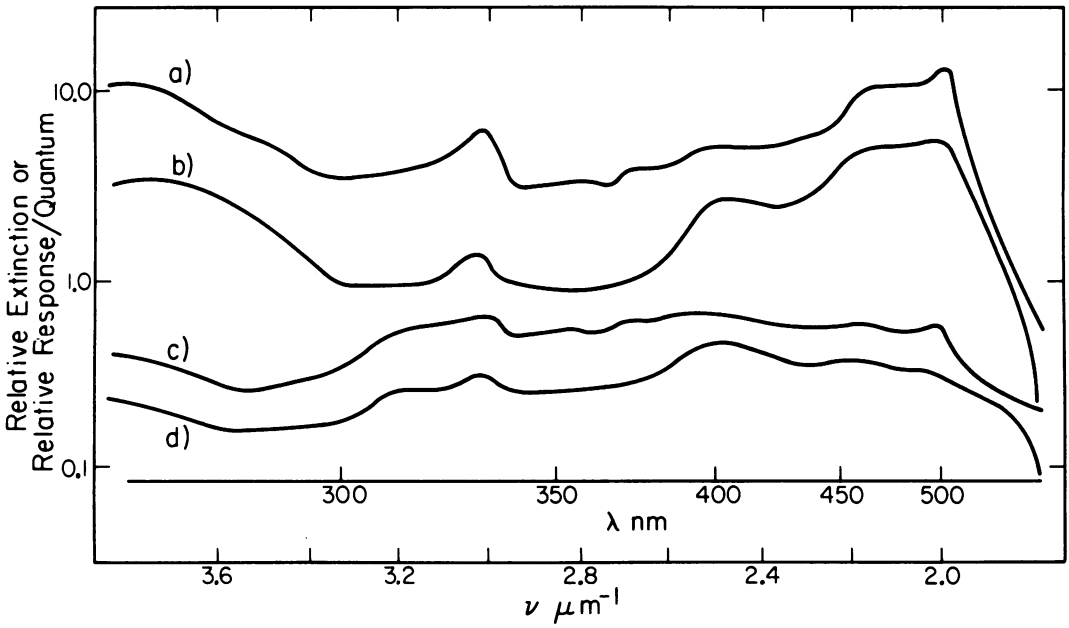

FIG. 18. *Platymonas spectra. (a) Threshold action spectrum for positive phototaxis (102). (b) Threshold action spectrum for negative phototaxis (102). (c) Estimated extinction of screen during positive phototaxis calculated from (a) and absorption spectrum of rhodopsin (24) using equation 40. (d) Estimated extinction of screen during negative phototaxis calculated from (b) and the absorption spectrum of rhodopsin (24) by using equation 40.*

(101), and *Gonyaulax* (101). Figure 19 shows the action spectra for phototaxis and the stop response in *Gymnodinium*. In all of these action spectra there is a peak around 280 nm and one in the region of 450 to 475 nm. There is little absorption in the 370-nm region, where flavoproteins usually have a peak. The spectra are sufficiently similar to each other and sufficiently different from those of other algae to suggest that a distinctive receptor pigment is involved. The visible peak is at a shorter wavelength than that of ordinary rhodopsin, but the spectrum resembles that of many carotenoids.

One possible receptor is a peridinin protein, an accessory pigment for photosynthesis (232). The very high threshold of *Gymnodinium* shown in Table 1 indicates that only a small portion of the total peridinin would be involved in phototaxis. Unfortunately, the threshold of *Peridinium balticum* has not been investigated. According to this interpretation the dinoflagellates resemble *Cryptomonas*, for which there is good evidence that a small portion of an accessory pigment is used for phototaxis.

Another possibility is that the receptor pigment is a form of rhodopsin in which the main absorption peak is shifted toward the blue from the position seen in Chlorophyceae. Such rhodopsins have been found in higher organisms (155). The probable location of the receptor pigment in the plasmalemma (see Tracking Antenna Designs), as in Chlorophyceae, makes rhodopsin a plausible choice.

Prorocentrum is different from the dinoflagellates discussed above, a desmophycean rather than a dinophycean in some classifications (23). Consistent with this difference is a marked difference in the action spectrum, which peaks at 570 nm, like *Cryptomonas*, instead of at 450 to 475 nm (101). As in *Cryptomonas*, some accessory pigment is probably involved.

Cryptomonas. The equal-stimulus action spectrum for phototaxis in *Cryptomonas* (244) is shown in Fig. 20a. The absorption spectrum of the extracted phycobiliproteins, mostly phycoerythrin with possibly some phycocyanin, is shown in Fig. 20b. The screen extinction, calculated by equation 38, is shown in Fig. 20c. This suggests a carotenoid shade such as that provided by the large pigment granules of the eyespot. The peak at 600 nm (if significant) may indicate that phycocyanin is more effective in producing the response than is phycoerythrin. (If a small amount of phycocyanin produced a disproportionally large receptor activity, the estimated photoreceptor spectrum of Fig. 20c would be too small at 600 nm, and the estimated screen would be too large there.) This is plausible if phycoery-

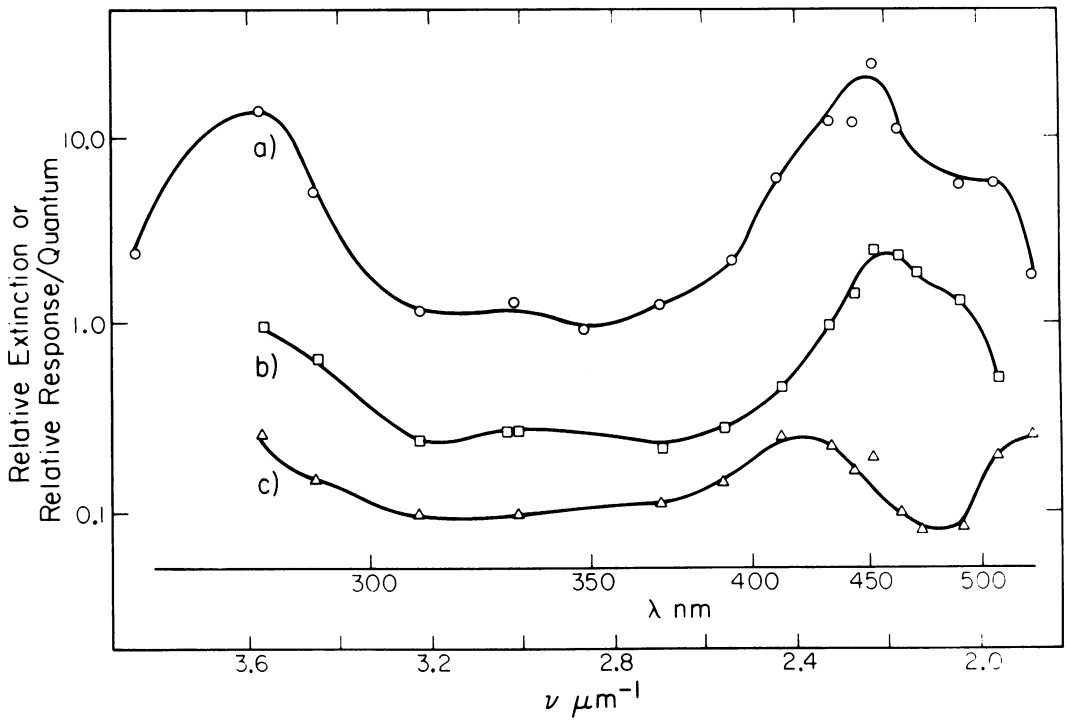

FIG. 19. *Gymnodinium spectra. (a) Phototactic action spectrum calculated from the data in Fig. 2b of Forward (79) and by using his Fig. 3 to convert ordinate to relative response per quantum. (b) Threshold action spectrum for stop response (79). (c) Estimated extinction of screen calculated from (a) and (b) by using equation 39.*

thrin and phycocyanin are in close proximity and phycoerythrin, which absorbs at the shorter wavelength, transfers its excitation energy to phycocyanin, as occurs in photosynthesis (85).

Euglena. Fig. 21a shows a response-per-intensity action spectrum for accumulation in a lighted region of a cell suspension (38). We ask whether light modulated by the stigma could produce the result observed. From the experimental design, it appears that the accumulation is caused by more than one stimulus: by phototaxis, by transient response to turning on the light, and by transient response when cells swim across the light-dark boundary. As pointed out by Diehn (53) and Checcucci et al. (38), the action spectrum resembles the absorption spectrum of a flavoprotein. This does not rule out participation of the stigma in the response. The extinction spectrum of the stigma, measured in the living cell by Wolken (248), is shown in Fig. 21b. This extinction spectrum, rather than the absorption spectrum of the extracted pigments, is the proper one to use because it includes attenuation of the light by both absorption and scattering. Because of scattering, the spectrum is almost flat from 420 to 510 nm. Consequently, the screen has little effect on the action spectrum in this region, and the estimated photoreceptor absorption, shown in Fig. 21c and calculated from equation 39, differs from the action spectrum mainly in the relative height of the peak at 380 nm, where stigma screening is lower. Fig. 21d shows the action spectrum for response to repetitive flashes of light, a response that should be less influenced by phototaxis. The similarity of this curve to Fig. 21c is consistent with involvement of screening by the stigma in phototaxis.

Intensity-Response Curve: Identity of Receptor Pigment, Mechanisms of Producing Directivity, and Pigment Regeneration Rate

Rate-sensitive, matched-filter processing by the detector provides a good signal independent of absolute intensity (see Signal Processing). Nevertheless, some important properties of photosensory systems change markedly with light intensity. Examples of such systems among the microorganisms are the light-growth response and phototropism in *Phycomyces* (see Fig. 8 of reference 83) and the probability of reversal of

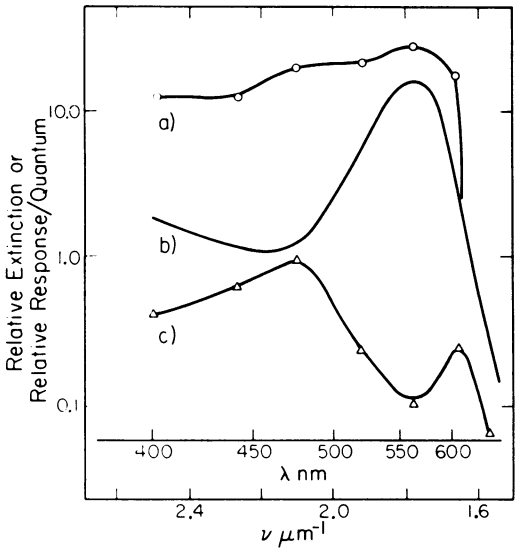

FIG. 20. *Cryptomonas spectra. (a) Equal-photon action spectrum. (b) Absorption of extracted phycobiliprotein. (c) Estimated extinction of screen calculated from (a) and (b) by using equation 38. Cryptomonas data are from Watanabe and Furuya (244).*

swimming direction by *Halobacterium* in response to blue-green light (K. W. Foster and H. C. Berg, manuscript in preparation). The processing filter of algae is also likely to change with intensity. By analogy with well-studied systems, we would expect the memory time to become shorter with increasing intensity and the error in phasing of the response to decrease. In this section we show how we can learn more about modulating screens and receptor pigments from studying behavior as a function of intensity.

When considering the relationship between magnitude of response and stimulus intensity in algal phototaxis, it is important to keep in mind the various ways in which sensory physiologists have studied this relationship in other organisms. There are three main methods, which differ in the variable that is held constant. In the classical technique pioneered by Weber, the response is held constant, the background level of stimulus is varied, and the fractional increase in stimulus required to produce the fixed response is measured. In the second method, the background stimulus is held constant, and the response is measured when the stimulus is raised to different levels above the background. As the stimulus intensity increases, the response typically rises in a hyperbolic curve to some maximum (149). In the third method, the fractional change in stimulus is held constant and the response is measured at different background levels of stimulus. In these experiments, as the background level increases, the response rises to a maximum and then declines, forming a more or less symmetrical peak when response is plotted against log intensity. For interpreting phototaxis, it is important to understand that only the third type of experiment can be done on freely swimming algae. The cells respond to light modulated by screening, and a screen removes a fixed fraction of incident light. As would be expected, when rate of aggregation is plotted as a function of log light intensity, curves with a single maximum are obtained (76, 198, 201).

In the Appendix we describe how we believe intensity-response curves for phototaxis should be analyzed. Because they yield action spectra for both the receptor and the screen and provide a value for the regeneration rate of the receptor pigment, they are fundamental for studying phototaxis. In the next section we apply the approach derived in the Appendix to published data on *Chlamydomonas*.

***Chlamydomonas* action spectra and regeneration rate.** Nultsch and co-workers (201) studied phototaxis in *Chlamydomonas*, a unicellular green alga with two flagella. Using the rate of phototactic accumulation as a measure of response, they obtained the equal-response action spectrum reproduced in Fig. 17a. The

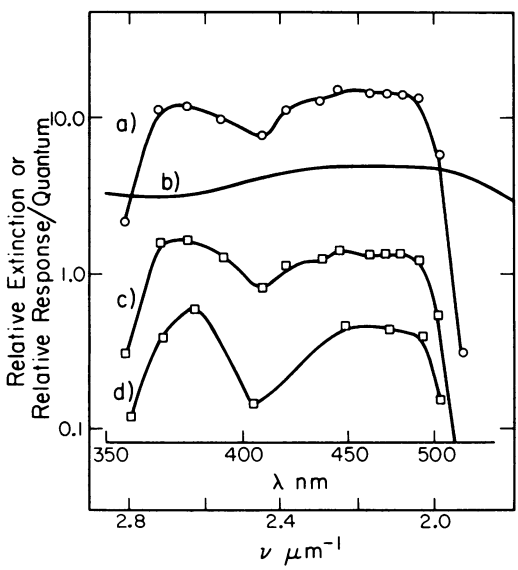

FIG. 21. *Euglena spectra. (a) Response-per-intensity action spectrum for accumulation in a lighted region after light turned on (38). (b) In vivo extinction spectrum of stigma (248). (c) Estimated extinction of photoreceptor pigment, calculated from (a) and (b) by using equation 39. (d) Response-per-intensity action spectrum for accumulation in region illuminated by repetitive 250-ms pulses of light (38).*

action spectrum is bimodal, with a main peak at 503 nm and a secondary peak at 443 nm. Such bimodal action spectra are characteristic of phototaxis in green algae and many dinoflagellates (101). To calculate the action spectrum, Nultsch et al. measured at each wavelength the response at three different light intensities in the linear part of the log intensity-response curve. They then found by interpolation the light intensity that gave a particular (arbitrarily chosen) magnitude of response. We will now show that the same data can be used to construct intensity-response action spectra as described in the Appendix.

From the log intensity-response curves we obtain intercept values I_0 whose reciprocals are plotted against wavelength in Fig. 17b. The action spectrum has a single maximum around 500 nm. This curve should represent the absorption spectrum of the photoreceptor pigment, and we have plotted for comparison the absorption spectrum of cattle rhodopsin (242). Except for the point at 513 nm, the agreement between the two curves is very close, though more points above 500 nm are needed to complete the comparison. Evidence from two other green algae agrees with this, showing that the photoreceptor pigment has a single absorption maximum around 500 nm: the action spectrum for the stop response in *Volvox* (221, 226) (see Action Spectra), and the action spectrum for a light-induced change in electrical potential in *Haematococcus* (151). (The latter action spectrum has a number of secondary maxima and minima which may be artifacts. They could be caused by variation in light intensity from one flash to another.)

Slopes of the log intensity-response curves are plotted in Fig. 17c. Since theory predicts that this action spectrum is proportional to the extinction spectrum of the screen, we have plotted for comparison the combined absorption of the bulk pigments (Fig. 17d), estimated from the measured pigment composition (201). The action spectrum of the screen has a single broad peak coinciding with the maximum absorption of the bulk pigments, an indication that these pigments contribute significantly to the screen. (Curry and Thimann [46] have argued that screening should produce only a small effect on an action spectrum. We see that this conclusion, when applied to phototaxis, is sometimes valid [*Euglena*] and sometimes not [*Chlamydomonas*].)

The extinction spectrum for the screen in *Chlamydomonas* (Fig. 17c) is much flatter than the absorption spectrum of the pigments, suggesting that reflection from the eyespot and scattering are also involved. Even though the absorption maximum of the photoreceptor pigment occurs at 500 nm, where the screening pigments have weak absorption, reflection and interference are strong enough there to produce adequate contrast for phototaxis.

The absolute I_0 values from the intensity-response curves were used to estimate the rate constant for photoreceptor pigment regeneration, k_2 from equation A7 of the Appendix. The calculation requires I_{max}, the intensity that gives maximum response. If the data fit the ideal curve of Fig. 27, then I_{max} would be $21 \times I_0$. But the data do not fit this curve closely. Nultsch et al. determined the complete intensity-response curve for white light, and on this curve $I_{max} = 55 \times I_0$. We argue in the Appendix that I_0/I_{max} is the same in white light as in monochromatic light. We therefore used $k_2 = \phi_r \sigma_r(\lambda) I_0(\lambda) \times 55$, assuming that $\phi_r = 0.67$ and calculating $\sigma_r(\lambda)$ from the absorption spectrum of cattle rhodopsin (242). Omitting the possibly aberrant point at 513 nm, we had 8 estimates of k_2, which averaged 0.0046 ($\pm$0.0003) s^{-1}. This gives $1/k_2 = 3.6$ min, comparable to the value $1/k_2 = 1$ min found by Rushton and Henry (219) for human cones and 4 orders of magnitude greater than the value found by Marcus and Aaron (168) for *Halobacterium* rhodopsin.

I_{max} is the light intensity at which phototaxis is most effective, and presumably it is set by selection to the light intensity at which phototaxis is most advantageous. I_{max} is determined by k_1 and k_2. During its evolution the organism probably had little control over k_1. The small number of compounds that serve as photoreceptors appear to have been selected to provide the highest attainable absorption and quantum efficiency. On the other hand, the organism does have control over k_2, and this quantity is probably varied to adapt different algae to different photic environments. (The organism also has control over the amount of photoreceptor pigment, which by determining threshold determines the range of phototactic sensitivity [see Threshold].) Comparative studies of k_2 should be informative, but little information is available. For *Chlamydomonas*, Nultsch et al. found in white light that $I_{max} = 10^3$ lx, equivalent to 10^{-2} times full sunlight. This low value may imply that this strain, and possibly soil algae in general, use phototaxis more to guide the organism out of the soil, where the light intensity is low, than to keep the cells oriented once they are in the light. I_{max} for phototropism in *Phycomyces* (83) is about the same as I_{max} in *Chlamydomonas* (198), whereas I_{max} for blue-green response in *Halobacterium* corresponds to full sunlight (Foster and Berg, in preparation).

Polarized Light: Characterization of the Dichroic Crystal Detector in *Euglena*

We discussed above the ultrastructural and physical evidence that *Euglena* has an oriented crystal detector (see Antenna Structures) and the evidence that the receptor pigment is a flavoprotein (see Action Spectra). In this section, we consider the behavioral consequences of this kind of detector, basing our discussion on the polarized light experiments of Diehn and coworkers.

To interpret these behavioral results it is necessary to consider how the electronic transition moments for absorption at different wavelengths are oriented with respect to the flavoprotein molecule. The action spectrum (Fig. 21a, d) resembles the absorption spectrum of flavoquinone, the oxidized form of flavin (111), modified by stacking interaction between the isoalloxazine ring of the flavin, and tyrosine or tryptophan in the protein (177, 178). Flavins typically have three main absorption peaks, one in the blue around 450 nm, one in the near ultraviolet around 370 nm, and one at 280 nm. Stacking interaction adds absorption around 390 and 485 nm. The action spectrum of *Phycomyces* (49, 81) implies that this receptor also has strong absorption at these wavelengths and significant stacking interaction. Probably this interaction is significant for function in both *Euglena* and *Phycomyces*.

The main electronic transition moments for each of these peaks are not parallel. To a first approximation we may suppose that the 450- and 280-nm transition moments are in the plane of the isoalloxazine ring, with the 450-nm moment close to its longest dimension and the 280-nm moment close to its shortest dimension; the 370- to 390-nm transition moment has a significant component normal to the 450-nm transition moment (231). With such an arrangement of the transition moments, a receptor could be formed that would absorb primarily blue but not near-ultraviolet light in one orientation, and primarily ultraviolet but not blue light in another orientation. This is the effect observed by Diehn (53) in action spectra measured in polarized light. Diehn measured aggregation changes of cells in a tube, a small region of which was illuminated with stimulating light. He found opposite effects in blue and near-ultraviolet light depending on whether the plane of polarization was parallel or perpendicular to the tube. This result implies that the cells were oriented in the tube at the time they were stimulated, but the experimental arrangement makes it uncertain what the orientation was. The experiment therefore detects dichroism, but does not give the orientation of the molecules in the photoreceptor.

Another effect of polarized light, discovered by Creutz and Diehn (45), does permit a conjecture about the orientation of the receptor molecules. Cells swimming in a thin cuvette were illuminated from above with blue (472-nm) polarized light. The cells accumulated at the upper wall, many swimming in the horizontal plane. The horizontally swimming cells showed a marked tendency to orient with their long axes perpendicular to the plane of polarization. Creutz and Diehn interpret this result on the basis that the cells accumulate in the orientation where the receptor absorbs the most light. It seems more likely to us that they accumulate in the orientation where the receptor absorbs the least light. The argument, briefly, is this. The cells are positively phototactic. This means that when the light is modulated by rotation of the cell, the cell turns toward the direction where it senses the least light. If a cell moving mostly in the horizontal plane and exposed to polarized light senses light modulated by receptor dichroism, it will still turn in the direction where it senses the least light. Since the cells line up perpendicular to the plane of polarization, this implies that the resultant (vector sum) of the blue light transition moments of the receptor molecules lies parallel to the long axis of the cell.

Two testable predictions can be made from this interpretation. One is that negatively phototactic cells should orient with their long axes parallel to the plane of polarization. The other is that polarized light at 370 nm should not cause orientation perpendicular to the plane of polarization in positively phototactic cells. It is unclear whether ultraviolet light will produce orientation parallel to the plane of polarization. The approximate orientation in the photoreceptor of the resultant transition moments at the three absorption peaks could be determined by observations on single cells. The probability of response to a step change in light intensity should show a maximum at a particular orientation of the cell with respect to the plane of polarization.

Polarized light is useful in detecting receptor dichroism, but light in the natural environment of algae is only partially polarized (155). It is unlikely that polarization of the light is an important cue for phototactic orientation. As discussed above, however, dichroism produces directivity in unpolarized light. If, as we suspect, the transition moment for blue light is parallel to the long axis of the cell, absorption will be minimum when the cell is parallel to the light and increase with increasing inclination to the light. As we will show (see Signal Processing), this arrangement seems necessary for close-an-

gle tracking. This increase in directivity due to the orientation of the dichroic crystal receptor supplements the directivity caused by stigma screening.

Discussion of Receptor Pigments

This survey of receptor pigments reveals that there have been at least three different patterns in the selection of a pigment for phototaxis from among the pigments available in the cell. First, the algae that we believe use rhodopsin have used a single pigment with unique properties to perform a single function. Presumably, retinal, the chromophore of rhodopsin, is produced as a branch from the pathway of carotenoid biosynthesis. Second, the forms that use flavoproteins have taken one of the dozens of flavoproteins in the cell and incorporated it into the photoreceptor. Third, other forms have taken a photosynthetic accessory pigment system present in high concentration and incorporated part of it into a specialized structure.

It seems likely that rhodopsin is the pigment used in the chlorophycean receptors and possibly in the quarter-wave stack antennas of dinoflagellates. (Present evidence cannot distinguish between the possibilities that the receptor pigment is rhodopsin or a carotenoprotein such as that which serves as an accessory pigment in chloroplasts.) In these forms the retinal chromophore probably lies in the plane of the membrane layers of the antenna just as it does in the *Halobacterium* membrane (235) and in vertebrate rods (74). This orientation of the chromophores would produce the greatest contrast at the interference maximum. Rhodopsin could provide rapid communication of a signal to the flagella via ion currents or potential changes (151), as it may in higher organisms (100). It is even possible that the receptor in green algae, if it is rhodopsin, is homologous with vertebrate rhodopsin. These protists might therefore serve as excellent eucaryotic model systems for vertebrate photoreceptors. This is particularly true of forms such as *Chlamydomonas*, whose genetics is well developed.

The second pattern of pigment development, best characterized by the crystalline paraflagellar body of *Euglena*, is probably common to all of the euglenoid algae. The interesting, and possibly unique, property of these receptors is that they are three dimensional. The low threshold of *Euglena*, the lowest of all of the algae in Table 1, implies that all of the pigment molecules in the crystal are effective in photoreception. Probably very few biological receptor pigments could be placed in a three-dimensional array and still retain their function. Taken together with the dichroic properties of the receptor, which show that the array is ordered, this implies that some process such as excited-state transfer must occur within the crystal to allow each pigment molecule to communicate with the processor. One clue to the physical mechanism comes from the detailed action spectrum, which implicates stacking interaction of the chromophores with tyrosine or tryptophan from the protein. Analysis of the mechanism of excited-state transfer in *Euglena* and investigation of whether similar crystalline structures occur in *Phycomyces* might be useful approaches to studying these flavin-response systems.

The third pattern, modification of a chloroplast structure and use of accessory pigments as receptor, is seen in *Cryptomonas*. The dinoflagellates might follow the same pattern, with peridinin-protein being used by *Gonyaulax*, *Peridinium*, *Gymnodinium*, and *Gyrodinium* and an unknown accessory pigment being used by *Prorocentrum micans*.

In warnowiacean dinoflagellates with ocelli, the retinoid is the presumed receptor structure. It is formed of lamellae arranged approximately end on with respect to the light. Lack of behavioral information prevents any conjecture about either the chemical nature of the receptor pigment or the orientation of the chromophore.

For the purpose of this article we made the assumption that we know the chemical nature of the photoreceptor pigments well enough that we could use the known absorption spectra of these compounds to analyze the phototaxis action spectra. This enabled us to obtain information about the spectral properties of the screen. This approach was particularly successful with the green algae. Here, the degree of effect of the screen between 475 and 550 nm is roughly proportional to the number of quarter-wave layers it contains. An important conclusion emerges from this comparison. For the quarter-wave properties of the stack to be effective, the receptor pigment must be an integral part of the structure. Moreover, its effectiveness requires that the interference properties of the stack (as opposed to its reflective properties alone) be utilized. Therefore, the receptor pigment must lie in the membranes at the interference maxima of the stack. Knowledge of the location of the receptor pigment is essential for isolation and biochemical identification of the pigments, study of communication from the pigments to the site of action, and investigation of the molecular details of signal processing. Ultrastructural studies using the freeze-fracture technique (29, 182, 193) should be particularly valuable for studying pigment location and other aspects of the design.

ANTENNA FUNCTION IN PHOTOTAXIS

In previous sections we presented structural evidence that algal cells contain directional light detectors, and we considered behavioral evidence that these detectors are used in phototaxis. We shall now consider how the detectors work. We can understand their function in phototaxis in broad outline, even though important experimental details are still lacking. In brief, the organism by its own motion performs a spatial scan of its light environment. The resulting signal is processed so that information about the direction and amplitude of the error in tracking is sent to the responder. This signal feeds back to control the flagella as indicated in Fig. 3, and the system orients the cell body to the light direction. We now consider each of these processes in detail.

Signal Production: Scanning by Cell Motion

The spatial scan performed by an algal cell is similar to the familiar process of rotating a home TV antenna to pick up the strongest signal. But there are important differences. The algal cell does not rest on a stable platform relative to the source, and it must scan continuously to maintain its orientation. Moreover, the cell does not look for brightest intensity, but for light direction. A better, but less familiar, analogy is a conically scanned tracker, sometimes used for tracking planes, missiles, or stars. All available evidence indicates that algae track by means of conical scanning. One of the major advantages of this technique, in both engineering and biological applications, is that only one sensor is required, and only one signal must be processed.

We explain the principle of conical-scan tracking, which is basic to subsequent discussion, by reference to fire-control radar, used for tracking airplanes in World War II (see Biberman, Chapter 4 [19]). In such trackers, a radar antenna is continuously rotated about a single axis, but the antenna is tilted slightly so that its direction makes an angle of a few degrees with the rotation axis (Fig. 22a). The signal consists of radiation reflected from the target and would be maximum if the target were on the optical axis of the antenna, but the antenna does not point at the target. It scans a circle in space, with the target situated somewhere within the field of the scan. The direction toward which the rotation axis points can be changed by servomotors. The purpose of the servo control is to position the target in the center of the scan. The essential point is that when the tracker is on target, the rotation axis, and not the antenna direction, is aligned with the target. From now on we will refer to the rotation axis as the tracking direction.

Because the antenna points at an angle to the target, the signal it receives is less than maximum. If the target were not moving, and the tracking direction were aligned with the target, the signal would be constant during the entire scan. When the target moves away from the axis, the signal becomes greater in one part of the scan and smaller in the other parts. It is greatest when the antenna points most closely toward the target, that is, when both the target and antenna directions are on the same side relative to the tracking direction. This periodic signal, usually called the error signal, contains two pieces of information: the phase gives the direction of the target from the tracking direction, and the amplitude gives the angular distance. During tracking, the servomotors turn the device toward the direction from which the signal is maximum, thus nulling the amplitude of the error signal (Fig. 22b). Phase information is both necessary and sufficient for tracking, but smoother tracking is obtained when the amplitude information is also used, that is, by making the rate of servo turning proportional to the amplitude. The error signal is not, of course, a simple sine wave. It is constantly being altered by both the motion of the target and the response of the servo drive. The tracker thus operates in a closed loop, the tracking servo loop.

Although algae use the same tracking principle (Fig. 22c), there are quantitative differences that are instructive to consider. First, we define two angles, the scan angle ϕ and the phasing angle θ, that describe the orientation of the algal antenna to its tracking direction (Fig. 23). We assume that the organism is swimming in a uniform helical path, and that its body maintains a fixed orientation to the axis of the helix. The axis of the helix is the tracking direction of the phototactic system, pointed in the direction of the net movement of the cells. We have already defined the direction of the antenna as the direction of maximum directivity (see Antenna Structures). The scan angle is simply the angle between the antenna and the tracking direction. To define the phasing angle, consider the plane formed by the tracking direction $\vec{\Omega}$ and its normal $\vec{R}$ passing through the center of the cell (Fig. 23b). The angle between this plane and the plane formed by the antenna and tracking directions is the phasing angle θ, positive in the direction of rotation.

For a particular tracking direction, the scan angle and the directivity of the antenna determine the pattern of light intensity received by the antenna. A change in the phasing angle will

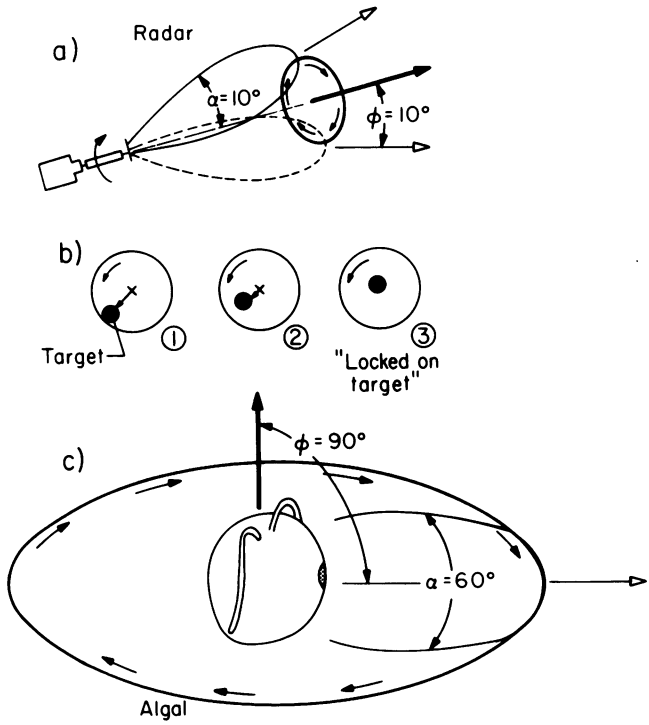

FIG. 22. *Scanning. (a) Airplane tracker in which a highly directional radar antenna is scanned in a circle around the tracking axis (after Fig. 4.5 of Biberman [19]). Solid and dashed lines are polar plots of antenna directivity in two positions of the antenna. Small arrows show direction of rotation of antenna. (b) Projection of the direction of the antenna (outer circle) onto the plane of the target, showing how successive scans and corrections (in the direction of the arrow) lock the tracker onto the target. (c) Analogous scanning by an algal cell, illustrated by Chlamydomonas. α is the half-beam width, the angle between half-maximum directivities of the antenna, and φ is the scan angle. Solid arrow indicates the tracking direction. Open arrow indicates the antenna direction.*

not change this pattern, but will change the timing of the stimulation relative to the orientation of the cell to the light.

Let us return to the radar analogy. Fire-control radar was a high-resolution instrument. Both the scan angle and the antenna beam were only a few degrees wide. When the tracker lost the target, the operator intervened to put it back on again. In algae, on the other hand, both the scan angle and the beam width are large. In *Chlamydomonas*, for example, the scan angle is 90°, and the half-beam width of the antenna is about 60° (Fig. 22c). The phasing angle is not known in *Chlamydomonas* (and is not relevant in the radar example).

A wide scan is acceptable in phototaxis, because in normal algal environments there is only one source of light, albeit a diffuse source, and it is quite dark in other directions (155). A wide scan means that algae never lose their target, but can acquire it from any initial orientation. A wide scan also makes it possible for the cell to measure the amplitude of the tracking error (the angle between the average light direction and the tracking direction over a wide angle.

A wide beam width implies that the antennas are designed to track diffuse light rather than point sources. This was first emphasized by Buder (31), who found that algae exposed to multiple light sources track the mean light direction, not one of the sources. Mast (174) made similar observations. This behavior is a direct consequence of the antenna design we have described.

Not all biological trackers are designed for diffuse light. For example, when the fungus *Pilobolus* grows under a canopy with several holes in it, it can shoot its spores through one of the holes, even when the separation is only 7° (calculated from Jolivette [133]). If one assumes that the directivity of a biological antenna is the result of natural selection, then one expects the directivity to be optimized for distinguishing the source to which response is most advantageous. The design is optimal when the directivity matches the source, that is, when the sensitivity

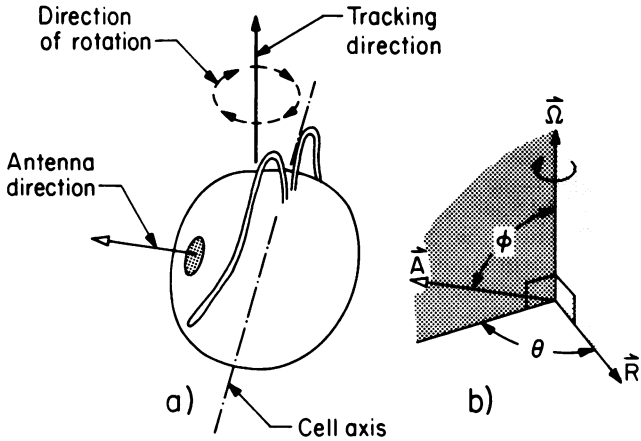

FIG. 23. *Definition of antenna scanning parameters: scan angle ϕ and phasing angle θ. $\vec{\Omega}$ is the direction of net swimming path, or tracking direction, i.e., the axis of the helix describing the swimming path. $\vec{A}$ is the antenna direction, and $\vec{R}$ is the normal from the net swimming path through the cell center. (If the center of the cell lies on its net swimming path, then θ will not be defined. Nevertheless, there is an angle between the direction of the antenna and the plane of response of the cell. It is not known whether this angle is the same as angle θ.) (a) Hypothesized orientation of cell; (b) direction of vectors.*

of the antenna as a function of angle is proportional to the light intensity of the source as a function of angle (224). If the antenna is too sharply directional, the direction of the source will not be distinguished within the width of the source. If the antenna is too broad, the source will not be resolved.

If algae are designed for diffuse light, why do they do such a good job of tracking nearly parallel light (Fig. 1)? This appears to be an example of engineering for the worst case. Biberman (19) emphasizes that even if a tracker is designed for the worst signals it is required to handle, it can still be relied upon to track when the signals are better. In direct sunlight (parallel light) the intensity distribution at the surface of a body of water is very narrow (155). Because there is plenty of light, almost any design will work. Under conditions in which it is critical for the system to work (for example, if the sun is not fully out, or if the algae are deep in the water), the distribution of the light more nearly coincides with the directivity of the antenna, and the algae receive the light distribution that they are optimized to track. It would be an informative study to determine how much, if any, correlation exists between the directivity of algal antennas and the distribution of light in the natural environments of the algae.

Despite the great structural diversity from one group to another, a single design is found in all of the antennas that have been well described. The signal is maximum when light is normal to the helical axis of the cell's swimming path. Because the cells mostly swim in shallow helices, this is about the same as saying that the signal is maximum when the light is normal to the swimming direction. In most cases the antenna points more or less normal to the helical axis and so is scanned 90° from its own rotation axis. The directivity diagrammed in Fig. 9b may be taken as typical, though exceptions may be found. This directivity creates a signal that contains information about both error direction and error amplitude.

The antenna may have an appreciable phasing angle. The phasing angle determines how the cell body will be oriented to the light at the time the cell responds. We do not know the phasing angle in unicellular algae, but we can make a prediction. Most likely it is set so that the antenna has a slight lead over the direction of response. The argument is as follows. The cell must turn toward or away from the direction of the light. In other words, it must turn in the direction that the antenna points at maximum or minimum light intensity. Response is delayed until after maximum or minimum light intensity (see Signal Processing). The phasing angle can be advanced to compensate for this delay, causing the direction of response to align more closely with the light direction. This appears to happen in *Euglena*, in which the cell turns toward its dorsal side somewhat after the receptor has entered the shadow of the stigma (54). In some colonial algae, discussed next, advance of the phasing angle is obvious.

Among the colonial algae in which phototaxis has been observed are *Volvox*, *Gonium*, *Eudorina*, *Pandorina*, *Astrephoneme*, and *Stephan-*

osphaera (118). In these algae the colony contains many antennas, usually one per cell, but each antenna is scanned in much the same way as the antennas of unicellular algae. As the colony moves forward and rotates about its fixed rotation axis, each antenna passes along a helical path. *Gonium* (173) and *Volvox minor* (175) both rotate left-handedly, and their eyespots are aimed counterclockwise (when the colony is viewed from the rear). In this orientation, light changes occur at the antenna a short time before the cell is in the correct orientation to respond to the change. Thus, the phasing angle advance is similar to what we hypothesize occurs in unicellular algae.

In most colonial algae, the individual cells show differentiation based on their anterior-posterior position in the colony. Therefore, the colony as a whole performs a more sophisticated spatial scan of the surrounding light than does a unicellular alga. In *Volvox* the cells show two kinds of differentiation. First, the eyespots decrease in size from front to back, the anterior eyespots having more layers and greater diameter or aperture. The anterior eyespots are also more curved, so that light is restricted to the maximum acceptance angles of 90° to 110° (175). Posterior cells may entirely lack eyespots. Second, farther back in the colony, the eyespots point more and more toward the rear. Usually, the most anterior eyespots point about 60° from the rotation axis, the eyespots a quarter of the way back point about 120° from the axis, and the eyespots in the back half point 180°, i.e., toward the rear (173).

If the colony is moving nearly toward the light, the light intensity on each cell remains nearly constant throughout the rotation cycle, and very few cells are stopped at any one time. Maximum force is therefore available to propel the colony. Because speed appears to be one of the main advantages of the colonial form (see Response), this effect is probably important. If the direction in which the colony is moving deviates from the light direction, some cells stop in the lit part of the colony while those in the shade are accelerated (221). The greater the angle of deviation, the greater the number of cells that stop. This means that in positive phototaxis, the greater the error in direction, the greater the torque turning the colony back toward the light. This proportional control probably occurs up to angles of deviation of 120 to 150°. Note that all antennas in the colony scan at wide angles, as described for unicellular algae. Each cell acts temporally as if it were unicellular, but the colony has antennas pointing in nearly all directions, enabling the colony as a whole to react much faster than a unicellular alga.

The antenna array provides proportional control over a large angle in positive phototaxis, but over a much smaller angle in negative phototaxis. This design seems advantageous because negative phototaxis usually occurs at higher light intensities, when the signal is large and less optimal performance is demanded of the tracking system. In this respect the colonial algae differ from the unicellular algae, which have proportional control of up to 90° in both positive and negative phototaxis.

Signal Processing

A fundamental property of sensory systems is that when an instantaneous stimulus (a pulse) is given, the response is not instantaneous, but is spread out in time. As we will see, this property is essential to phototaxis and in fact is essential to the biological usefulness of any sensory system. The impulse response, the time course of response after a pulse stimulus, largely determines the consequences of particular patterns of stimulation. The impulse response has not yet been adequately measured for the phototactic response of any alga. The best published measurements are those (Sakaguchi and Iwasa, 221) for the time course of flagellar activity in *Volvox carteri* in response to large non-physiological step changes in light intensity. Positively phototactic colonies show a transient increase in flagellar movement after a decrease in light and a transient decrease or stopping of flagellar motion after an increase in light. Because the impulse response is the derivative of the step response, and because we would expect it to resemble the impulse response measured in other systems with similar types of response, we can predict its form in phototaxis. The predicted form as shown in Fig. 24 is the same form as the impulse response measured for the light-growth response of *Phycomyces* (150). Here, the response, growth rate, is graded. But all-or-nothing responses may also have the same form of impulse response. For example, *Halobacterium* responds to blue-green light by reversing its direction of swimming. The impulse response describes the probability of reversal as a function of time after a pulse of light, and also has the form shown in Fig. 24 (Foster and Berg, in preparation). The assumption that the impulse response for phototaxis has this form leads to some useful insights into the handling of light signals in a noisy environment.

The impulse response itself is a laboratory artifact, because the laboratory is the only place where receptors receive pulse stimuli. In nature they receive a constantly fluctuating signal. The

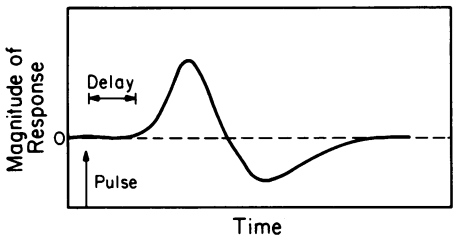

FIG. 24. *Impulse response for a rate-sensitive detector. A short pulse of sensory stimulus produces a response whose time course has the form shown.*

impulse response nevertheless can be used to predict phototactic behavior under normal illumination. By normal illumination we mean that changes in light intensity are caused by fluctuations and cell motion, but not by large changes in the source. Under these conditions we can assume that the system is approximately linear. This means that (i) the magnitude of the impulse response is directly proportional to the intensity of the pulse, and (ii) the principle of superposition holds. Superposition implies that the response to a series of pulses is the sum of the impulse responses to each individual pulse. Therefore, we can think of the time-varying stimulus as being made up of a series of pulses. The resulting behavior is the summation of all the impulse responses produced by the series of pulses (205). The equivalent statement in mathematical terms is: phototactic behavior is the convolution of the light intensity with the impulse response. This principle is basic to our interpretation of signal processing. Figure 3 shows a possible pattern of light intensity and the appearance of the signal after it has been convoluted with the impulse response to produce the processed signal.

Convolution of the light intensity with the impulse response implies that the impulse response acts as a filter through which the organism perceives its past experience. The shape of the impulse response determines the aspects of its experience that the cell remembers. An essential property of the impulse response shown in Fig. 24 is its biphasic nature. Part of the response is positive, and part is negative; the areas under the positive and negative parts are equal. Figure 24 shows a positive impulse response. The impulse response can also be negative, having the same form but with the sign reversed. Probably, some kinds of algae have a positive impulse response for positive phototaxis, and others have a negative impulse response. When a positively phototactic individual becomes negatively phototactic, the sign of the impulse response probably changes (221). For simplicity, we talk about positive phototaxis and positive impulse response in the next paragraph, but the principle is the same for all four sign combinations.

An impulse response of the form predicted has a number of important consequences for behavior. (i) The first consequence is finite memory time. The effect of stimulation lasts only for the duration of the impulse response. (ii) The second consequence is suppression of high-frequency noise by integration. A convolution is a summation or, strictly speaking, an integral. Each point on the response curve is therefore a kind of weighted running average of the light intensity taken over the memory time. This tends to average out any noise in the signal having a period significantly shorter than that of the impulse response. (iii) The third consequence is rate sensitivity. Because the impulse response is biphasic, its convolution with the light intensity amounts to subtracting one part of the remembered signal from the other part. By measuring the difference between two parts of the previous signal, the impulse response measures how rapidly the signal is changing. In other words, it acts as a differentiator. (iv) The fourth consequence is suppression of low-frequency noise by differentiation. Rate sensitivity implies that only changes that are appreciable over the length of the memory time are measured. Low-frequency changes, those that cause a slow rise and fall in the base level of the received intensity, are strongly suppressed. (v) The fifth consequence is independence of mean light level. Because the behavior depends only on the rate of change of the light intensity, not on the absolute level, phototaxis is effective over a wide range of intensities. (vi) The sixth consequence is bandpass filtering. We have seen that both high and low frequencies are suppressed. This means that the cell is most sensitive to frequencies whose period is comparable to the memory time. (vii) The seventh consequence is filter matching. Maximum response occurs when the impulse response (reversed in time) exactly coincides with the variation in light intensity. In general, the more nearly the pattern of stimulation matches the impulse response, the greater the response. The implications of this fundamental property are discussed below. (viii) The eighth consequence is phase detection. Rate sensitivity not only suppresses low-frequency noise but also guarantees that the cell will know the phase of the signal, as required for tracking. (ix) The ninth consequence is phase advance. As we will see, it is advantageous to the cell that maximum response should roughly coincide with maximum light intensity (see Response). However, the

maximum of the derivative, the quantity sensed by the cell, occurs a quarter cycle before the maximum of the light intensity, as is characteristic of periodic signals. The delay inherent in matched filter processing compensates for this phase advance and moves the maximum response closer to the maximum intensity. Although the cell senses rate of change, it responds approximately in phase with the intensity. (A similar phase advance is important in the phototropic response of *Phycomyces* [50, 81, 82].) Maximum response actually appears to occur somewhat after maximum intensity, the difference being compensated by the advance of the phasing angle of the antenna direction (see Signal Production). (x) The tenth consequence is proportional control. The magnitude of the processed signal is proportional to the amplitude of the modulated light intensity. We have already seen that the latter amplitude is proportional to the tracking error (see Signal Production). The cell therefore takes advantage of the tracking error, achieving more stable tracking through proportional control of the response.

Matched filter processing is highly immune to noise because it uses information available throughout the memory time to detect the signal. The scheme is widely used in electronics to extract a known signal from noise (for example, see Papoulis [205]). Phototaxis uses a known signal. The purpose of cell rotation and antenna directivity is to impart to the signal a known form that enables the processor to find it in the noise. We would expect the impulse response to reflect the pattern of light intensity that the processor is designed to detect. Since the pattern of light intensity varies, depending, for instance, on the orientation of the cell, we can say that the system is optimized for a temporal pattern of light that is the same as the time-reversed impulse response.

Full characterization of the phototactic response of any alga requires measurement of two functions: (i) the impulse response and (ii) the directivity of the antenna. The impulse response might be measured by observing the response to pulse signals, but a more effective method, and one that could also measure antenna directivity, is white noise analysis (170). Applied to phototaxis, this would require modulating the incident light in a known way and cross-correlating the observed track with the incident intensity. This would show the correction that the cell makes to a source that undergoes small changes. Once the impulse response was known, it could be used to determine the correlation between response and orientation to the light, a measure of the antenna directivity.

White noise analysis has another advantage. We have simplified our story by assuming linear behavior, but there are always nonlinearities, which may or may not be important in a particular experiment. White noise analysis gives the nonlinear terms, allowing us to assess their significance and providing us with an objective way of deciding between different measures of response. The more linear a response, the more likely it is to be useful for analyzing behavior. Nonlinearities in some measures of response may occur even when the primary response is linear. Examples of common forms of nonlinearity that might occur at some stage of signal processing in phototaxis are rectification (response to only one direction of the signal) and saturation.

The signal possesses one other known characteristic, in addition to the component caused by cell rotation, that could be used to aid detection, although there is no clear evidence of whether it is used. This is the component caused by the flagellar beat. As described above, the cell body rocks back and forth during each beat of the flagella. This changes the orientation of the cell with respect to the light, causing the light intensity on the antenna to modulate in phase with the flagellar beat. This component could be selected from the noisy signal by cross-correlation with the flagellar beat, with a great reduction in high-frequency noise (for example, see Lee [143]). There are many ways that such cross-correlation could arise rather simply. As an example, imagine that the signal picked up by the antenna is transferred to the flagellum, where it exerts the effect described by the impulse response. Then imagine that the sensitivity of the flagellum to the signal varies in some systematic way throughout the beat cycle. This property alone would cause the signal to be enhanced over the noise. One attractive feature of such a cross-correlation scheme is that the cross-correlation occurs no matter what irregularities occur in the flagellar beat. Moreover, the exact form of the flagellar sensitivity is not critical, provided it is in phase with the flagellar beat. The two methods of signal production, rotation and flagellar beat, would affect the processed signal in the same way. In other words, the component due to the flagellar beat would be large when the antenna is lit and small when it is shaded. We think it likely that some form of cross-correlation with the flagellar beat occurs. This could be tested by determining whether phototaxis can be disrupted by modulating the stimulus light at frequencies near the flagellar beat. Cross-correlation of the input signal with the flagellar beat might be the explanation of

why *Chlamydomonas* cells sometimes track for a few seconds normal to the light (Fig. 25). (When the antenna points directly at the light, the cross-correlated signal would be low.)

How could the signal processor work at the molecular level? The processor makes the detector rate sensitive, so the signal must be compared at two different times. This can be done enzymatically as demonstrated in the chemotaxis system of *Escherichia coli*. Here, behavior depends on the rate of change of chemical attractant bound to a receptor (30, 47). The methylation level of a methyl-acceptor protein provides a record of the low-frequency changes of the concentration of bound attractant (89, 233). A comparison to the present level of bound attractant provides the differentiated signal (17). Comparable biochemical studies relating to processing in algae have not yet been carried out.

Another form of signal processing, based on ionic control mechanisms, has been studied in detail in *Paramecium* (reviewed in references 66 and 138). Here, ciliary beat frequency and direction of beating are controlled by the membrane potential of the cell and the internal Ca^{2+} concentration. Membrane potential and internal calcium concentration are interdependent, and both change in response to stimulation. Several lines of evidence suggest that at least some algae have similar mechanisms of signal processing. The experiments of Litvin et al. (151) on the volvocalian alga *Haematococcus* are instructive. These investigators inserted one end of the alga cell into a micropipette and measured the potential difference between the inside and the outside of the pipette. This potential provides an indirect measure of the membrane potential of the cell and was found to change in response to light. Because the action spectrum of the change is similar to the absorption spectrum of the receptor pigment for phototaxis (see Action Spectra), change in membrane potential is thought to play a role in phototaxis.

Litvin et al. used both pulse and step changes in light intensity. After a step change, the inside of the pipette became transiently more positive, reaching a peak in 20 to 85 ms depending on the light intensity; the change lasted about 200 ms. These times are comparable to the 20-ms minimum time required for a behavioral response in *Chlamydomonas* (227; stop response delay, Smyth, unpublished data), and the cell rotation time of 500 ms. The change in membrane potential is probably involved in conducting the signal from the receptor to the flagella and represents an early stage of the processed signal. We can suggest, by analogy with vertebrate photoreceptor rods (6, 73), that lights controls one ion gate, whereas a second ion gate is voltage controlled in the opposite direction to make the resultant response transient. In *Volvox* it has been observed that transient changes in flagellar activity (i.e., probably beat frequency) occur with changes in light intensity (221, 222).

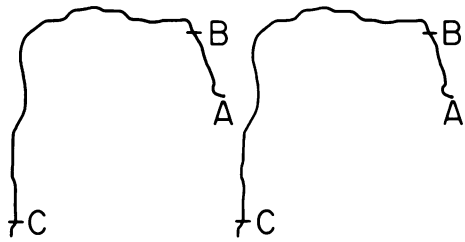

FIG. 25. *Stereo plot of the path of Chlamydomonas. After blue stimulating light was turned on at B, the cell swam approximately normal to the light. Total duration of path was 13.6 s. Path length was 1.2 mm (see legend to Fig. 1).*

Several lines of evidence indicate that the mode of flagellar activity of algae is affected by internal Ca^{2+} concentration. Litvin et al. (151) found that a large step change in light intensity caused a second potential change, opposite in sign to that caused by a smaller stimulus, to be superimposed on the first, the second change requiring free Ca^{2+} in the external medium. This potential change may be involved in backward swimming, a response algae made to strong stimulation, and known in *Chlamydomonas* to require Ca^{2+} (125, 227). Nichols and Rikmanspoel (194) injected small volumes of solution into *Chlamydomonas* and *Euglena* cells. Injection of positive-current or Mg^{2+} ions increased the flagellar beat frequency, whereas negative-current or Ca^{2+} ions decreased flagellar activity.

Although the interpretation of these various observations on ionic control mechanisms in algae is not yet clear, it may be that small-signal effects, mediated through changes in membrane potential, control flagellar beat frequency and tracking, whereas large-signal effects, which cause the cell to reverse or stop, are mediated through internal Ca^{2+} concentration. Note, however, the *Chlamydomonas* growth without added Ca^{2+} is not phototactic (199). It is not known whether individual flagella are differently affected by stimulation.

We have described the processor as a temporal filter of the light intensity received by the antenna, but because the antenna scans the environment, we can say with equal justification that the processor acts as a spatial filter of the light environment (224). This description relates the processor more directly to its biological role.

Acting as a spatial filter, it enhances the sensitivity of the cell to certain distributions of light intensities and suppresses the response of the cell to other distributions. This optimizes the ability of the organism to find the light direction in a particular light distribution.

Response: Tracking the Light Direction

We will now consider the behavior of a few organisms. Although tracks of the net phototactic response exist (Fig. 1), few of the essential facts have been firmly established for any alga. Here, we tie together what is known about the response with what we have already said about function.

Chlamydomonas. We assume that positively phototactic *Chlamydomonas* (like *Volvox* [221, 222]) responds with decreased flagellar beating to an increase in light intensity and vice versa. The evidence for this is that *Chlamydomonas* stops after step increases in light intensity, but not after step decreases. Although experiments to determine the time course and direction of the asymmetric corrective force of the flagella are straightforward in principle, they have not been done. One would like to know whether the two flagella respond symmetrically or asymmetrically. The asymmetrical position of the eyespot (Fig. 2) shows that the two flagella are not topologically equivalent. Moreover, B. Huang (private communication) has obtained mutants in which the development of the *cis*-eyespot flagellum is different from that of the *trans*-eyespot flagellum. Also, occasional asymmetric beats are seen by microcinematography (see Introduction). Thus, there is sufficient asymmetry between the two flagella that the corrective response could involve asymmetric action of the flagella. The main effect, however, is more likely a symmetrical change in the beat (194, 221). We do not know how the corrective maneuver is phased with the stimulus.

The swimming paths are helical, though often the helices are quite shallow and the paths are nearly straight. We do not know whether the antenna points toward the inside of the helix (large θ) or the outside (small θ) during tracking. Because the amplitude of the light modulation during the rotation cycle would be greater if the antenna pointed inward, this orientation seems somewhat more likely. (The antennas of *Euglena* [54] and *Ceratium* [185] point inward.) The cells could track with the antenna in either position, and when the helices are shallow, the orientation probably does not make much difference. But smooth tracking, such as we see in Fig. 1, implies that both the phasing and scan angles remain relatively constant. If the antenna flipped from inside to outside, there would be a 180° phase shift that should be visible in the track. Therefore, we suspect that the angle between the cell axis and the tracking direction is great enough to overcome noise in the cell orientation that could cause ambiguity as to whether the antenna faces inward or outward.

At the time that the cell responds, the processing delay (see Signal Processing) and phasing angle advance (see Signal Production) have combined to place the cell in an orientation where a small corrective response will make it turn toward the light. However, the timing, direction, and magnitude of the response probably depend on the size of the stimulus in such a way that more than one kind of behavior is possible. At least two kinds of tracking are seen in *Chlamydomonas*, close-angle tracking (Fig. 1) and superhelical tracking (Fig. 26). Stable superhelical tracks are rather common, with the superhelical axis coinciding with the light direction and with 5 to 6 rotations of the cell per superhelical rotation. In superhelical tracking, the plane in which the cell turns when it makes its main corrective response must be inclined to the light direction in such a way that after one rotation cycle, the cell retains the same orientation to the light that it had at the beginning of the cycle. The tracks are left-handed for positively phototactic cells, right-handed for negatively phototactic ones. This handedness implies that the plane in which the cell turns is rotated counterclockwise (as seen from in front, see Fig. 23) as compared with the clockwise cell rotation. There is a way the cell could do this. Compared with the close-angle-tracking cell, which reorients precisely in the direction which corrects its error, the superhelical-tracking cell could respond earlier in each rotation cycle. One reason for this apparently less-than-optimum

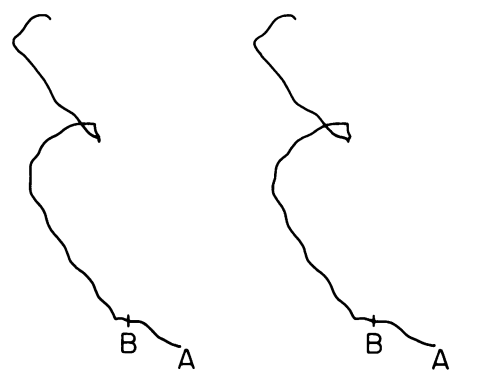

FIG. 26. *Stereo plot of the path of Chlamydomonas, showing phototactic tracking (negative) in a superhelical path. Blue stimulating light was turned on at B. Path duration was for 7.6 s. Path length was 1.4 mm (see legend to Fig. 1).*

design may be the need to be optimum at lower light intensities (i.e., worse conditions) when response time is inevitably slower. In summary, there is a significant difference between close-angle and superhelical tracking. In close-angle tracking a small error signal is nulled at all times, the cell maintains its same face toward the light, a small response makes the realignment, and the axis of the cell rotation is aligned with the light direction. In superhelical tracking the error signal is periodic with cell rotation, and there is a larger and earlier periodic correction which keeps the cell going through a constant cycle of orientations that align the axis of the superhelix (not the axis of the rotation of the cell) with the light direction.

The cells sometimes swim normal to the light direction for short intervals (Fig. 25). Although these paths lack long-term stability, they appear to result from active response to the light rather than from random swimming without stimulation.

Microthamnium. Watson has observed stable swimming paths of the green alga *Microthamnium* that are normal to the light direction (see Fig. 2c of reference 245). The cells were stimulated with continuous dark-field illumination and appeared to respond to the light once each rotation. Each time they responded, they changed their orientation to the helical path by 180°. At each response the curvature of the path changed by 180°, giving it a zig-zag appearance. This study raises an important point: little attention has been paid to the effect of light distribution on the behavior of microorganisms. Because the light antennas of algae are designed to match a particular distribution of light, this could have a significant effect. It is not clear to what extent the observed behavior of *Microthamnium* depends on the unusual light distribution (dark field) used.

Euglena. The antenna of *Euglena* is directed inward toward the helical axis (54), and the response is directed opposite to the antenna direction. In positive phototaxis the organism responds to a decrease in light intensity; in negative phototaxis it responds to an increase in light intensity (54).

Dinoflagellates. In dinoflagellates with both a transverse and a longitudinal flagellum, the flagella may be under separate control. Both Metzner (185) and Hand and Schmidt (105) have the impression that in continuous light the transverse flagellum rotates the cell to align the antenna toward the light, after which the longitudinal flagellum steers the anterior end toward the light. In *Ceratium* (185) the longitudinal flagellum is stimulated to turn the cell in the direction of the antenna, and probably it alone is responsible for making small tracking corrections. During tracking the antenna is pointed toward the inside of the helix, and correction is made toward the same direction. This implies that the cell responds to an increase in light (positive impulse response).

So far we have discussed only the usual case of antennas that are directed normal to the swimming path of the cell, but in some cells the antennas are directed more forward. The conspicuous ocelli found in the family Warnowiaceae appear to be angled in different species from normal to the longitudinal axis of the cell in *Nematodinium armatum* (191) to perhaps 30° from the longitudinal axis in *Erythropsidinium* (97). In one warnowiacean, a completely different principle may be employed. *Leucopsis cylindrica* (95) is a large cell 45 μm in diameter and 115 μm long with its anterior face covered with 15 or so ocelli directed forward. We have no behavioral information. This might be an antenna array that forms an image and can therefore work like the man-made multiple-element tracker mentioned earlier (see Introduction). In that case it would compare the intensity at each antenna to make flagellar control decisions.

Colonial algae. Colonial algae are superbly phototactic as they swim rapidly and respond immediately to changes in light direction. They swim at speeds up to ten times the speed of unicellular organisms that are comparable to the individual cells of the colony. This increased speed is a consequence of Stokes' law. The speed of a body in a viscous medium is directly proportional to the propulsive force and inversely proportional to the viscous resistance. The propulsive force is proportional to the number of flagellated cells in the colony, which in turn is proportional to the area. Because the area increases as the square of the radius and the viscous resistance increases as only the first power of the radius, the swimming speed increases as the radius increases. Rapid response is a consequence of the many independent sensors of the colony. Unlike a unicellular alga, the colony need not complete a rotation to detect a change in light direction. When the light direction changes, some cells pass from dark to light and respond quickly by beating their flagella with less force (123, 173, 194). Unequal force on the two sides of the colony generates a torque that immediately starts turning the colony toward the light. Because rotation of the colony continuously brings dark-adapted cells into the light, the torque is sustained until the colony is realigned with the light.

Gonium pectorale (173) contains 16 cells arranged in a square flat plate 100 μm across. Each cell has an eyespot and two flagella. The colony

swims with its flat surface perpendicular to the direction of motion and with the flagella all on the front surface. The colony rotates counterclockwise (left-handedly) as seen from the rear. Each antenna points normal to the direction of travel of the colony, making the scan angle about 90° as in unicellular algae. In the plane of the colony, each antenna points more counterclockwise than the radius from the center of the colony to the antenna. Thus, there is an appreciable positive phasing angle, and we can say that the antenna anticipates the signal (see Signal Production). If the position of the light source is changed so that the rays strike the anterior surface of the colony obliquely, it correctly turns at once. It never turns in the wrong direction or makes a random motion. If the light intensity is suddenly decreased, the rate of movement suddenly increases for a short period. Although not reported, there is probably also a transient decrease in activity in response to an increase in light. The distribution of beating rates on the cell reorients the colony. Once aligned with the light each cell has nulled its own error signal. In fact, each individual cell acts independently to give the immediate collective response.

Volvox is more complicated, its coenobium consisting of 1,000 or more individual cells arranged in a hollow sphere. As already discussed (see Signal Production), *Volvox* antennas are strategically oriented in specific directions to make the colony orient to the light. Mutants with incorrectly oriented antennas cannot track (122). The coenobium is densest in the rear, where there are large reproductive cells and autocolonies (171, 215). Because of this asymmetry, motile colonies swim upward in the dark, and nonmotile colonies sink with the posterior end downward (171, 215). When the cell is in any other orientation a torque is produced by gravity which tries to return it to the vertical orientation. When illuminated from above, positively phototactic colonies swim upward in a helix (171).

In experiments on phototaxis, horizontal light has most commonly been used as the stimulus. Under these conditions *Volvox* colonies swim in a nearly straight line. The line deviates to the left of the light direction (when the colonies are viewed from above) (124, 171, 226) and somewhat upward (171). More rapidly rotating colonies show less deviation to the left (124). As the light intensity is raised, the paths become more nearly horizontal (171). The angle of lateral deviation, on the other hand, remains almost constant over an intensity range of 3 orders of magnitude (124, 226). The amount of lateral deviation varies with wavelength, becoming greater at wavelengths at which screening pigments absorb less (226).

This behavior is a consequence of two effects that act to turn the colony, the torque due to gravity and the torque produced by the asymmetrical response to light changes. Whereas the gravitational torque always acts to turn the anterior end of the colony upward, the net torque direction due to photoresponse is variable, depending on the direction of the light. To reach stable paths such as those observed in horizontal light, the torque due to photoresponse must act straight downward in the vertical plane (i.e., the leftward and rightward torques must cancel) and be of the same magnitude as the gravitational torque at that particular angle. Given the specialized directivities of the antennas in *Volvox* and their unknown responses, it is impossible to predict the magnitude and direction of the torque produced as a function of the angle of the colony axis to the light direction. However, it is reasonable to assume that the magnitude increases monotonically with the angle of deviation between the swimming path and the light direction (see Signal Production). The direction of the torque would also be expected to change with the angle of deviation, the response most likely occurring earlier as the amplitude of the signal increases. It is possible that this variation in direction of response has been selected to some extent to lessen the time required for the cell to realign its path with the light direction when it deviates under normal illumination. In any case, the leftward deviation under horizontal illumination shows that when the gravitational torque forces an appreciable deviation of the path from the light direction, the response is phase advanced, in effect occurring earlier than the time when response would cause the colony to turn directly toward the light. The paths are stable because the magnitudes of the two torques vary in opposite directions, the gravitational torque ranging from zero when the colony is vertical to a maximum when it is horizontal.

In the more rapidly rotating colonies, the phototactic torque is probably greater than in the slower ones, and the cells have rotated farther when they respond. Therefore, the lateral deviation is less. At higher light intensity, the phototactic torque is stronger, and the delay in response is shorter; a new equilibrium is found closer to the light direction. The independence of the lateral deviation from the light intensity indicates, however, that the two effects approximately cancel in the horizontal plane. Increasing the screen increases the torque substantially without changing the delay, which primarily

depends on the mean light intensity; therefore, when the screen is larger, the lateral deviation is reduced.

We have simplified the discussion by supposing that the colonies always rotate in the left-hand sense and always deviate to the left when exposed to a horizontal light beam. Although this is the predominant behavior, the colonies sometimes rotate to the right (171, 215) and sometimes deviate to the right (171). Our interpretation predicts that right-rotating colonies should deviate to the right, and that left-rotating colonies should deviate to the left.

Both the superhelical swimming in *Chlamydomonas* and the lateral deviation in *Volvox* illustrate that the phase relationship between the response and the orientation of the organism to the light has an important effect on behavior. In both cases maximum response occurs earlier in the rotation cycle that would be required to turn the colony or cell directly toward the light.

Discussion

We hope that this analysis of function will be useful not only in physiological studies of algae but also in more general characterization of algal species. Therefore, we do not want to leave the impression that progress depends solely, or even primarily, on specialized techniques like white noise analysis or single cell tracking. Straightforward observations are needed on the location of the eyespot, the direction and rate of rotation, and rates of translational and rotational diffusion, all of which can be measured by using the light microscope. Also needed, but harder to obtain, is information about the orientation of the cell to its helical swimming path. We have seen that some groups of algae have a positive impulse response, and others have a negative one. This appears to be a basic phylogenetic trait. Its measurement requires observation of the effect of small changes in light intensity, up and down, on the behavior of the cell as a function of the orientation of the cell to the light. Such studies will be more valuable if ultrastructural studies to determine antenna properties and threshold and intensity-response measurement to determine light requirements are done on the same species.

Many photosynthetic bacteria use the photosynthetic receptor in a dual role as sense receptor. Algae are different, using specialized pigments or separate structures for phototaxis. At first this seems surprising, because presumably the purpose of phototaxis is to optimize photosynthesis. The reason for specialized structures cannot be any need for elaborate antennas because, as we have seen, phototaxis can work passably well without them. Apparently, specialized structures are necessary because the receptor must be small. Only then can it produce a phased signal containing the directional information essential to tracking. Again and again in different groups of algae this adaption for finding appropriate light conditions has justified the cost to the cell of building specialized structures.

PROSPECTS AND CONCLUSIONS

Different groups of algae have evolved different solutions to the problem of orienting to the light direction. Evolving in parallel, each group has developed dramatically different machinery for its phototaxis control system (Fig. 3). Dodge (58), in particular, has emphasized this viewpoint when describing eyespots. The same basic principle for tracking light is used in all designs. The rotational motion of the cell causes the antenna to scan the environment. The sensor receives a temporal pattern of intensity. The sensor output is filtered by the signal processor, and the signal is communicated to the responder to regulate the flagellar response. A succession of flagellar maneuvers of the right phase and amplitude keep realigning the organism with the average light direction. This is done over a wide range of external light intensities in spite of noise. In each design the antenna points normal to the swimming path of the cell. Therefore, when the organism swims normal to the light direction, the change in light intensity at the sensor during one rotation is maximal. This change in light intensity is the error signal for tracking. As the angle between the light direction and the cell axis decreases, the amplitude of error signal also decreases. One important result of this design is that the cell, no matter what its orientation, has an appropriate signal to correct its motion. The light antenna system functions as a spatial filter eliciting for a particular pattern of light a response that aligns the organism with the light direction. The ways that different phototaxis systems achieve their results provide us with lessons in wave optics and control analysis.

Clearly, the methods have been different. Chlorophycean algae, for example, have medially located eyespots and use the following optical strategies to create a directional antenna: reflection and interference from a quarter-wave stack of differing refractive index layers, absorption in the high refracting layers, wave guide action for light at high incidence, absorption and scattering of light passing through the cell, and probably orientation of the chromophore molecules in the receptor membrane. They use a carotenoprotein or rhodopsin as photoreceptor

and probably use the electrical properties of the plasmalemma to communicate with the flagellum. *Cryptomonas* uses slab wave guides in its antenna, combined with an absorbing stop or eyespot. The photoreceptor pigment is phycoerythrin, and communication from pigment to flagellum may involve diffusion. *Euglena* uses a three-dimensional dichroic crystal receptor in combination with an absorbing eyespot. The photoreceptor pigment is a flavoprotein, and signal communication probably involves solid-state conduction.

Each of these antenna designs employs two or more optical principles that operate simultaneously and reinforce each other. This diversity raises the expectation that if we figure out some mechanism that could be used for phototaxis, an organism may eventually be found that uses it. Antenna structures have not been identified in all phototactic organisms. In some of these a specialized antenna may not have been required. In organisms in which good tracking and low threshold are not needed for survival, a localized patch of membrane could serve as receptor, and absorption and scattering from the cell body could serve as screen. In other cases we probably have not seen the antenna because we do not know what to look for, and we have no behavioral data to tell us that it is there. We have seen various ways that algae have modified parts of their chloroplasts and flagella to make parts of their antennas. Presumably, other organelles have been modified for antenna function, but the antennas have not been recognized yet. One of the exciting prospects for work on phototaxis is the discovery of these new antennas.

We have emphasized in our discussion the importance of the environment for understanding phototaxis, but we can use phototaxis to understand the environment. The color, intensity, temporal pattern, and spatial pattern of light that the cell is designed to detect describe the environment that elicited the design. It is often unclear to the researcher what physical variables of the environment are important to microorganisms. Comparative study of phototaxis, by giving us an alga's-eye view of the world, may provide us with ecological insights that would be difficult to arrive at by other means.

An example may make the point clearer. Piccini and Omodeo (212) have suggested that some warnowiacean dinoflagellates, instead of tracking the overhead light in the sea, use their sensory apparatus to see their prey, which they could then attack with their nematocysts. How do we decide between these two possible roles for photosensitivity? One way, of course, is to watch the organisms and try to figure out what they are doing, but another way is to make laboratory observations on how they respond to patterned stimulation. Do they respond to a shadow that gets bigger, suggesting that they see prey, or do they respond to light of a certain optimum distribution, suggesting that they see the light in the ocean? To answer this kind of question, white-noise techniques for the analysis of spatial stimuli could be applied to single algal cells. These techniques have already been successfully applied to analyzing interactions in the vertebrate retina (170).

Recognition that most flagellated algae have antennas is crucial to the study of these organisms. We do not overstate the case by saying that it is as important to the phycologist to know about the antenna and its function as it is for the ornithologist to know that birds fly. Lack of this knowledge about algae has led to many errors in the past. For example, we find clear errors in the placement of eyespots in drawings of algae; sometimes authors place them in positions that disagree with their own electron micrographs. We find suggestions that algae do not rotate, failure to recognize the consequences of rotation in data on phototaxis, or suggestions that tracking the direction of the light is not the physiologically relevant response.

Our analysis of phototaxis also has some broader implications for sensory physiology. The algae are a dramatic example of a cell that must detect a pattern to its stimulation. Considerations of how such a signal must be processed led us to see features of design that might otherwise have escaped our notice. Similar analysis could be applied to any sensory system in which a pattern must be detected and in which matched filter processing is likely to be involved. This could be especially useful in studying communication between individual cells, where both the transmitter and the receiver are under biological control.

To make the scheme of phototaxis outlined in this paper clear, we have asserted some conclusions more strongly than present data warrant. We have tried to indicate where we have done so. Undoubtedly, some details will prove wrong, or reality will prove to be more complex, but the convergence of evidence from diverse sources makes us confident that the broad picture is correct.

Although much descriptive work remains to be done on phototaxis, the time appears ripe for learning from biochemical, genetic, and electrophysiological approaches the largely unknown molecular details of light reception, signal processing, antenna structural design, signal conduc-

tion, and response. *Chlamydomonas,* with its quarter-wave stack antenna and probable rhodopsin receptor, and *Euglena,* with its flavoprotein crystal detector, have been popular organisms in the past and will probably serve as good model systems in the future. We hope that by surveying present knowledge from a modern physical viewpoint, we have augmented the challenge to find out how the molecules really work in the complicated behavior of these simple creatures.

ACKNOWLEDGMENTS

Most of this work was done in the laboratory of H. C. Berg, University of Colorado, Boulder, and California Institute of Technology, Pasadena. We thank H. C. Berg, Jeremy Pickett-Heaps, and L. A. Staehelin for critical comments on the manuscript and L. A. Staehelin for allowing us to publish his electron photomicrograph of *Chlamydomonas.*

This work was supported in part by Public Health Service grant EY 01263 from the National Institutes of Health and by grants PCM77-08543 and PCM79-22601 from the National Science Foundation.

APPENDIX

Analysis of Intensity-Response Curves

Independent effect of photoreceptor and screen. From the intensity-response curve, one can construct separate action spectra for the receptor and the screen. The response is dependent on the number of captured photons ($I\sigma_r$), the fractional absorption of the screen (A), and the wavelength (λ). Hence, we can write the response as $R(I\sigma_r,A,\lambda)$. Under conditions that we will examine below, the response can be represented as the product of two functions, f and s, for the receptor and screen functions, respectively: $R(I\sigma_r,A,\lambda) = f(I\sigma_r,\lambda)\cdot s(A,\lambda)$. At the intensity I_{max} that produces maximum response, we have $\partial R/\partial I = (\partial f(I\sigma_r)/\partial I)\cdot s(A,\lambda) = 0$, $\partial f(I\sigma_r)/\partial I = 0$, and $I_{max}\sigma_r = c$, where c is a constant independent of wavelength. For the maximum response R_{max}, we have $R_{max} = f(c)\cdot s(A,\lambda)$. If response to the screen is linear with absorption, we can replace $s(A,\lambda)$ with $A(\lambda)$. Therefore, we have two action spectra

$$R_{max}(\lambda) \propto A(\lambda) \quad \text{(A1)}$$

$$1/I_{max}(\lambda) \propto \sigma_r(\lambda) \quad \text{(A2)}$$

A plot of R_{max} versus λ approximates the screen extinction; a plot of $1/I_{max}$ versus λ approximates the photoreceptor absorption spectrum.

We can generalize this approach by noting that it is not really necessary to measure R_{max} or I_{max}. All that is required is a set of corresponding points on the intensity-response curves at different wavelengths.

We define corresponding points as the points on each intensity-response curve where I/I_{max} equals some constant. At these points, $I\sigma_r$ and $f(I\sigma_r)$ are constant. Therefore at corresponding points

$$R(\lambda) \propto A(\lambda) \quad \text{(A3)}$$

$$1/I(\lambda) \propto \sigma_r(\lambda) \quad \text{(A4)}$$

We show below how to obtain a set of corresponding points from the linear portion of a plot of R versus log I.

Under what conditions can we expect the receptor and screen functions, $f(I\sigma_r)$ and $s(A,\lambda)$, to be independent? First, we assume a single photoreceptor pigment. If there are two receptor pigments, the action spectrum is a composite of $I\sigma_{r_1}$ and $I\sigma_{r_2}$ and is a different function of light intensity at different wavelengths. As long as there is a single photoreceptor pigment, the light need not be monochromatic. The response is the same function of light intensity for white light of constant spectral quality as for monochromatic light. Even when there is a single receptor pigment at low intensity, photosensitive intermediates usually accumulate at high intensity and may complicate analysis. We assume that the quantum efficiencies (ϕ_r) are nearly constant with wavelength. We assume that at a particular wavelength the proportion of light screened is the same at different light intensities, an assumption that is probably valid over short intervals, but is known not to be valid over periods of many hours. Finally, the effective light intensity in the cell is less than the measured light intensity by an amount that depends on the "average" screening. We do not know how to measure or compute this average, although it must lie between incident intensity and the minimum of the modulation cycle. We assume that the absolute variation in the screen as a function of wavelength is small enough so that this additive correction can be neglected in the determination of relative action spectra. The effect of photoreceptor and screen cannot be precisely separated easily in the presence of a quarter-wave stack. The wavelength dependence of the interference of the stack will affect f in the same way as variations in quantum efficiency, while at the same time contributing to the screen. The magnitude of the effect is difficult to estimate and depends on the orientation of the cell that determines the observed behavioral response.

Derivation from receptor kinetics. We have outlined above a general scheme for constructing action spectra from the intensity-response curve. To make this approach more concrete we apply it to a particular derivation of the intensity-response curve, with the understanding that the validity of the general approach to action spectra just described does not depend on the validity of the additional assumptions made in this particular derivation. We also show that this derivation provides an estimate of the regeneration time of the photoreceptor pigment.

A derivation of the intensity-response curve is suggested by the analogous case of bacterial chemotaxis, for which abundant data are available. Several workers (30, 47, 183) have shown that kinetic data on bacterial chemotaxis fit a model that assumes that the response is proportional to the rate of change of chemoreceptor protein bound to chemical attractant. Here, the critical process is the reversible binding of attractant to chemoreceptor protein, subject to the law of mass action. We assume that the analogous process in phototaxis is the destruction and regeneration of photoreceptor pigment. Following Rushton (218), we assume that the photoreceptor pigment exists in two states, an active state P_A and an inactive state P_I. Absorption

of a photon by a molecule of active pigment converts it to inactive pigment. Active pigment is regenerated from inactive pigment by a chemical process not requiring light. Diagrammatically, the relationship is

$$P_A \xrightleftharpoons{h\nu} P_I.$$

Such pigment conversion has been demonstrated by direct measurement of P_A and P_I in human vision (3, 219) and in insect vision (reviewed by White [247]). It has been inferred for the *Phycomyces* light-growth response (150).

The rate equation for interconversion of P_A and P_I is $dp/dt = -k_1Ip + k_2(1-p)$, where p is the proportion of photoreceptor pigment in the active form, I is the incident light intensity (in quanta per square centimeter per second), k_1 is the rate constant for photochemical inactivation (in square centimeters), and k_2 is the rate constant for dark regeneration (per second). Setting $dp/dt = 0$, we have at equilibrium $p = k_2/(k_2 + k_1I)$. We assume that the magnitude of the response is a monotonic function of the time rate of change in amount of active pigment. If we approximate the amount of active pigment by the equilibrium amount at incident light intensity, $R = C\ dp/dt = C[k_1k_2/(k_2 + k_1I)^2]dI/dt$, where C is a porportionality constant, independent of wavelength. We assume that dI/dt is proportional to the incident light intensity I and to the extinction of the screen A. The intensity-response curve is then

$$R = Ck_1k_2AI/(k_2 + k_1I)^2 \quad \text{(A5)}$$

We now show that this curve can be used to estimate k_1, k_2, and relative values of A at different wavelengths.

If we differentiate equation A5 with respect to I and set $\partial R/\partial I = 0$, we have

$$I_{max} = k_2/k_1 \quad \text{(A6)}$$

where I_{max} is the intensity of light that produces the maximum response. k_1 is equivalent to $\phi_r\sigma_r$, the quantum efficiency times the absorption cross section of the photoreceptor pigment. If these quantities are known or estimated, then the time constant for the regeneration of active pigment is

$$1/k_2 = 1/(I_{max}\phi_r\sigma_r) \quad \text{(A7)}$$

This is the time in the dark required to convert $1/e = 37\%$ of the inactive pigment to the active form.

If I_{max} from equation A6 is substituted for I in equation A5 we have $R_{max} = CA/4$, where R_{max} is the magnitude of the maximum response. Therefore, at different wavelengths

$$R_{max}(\lambda) \propto A(\lambda) \quad \text{(A8)}$$

the same result as equation A1. Since C is unknown, the method gives only relative values of $A(\lambda)$.

Replacing k_1 in equation A6 by its equivalent $\phi_r\sigma_r$ and rearranging, we have

$$1/I_{max} = (1/k_2)\phi_r\sigma_r(\lambda) \quad \text{(A9)}$$

Since k_2 is independent of wavelength and ϕ_r in most cases is nearly so, a plot of $1/I_{max}$ versus λ gives an action spectrum proportional to the absorption spectrum of the receptor pigment, as predicted by equation A2.

Often, monochromatic light of sufficient intensity to produce the maximum response is not available. Nonetheless, the two action spectra described above can be constructed using only the lower part of the intensity-response curve. Over a range of intensities below the maximum, the response is nearly linear with respect to log I. We can approximate the log intensity-response curve in this region by the tangent to the curve at the inflection point. Replacing I in equation A5 by 10^x and differentiating twice with respect to x, we find that at the inflection point $R = CA/6$ and $I = 0.268(k_2/k_1)$. The equation of the tangent at this point is

$$x = R/(0.222CA) + \log\,[0.0474(k_2/k_1)] \quad \text{(A10)}$$

where $0.222CA$ is the slope and $\log\,[0.0474(k_2k_1)]$ is the x intercept. Note that the slope is proportional to A and independent of k_1, whereas the intensity at the intercept is proportional to $1/k_1$ and independent of A. Plots of the slopes and of the reciprocals of the intercept intensity at different wavelengths therefore give action spectra representing the extinction of the screen and the absorption of the photoreceptor pigment, respectively. If sufficient points are available, it may be preferable to construct these action spectra by fitting equation A5 to the points instead of using the linear approximation. The principles involved in this construction of action spectra are illustrated in Fig. 27.

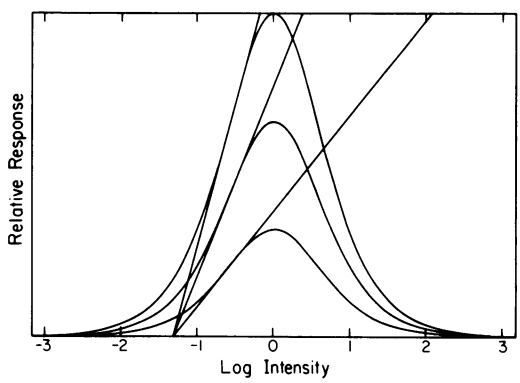

FIG. 27. *Intensity-response curves for different amounts of screening, computed from equation A5. The curves have been shifted along the log I axis to align their maxima. Construction of intensity-response action spectra requires identification of corresponding points on different curves, i.e., points that are vertically aligned on this plot. One set of corresponding points is required. Three possible sets are: (i) Points at log, if log I_{max} can be read from the curves; (ii) points where $R = R_{max}/2$, when R_{max} can be determined more accurately than log I_{max}; and (iii) intercept found by extrapolating linear part of R-log I curve, approximated here by the tangent at the inflection point. The plot shows that the tangents all intersect the log I axis at a point equidistant from log I_{max}.*

LITERATURE CITED

1. **Abelès, F.** 1950. Recherches sur la propagation des ondes électromagnétique sinusoïdales dans les milieux stratifiés. Application aux couches minces. Ann. Phys. (Paris) (12e série) **5**:596–640, 706–782.
2. **Abelès, F.** 1967. Optics of thin films, p. 143–188. *In* A. C. S. van Heel (ed.), Advanced optical techniques. Elsevier-North Holland Publishing Co., Amsterdam.
3. **Alpern, M., and E. N. Pugh, Jr.** 1974. The density and photosensitivity of human rhodopsin in the living retina. J. Physiol. (London) **237**:341–370.
4. **Arnott, H. J., and R. M. Brown, Jr.** 1967. Ultrastructure of the eyespot and its possible significance in phototaxis of *Tetracystis excentrica*. J. Protozool. **14**:529–539.
5. **Ascoli C., M. Barbi, C. Frediani, and A. Murè.** 1978. Measurements of *Euglena* motion parameters by laser light scattering. Biophys. J. **24**:585–599.
6. **Bader, C. R., P. R. MacLeish, and E. A. Schwartz.** 1979. A voltage-clamp study of the light response in solitary rods of the tiger salamander. J. Physiol. (London) **296**:1–26.
7. **Bartlett, C. J., P. L. Walne, O. J. Schwarz, and D. H. Brown.** 1972. Large scale isolation and purification of eyespot granules from *Euglena gracilis* var. *bacillaris*. Plant Physiol. **49**:881–885.
8. **Batra, P. P., and G. Tollin.** 1964. Phototaxis in *Euglena*. I. Isolation of the eye-spot granules and identification of the eye-spot pigments. Biochim. Biophys. Acta **79**:371–378.
9. **Belcher, J. H.** 1968. A study of *Pyramimonas reticulata* Korshikov (Prasinophyceae) in culture. Nova Hedwigia Z. Krytogamenkd. **15**: 179–190.
10. **Belcher, J. H., and E. M. F. Swale.** 1967. *Chromulina placentula* sp. nov. (Chrysophyceae), a freshwater nannoplankton flagellate. Br. Phycol. Bull. **3**:257–267.
11. **Belcher, J. H., and E. M. F. Swale.** 1967. Observations of *Pteromonas tunuis* sp. nov. and *P. angulosa* (Carter) Lemmermann (Chlorophyceae, Volvocales) by light and electron microscopy. Nova Hedwigia Z. Kryptogamenkd. **13**:353–359.
12. **Belcher, J. H., and E. M. F. Swale.** 1971. The microanatomy of *Phaeaster pascheri* Scherffel (Chrysophyceae). Br. Phycol. J. **6**:157–169.
13. **Belcher, J. H., and E. M. F. Swale.** 1972. The morphology and fine structure of the colourless colonial flagellate *Anthophysa vegetans* (O. F. Müller) Stein. Br. Phycol. J. **7**:335–346.
14. **Benedetti, P. A., and A. Checcucci.** 1975. Paraflagellar body (PFB) pigments studied by fluorescence microscopy in *Euglena gracilis*. Plant Sci. Lett. **4**:47–51.
15. **Benedetti, P. A., and F. Lenci.** 1977. *In vivo* microspectrofluorometry of photoreceptor pigments in *Euglena gracilis*. Photochem. Photobiol. **26**:315–318.
16. **Berg, H. C.** 1978. The tracking microscope. Adv. Opt. Electron Microsc. **7**:1–15.
17. **Berg, H. C., and P. M. Tedesco.** 1975. Transient response to chemotactic stimuli in *Escherichia coli*. Proc. Natl. Acad. Sci. U.S.A. **72**:3235–3239.
18 **Berning, P. H.** 1963. Theory and calculations of optical thin films, p. 69–121. *In* G. Hass (ed.), Physics of thin films, vol. 1. Academic Press, Inc., New York.
19. **Biberman, L. M.** 1966. Reticles in electro-optical devices. Pergamon Press, Inc., Elmsford, N.Y.
20. **Birkbeck, T. E., K. D. Stewart, and K. R. Mattox.** 1974. The cytology and classification of *Schizomeris leibleinii* (Chlorophyceae): II. The structure of quadriflagellate zoospores. Phycologia **13**:71–79.
21. **Blanchard, C. H., C. R. Burnett, R. G. Stoner, and R. L. Weber.** 1958. Introduction to modern physics, p. 257–260. Prentice-Hall, Inc., Englewood Cliffs, N.J.
22. **Blum, H. F., and D. L. Fox.** 1933. Light responses in the brine flagellate *Dunaliella salina* with respect to wave length. Univ. Calif. Berkeley Publ. Physiol. **8**:21–30.
23. **Bold, H. C., and M. J. Wynne.** 1978. Introduction to the algae: structure and reproduction. Prentice-Hall, Inc., Englewood Cliffs, N.J.
24. **Bonting, S. L., P. J. G. M. van Breugel, and F. J. M. Daeman.** 1977. Influence of the lipid environment on the properties of rhodopsin in the photoreceptor membrane, p. 175–189. *In* N. G. Bazan, R. R. Brenner, and N. M. Ciusto (ed.), Function and biosynthesis of lipids. Plenum Publishing Corp., New York.
25. **Born, M., and E. Wolf.** 1965. Principles of optics, 3rd ed. Pergamon Press, Inc., Elmsford, N.Y.
26. **Bouck, G. B.** 1970. The development and postfertilization fate of the eyespot and the apparent photoreceptor in *Fucus* sperm. Ann. N.Y. Acad. Sci. **175**:673–685.
27. **Bound, K. E., and G. Tollin.** 1967. Phototactic response of *Euglena gracilis* to polarized light. Nature (London) **216**:1042–1044.
28. **Bråten, T., and A. Løvlie.** 1968. On the ultrastructure of vegetative and sporulating cells of the multicellular green alga *Ulva mutabilis* Føyn. Nytt Mag. Bot. **15**:209–219.
29. **Bray, D. F., K. Nakamura, J. W. Costerton, and E. B. Wagenaar.** 1974. Ultrastructure of *Chlamydomonas eugametos* as revealed by freeze-etching: cell wall, plasmalemma, and chloroplast membrane. J. Ultrastruct. Res. **47**: 125–141.
30. **Brown, D. A., and H. C. Berg.** 1974. Temporal stimulation of chemotaxis in *Escherichia coli*. Proc. Natl. Acad. Sci. U.S.A. **71**:1388–1392.
31. **Buder, J.** 1917. Zur Kenntnis der phototaktischen Richtungsbewegungen. Jahrb. Wiss. Bot. **58**:105–220.
32. **Buetow, D. E. (ed.).** 1968. The biology of *Euglena*, 2 vol. Academic Press, Inc. New York.
33. **Burgess, P. R., and E. R. Perl.** 1973. Cutaneous mechanoreceptors and nociceptors, p. 29–78.

In A. Iggo (ed.), Somatosensory system. Handbook of sensory physiology, vol. 2. Springer-Verlag, Inc., New York.

34. **Burr, F. A., and J. A. West.** 1970. Light and electron microscope observations on the vegetative and reproductive structures of *Bryopsis hypnoides*. Phycologia **9**:17–37.
35. **Carlson, F. E., and C. N. Clark.** 1965. Light sources for optical devices, p. 43–109. *In* R. Kingslake (ed.), Applied optics and optical engineering, vol. 1. Academic Press, Inc., New York.
36. **Carter, N.** 1938. New or interesting algae from brackish water. Arch. Protistenkd. **90**:1–68.
37. **Castle, E. S.** 1965. Differential growth and phototropic bending in *Phycomyces*. J. Gen. Physiol. **48**:409–423.
38. **Checcucci, A., G. Colombetti, R. Ferrara, and F. Lenci.** 1976. Further analysis of the mass photoresponses of *Euglena gracilis* Klebs (Flagellata Euglenoidina). Monit. Zool. Ital. (N.S.) **10**:271–277.
39. **Clayton, R. K.** 1958. On the interplay of environmental factors affecting taxis and motility in *Rhodospirillum rubrum*. Arch. Mikrobiol. **29**:189–212.
40. **Clayton, R. K.** 1970. Light and living matter, vol. 1: The physical part. McGraw-Hill Book Co., New York.
41. **Collin, R. E.** 1969. Radiation from simple sources, p. 29–60. *In* R. E. Collin and F. J. Zucker (ed.), Antenna theory, part I. McGraw-Hill Book Co., New York.
42. **Crawford, R. M., J. D. Dodge, and C. M. Happey.** 1971. The dinoflagellate genus *Woloszynskia*. I. Fine structure and ecology of *W. tenuissimum* from Abbot's Pool, Somerset. Nova Hedwigia Z. Kryptogamenkd. **19**:825–840.
43. **Crawley, J. C. W.** 1966. Some observations on the fine structure of the gametes and zygotes of *Acetabularia*. Planta **69**:365–376.
44. **Crawley, J. C. W.** 1970. The fine structure of the gametes and zygotes of *Acetabularia*, p. 73–83. *In* J. Brachet and S. Bonotto (ed.), Biology of *Acetabularia*. Academic Press, Inc., New York.
45. **Creutz, C., and B. Diehn.** 1976. Motor responses to polarized light and gravity sensing in *Euglena gracillis*. J. Protozool. **23**:552–556.
46. **Curry, G. M., and K. V. Thimann.** 1961. Phototropism: the nature of the photoreceptor in higher and lower plants, p. 127–134. *In* B. C. Christensen and B. Buchmann (ed.), Progress in photobiology. Elsevier-North Holland Publishing Co., Amsterdam.
47. **Dahlquist, F. W., R. A. Elwell, and P. S. Lovely.** 1976. Studies of bacterial chemotaxis in defined concentration gradients. A model for chemotaxis toward L-serine. J. Supramol. Struct. **4**:329(289)–342(302).
48. **Dartnall, H. J. A.** 1972. Photosensitivity, p. 122–145. *In* H. J. A. Dartnall (ed.), Photochemistry of vision. Handbook of sensory physiology, vol. VII/1. Springer-Verlag, Inc., New York.
49. **Delbrück, M., and W. Shropshire, Jr.** 1960. Action and transmission spectra of *Phycomyces*. Plant Physiol. **35**:194–204.
50. **Dennison, D. S., and K. W. Foster.** 1977. Intracellular rotation and the phototropic response of *Phycomyces*. Biophys. J. **18**:103–123.
51. **Dera, J., and H. R. Gordon.** 1968. Light field fluctuations in the photic zone. Limnol. Oceanogr. **13**:697–699.
52. **Desikachary, T. V.** 1972. Notes on Volvocales I. Curr. Sci. **41**:445–447.
53. **Diehn, B.** 1969. Action spectra of the phototactic responses in *Euglena*. Biochim. Biophys. Acta **177**:136–143.
54. **Diehn, B.** 1979. Photic responses and sensory transduction in motile protists, p. 23–68. *In* H. Autrum (ed.), Comparative physiology and evolution of vision in invertebrates. A: Invertebrate photoreceptors. Handbook of sensory physiology, vol. VII/6A. Springer-Verlag, Inc., New York.
55. **Diehn, B., J. R. Fonseca, and T. L. Jahn.** 1975. High speed cinemicrography of the direct photophobic response of *Euglena* and the mechanism of negative phototaxis. J. Protozool. **22**: 492–494.
56. **Ditchburn, R. W.** 1963. Light, 2nd ed. Wiley-Interscience, New York.
57. **Dodge, J. D.** 1969. The ultrastructure of *Chroomonas mesostigmatica* Butcher (Cryptophyceae). Arch. Mikrobiol. **69**:266–280.
58. **Dodge, J. D.** 1973. The fine structure of algal cells. Academic Press, Inc., New York.
59. **Dodge, J. D.** 1974. Fine structure and phylogeny in the algae. Sci. Prog. (London) **61**:257–274.
60. **Dodge, J. D.** 1975. The fine structure of *Trachelomonas* (Euglenophyceae). Arch. Protistenkd. **117**:65–77.
61. **Dodge, J. D.** 1975. The Prorocentrales (Dinophyceae). II. Revision of the taxonomy within the genus *Prorocentrum*. Bot. J. Linn. Soc. **71**: 103–125.
62. **Dodge, J. D., and B. T. Bibby.** 1973. The Prorocentrales (Dinophyceae): I. A comparative account of fine structure in the genera *Prorocentrum* and *Exuviaella*. Bot. J. Linn. Soc. **67**: 175–187.
63. **Dolzmann, R., and P. Dolzmann.** 1964. Untersuchungen über die Feinstruktur und die Funktion der Plasmodesmen von *Volvox aureus*. Planta **61**:332–345.
64. **Drude, P.** 1959. The theory of optics, p. 136–141. Translated by C. R. Mann and R. A. Millikan. Dover Publications, Inc., New York. (Reprint of 1902 ed.)
65. **Dynesius, R. A., and P. L. Walne.** 1975. Ultrastructure of the reservoir and flagella in *Phacus pleuronectes* (Euglenophyceae). J. Phycol. **11**:125–130.
66. **Eckert, R., and P. Brehm.** 1979. Ionic mechanisms of excitation in *Paramecium*. Annu. Rev. Biophys. Bioeng. **8**:353–383.
67. **Enoch, J. M., D. G. Birch, and E. E. Birch.** 1979. Monocular light exclusion for a period of days reduces directional sensitivity of the hu-

man retina. Science **206**:705–707.
68. **Ettl, H.** 1964. Die feinere Struktur von *Pedinomonas minor* Korschikoff. I. Untersuchungen mit dem Lichtmikroskop. Nova Hedwigia Z. Kryptogamenkd. **8**:421–440.
69. **Ettl, H.** 1972. *Pedinomonas minor* Korschikoff, ein einfacher Modellorganismus aus dem Bereiche der kleinsten autotrophen Flagellaten. Arch. Hydrobiol. **41**(Suppl.):48–56.
70. **Ettl, H.** 1975. Die Teilung und Verformung des gegliederten Chromatophors Von *Stigeoclonium stagnatile*. (Chlorophyceae). Plant Syst. Eol. **124**:179–186.
71. **Ettl, H., and J. C. Green.** 1973. *Chlamydomonas reginae* sp. nov. (Chlorophyceae), a new marine flagellate with unusual chloroplast differentiation. J. Mar. Biol. Assoc. U.K. **53**:975–985.
72. **Evans, L. V., and A. O. Christie.** 1970. Studies on the ship-fouling alga *Enteromorpha*. I. Aspects of the fine-structure and biochemistry of swimming and newly settled zoospores. Ann. Bot. **34**:451–466.
73. **Fain, G. L., F. N. Quandt, B. L. Bastian, and H. M. Gerschenfeld.** 1978. Contribution of a caesium-sensitive conductance increase to the rod photoresponse. Nature (London) **272**:467–469.
74. **Falk, G., and P. Fatt.** 1972. Physical changes induced by light in the rod outer segments of vertebrates, p. 200–244. *In* H. J. A. Dartnall (ed.), Photochemistry of vision. Handbook of sensory physiology, vol. VII/1. Springer-Verlag, Inc., New York.
75. **Feinleib, M. E., and G. M. Curry.** 1971. The nature of the photoreceptor in phototaxis, p. 366–395. *In* W. R. Loewenstein (ed.), Principles of receptor physiology. Handbook of sensory physiology, vol. I. Springer-Verlag, Inc., New York.
76. **Feinleib, M. E. H., and G. M. Curry.** 1971. The relationship between stimulus intensity and oriented phototactic response (topotaxis) in *Chlamydomonas*. Physiol. Plant. **25**:346–352.
77. **Forward, R. B., Jr.** 1970. Change in the photoresponse action spectrum of the dinoflogellate *Gyrodinium dorsum* Kofoid by red and far-red light. Planta **92**:248–258.
78. **Forward, R. B., Jr.** 1973. Phototaxis in a dinoflagellate: action spectra as evidence for a two-pigment system. Planta **111**:167–178.
79. **Forward, R. B., Jr.** 1974. Phototaxis by the dinoflagellate *Gymnodinium splendens* Lebour. J. Protozol. **21**:312–315.
80. **Forward, R. B., Jr.** 1976. Light and diurnal vertical migration: photobehavior and photophysiology of plankton, p. 157–209. *In* K. C. Smith (ed.), Photochemical and photobiological reviews, vol. 1. Plenum Publishing Corp., New York.
81. **Foster, K. W.** 1972. The photoresponses of *Phycomyces*: analysis using manual techniques and an automated machine which precisely tracks and measures growth during programmed stimuli. Ph.D. thesis, California Institute of Technology, Pasadena.
82. **Foster, K. W.** 1977. Phototropism of coprophilous zygomycetes. Annu. Rev. Biophys. Bioeng. **6**:419–443.
83. **Foster, K. W., and E. D. Lipson.** 1973. The light growth response of *Phycomyces*. J. Gen. Physiol. **62**:570–617.
84. **Francis, D.** 1967. On the eyespot of the dinoflagellate, *Nematodinium* J. Exp. Biol. **47**:495–501.
85. **Gantt, E.** 1975. Phycobilisomes: light-harvesting pigment complexes. BioScience **25**:781–788.
86. **Gantt, E., M. R. Edwards, and L. Provasoli.** 1971. Chloroplast structure of the *Cryptophyceae*. Evidence for phycobiliproteins within intrathylakoidal spaces. J. Cell Biol. **48**:280–290.
87. **Gerisch, G.** 1959. Die Zelldifferenzierung bei *Pleodorina californica* Shaw und die Organization der Phytomonadinenkolonien. Arch. Protistenkd. **104**:292–358.
88. **Gössel, I.** 1957. Über das Aktionsspektrum der Phototaxis chlorophyllfreier Euglenen und über die Absorption des Augenflecks. Arch. Mikrobiol. **27**:288–303.
89. **Goy, M. F., and M. S. Springer.** 1978. In search of the linkage between receptor and response: the role of a protein methylation reaction in bacterial chemotaxis, p. 1–34. *In* G. L. Hazelbauer (ed.), Taxis and behavior. Receptors and recognition, series B, vol. 5. Chapman and Hall, London.
90. **Green, J. C.** 1973. Studies in the fine structure and taxonomy of flagellates in the genus *Pavlova*. II. A freshwater representative, *Pavlova granifera* (Mack) comb. nov. Br. Phycol. J. **8**: 1–12.
91. **Green, J. C.** 1975. The fine-structure and taxonomy of the haptophycean flagellate *Pavlova lutheri* (Droop) comb. nov. (= *Monochrysis lutheri* Droop). J. Mar. Biol. Assoc. U.K. **55**: 785–793.
92. **Green, J. C., and D. J. Hibberd.** 1977. The ultrastructure and taxonomy of *Diacronema vlkianum* (Prymnesiophyceae) with special reference to the haptonema and flagellar apparatus. J. Mar. Biol. Assoc. U.K. **57**:1125–1136.
93. **Green, J. C., and I. Manton.** 1970. Studies in the fine structure and taxonomy of flagellates in the genus *Pavlova*. I. A revision of *Pavlova gyrans*, the type species. J. Mar. Biol. Assoc. U.K. **50**:1113–1130.
94. **Greuet, C.** 1965. Structure fine de l'ocelle d'*Erythropis pavillardi* Hertwig, Péridinien Warnowiidae Lindemann. C. R. Acad. Sci. **261**: 1904–1907.
95. **Greuet, C.** 1968. *Leucopsis cylindrica*, nov. gen., nov. sp., Péridinien Warnowiidae Lindemann: considérations phylogénétique sur les Warnowiidae. Protistologica **4**:419–422.
96. **Greuet, C.** 1971. Étude ultrastructurale et évolution des cnidocystes de *Nematodinum*, Périndinien Warnowiidae Lindemann. Protistologica **7**:345–355.
97. **Greuet, C.** 1978. Organisation ultrastructurale

de l'ocelloide de *Nematodinium*. Aspect phylogénétique de l'evolution du photorécepteur des Péridiniens Warnowiidae Lindemann. Cytobiologie **17**:114–136.

98. **Gruber, H. E., and B. Rosario.** 1974. Variation in eyespot ultrastructure in *Chlamydomonas reinhardi* (ac-31). J. Cell Sci. **15**:481–494.
99. **Hagins, W. A., R. D. Penn, and S. Yoshikama.** 1970. Dark current and photocurrent in retinal rods. Biophys. J. **10**:380–412.
100. **Hagins, W. A., and S. Yoshikami.** 1974. A role for Ca^{2+} in excitation of retinal rods and cones. Exp. Eye Res. **18**:299–305.
101. **Halldal, P.** 1958. Action spectra of phototaxis and related problems in Volvocales, Ulva-gametes and Dinophyceae. Physiol. Plant. **11**: 118–153.
102. **Halldal, P.** 1961. Ultraviolet action spectra of positive and negative phototaxis in *Platymonas subcordiformis*. Physiol. Plant. **14**:133–139.
103. **Halldal, P.** 961. Action spectra of phototaxis in unicellular algae, p. 121–126. *In* B. C. Christensen and B. Buchmann (ed.), Progress in photobiology. Elsevier-North Holland Publishing Co., Amsterdam.
104. **Hand, W. G., and W. Haupt.** 1971. Flagellar activity of the colony members of *Volvox aureus* Ehrbg. during light stimulation. J. Protozool. **18**:361–364.
105. **Hand, W. G., and J. A. Schmidt.** 1975. Phototactic orientation by the marine dinoflagellate *Gyrodinium dorsum* Kofoid. II. Flagellar activity and overall response mechanism. J. Protozool. **22**:494–498.
106. **Haupt, W..** 1959. Die Phototaxis der Algen, p. 318–370. *In* W. Ruhland (ed.), Handbuch der Pflanzenphysiologie, vol. 17/1. Springer-Verlag, Inc., New York.
107. **Haxo, F. T., and K. A. Clendenning.** 1953. Photosynthesis and phototaxis in *Ulva lactuca* gametes. Biol. Bull. Woods Hole Mass. **105**: 103–114.
108. **Hecht, E., and A. Zajac.** 1974. Optics. Addison-Wesley Publishing Co., Inc., Reading, Mass.
109. **Hecht, S., S. Shlaer, and M. H. Pirenne.** 1942. Energy, quanta and vision. J. Gen. Physiol. **25**: 819–840.
110. **Heelis, D. V., W. Kernick, G. O. Phillips, and K. Davies.** 1979. Separation and identification of the carotenoid pigments of stigmata isolated from light-grown cells of *Euglena gracilis* Strain Z. Arch. Microbiol. **121**:207–211.
111. **Hemmerich, P.** 1976. The present status of flavin and flavocoenzyme chemistry. Prog. Chem. Org. Nat. Prod. **33**:451–527.
112. **Henderson, R.** 1977. The purple membrane from *Halobacterium halobium*. Annu. Rev. Biophys. Bioeng. **6**:87–109.
113. **Heussler, P.** 1972. Licht-und electronen-mikroskopische Untersuchungen zur Entwicklungsmorphologie zoosporebildender und coccaler Grünalgen. Thesis, Universität München, Germany.
114. **Hibberd, D. J.** 1976. The ultrastructure and taxonomy of the Chrysophyceae and Prymnesiophyceae (Haptophyceae): a survey with some new observations on the ultrastructure of the Chrysophyceae. Bot. J. Linn. Soc. **72**:55–80.
115. **Hibberd, D. J.** 1979. The structure and phylogenetic significance of the flagellar transition region in the chlorophyll *c*-containing algae. BioSystems **11**:243–261.
116. **Hibberd, D. J., and M. J. Chretiennot-Dinet.** 1979. The ultrastructure and taxonomy of *Rhizochromulina marina* gen. et sp. nov., an amoeboid marine chrysophyte. J. Mar. Biol. Assoc. U.K. **59**:179–193.
117. **Hibberd, D. J., and G. F. Leedale.** 1972. Observations on the cytology and ultrastructure of the new algal class, Eustigmatophyceae. Ann. Bot. **36**:49–71.
118. **Hobbs, M. J.** 1972. Eyespot fine structure in *Euderina illinoiensis*. Br. Phycol. J. **7**:347–355.
119. **Hoffman, L. R.** 1976. Fine structure of *Cylindrocapsa* zoospores. Protoplasma **87**:191–219.
120. **Hoffman, L. R., and I. Manton.** 1962. Observations of the fine structure of the zoospore of *Oedogonium cardiacum* with special reference to the flagellar apparatus. J. Exp. Bot. **13**:443–449.
121. **Holt, F. S.** 1969. Wave fronts, rays, and focal surfaces, p. 1–35. *In* R. E. Collin and F. J. Zucker (ed.), Antenna theory, part 2. McGraw-Hill Book Co., New York.
122. **Huskey, R. J.** 1979. Mutants affecting vegetative cell orientation in *Volvox carteri*. Dev. Biol. **72**:236–243.
123. **Huth, K.** 1970. Bewegung und Orientierung bei *Volvox aureus* Ehrb. I. Mechanismus der phototaktischen Reaktion. Z. Pflanzenphysiol. **62**: 436–450.
124. **Huth, K.** 1970. Bewegung und Orientierung bei *Volvox aureus* Ehrb. II. Richtungsabweichung bei taktischen Reaktionen. Z. Pflanzenphysiol. **63**:344–351.
125. **Hyams, J. S., and G. G. Borisy.** 1978. Isolated flagellar apparatus of *Chlamydomonas*: characterization of forward swimming and alteration of waveform and reversal of motion by calcium ions *in vitro*. J. Cell Sci. **33**:235–253.
126. **Jahn, T. L., and E. C. Bovee.** 1964. Protoplasmic movements and locomotion of protozoa, p. 61–129. *In* S. H. Hutner (ed.), Biochemistry and physiology of protozoa, vol. 3. Academic Press, Inc., New York.
127. **Jahn, T. L., and E. C. Bovee.** 1965. Movement and locomotion of microorganisms. Annu. Rev. Microbiol. **19**:21–58.
128. **Jahn, T. L., and E. C. Bovee.** 1967. Motile behavior of protozoa, p. 41–200. *In* T.-T. Chen (ed.), Research in protozoology, vol. 1. Pergamon Press, Inc., Elmsford, N.Y.
129. **Jeffrey, S. W., and M. Vesk.** 1976. Further evidence for a membrane-bound endosymbiont within the dinoflagellate *Peridinium foliaceum*. J. Phycol. **12**:450–455.
130. **Jenkins, F. A., and H. E. White.** 1976. Funda-

mentals of optics, 4th ed., p. 288–291. McGraw-Hill Book Co., New York.
131. **Jennings, H. S.** 1976. Behavior of the lower organisms. Indiana University Press, Bloomington. (Reprint of 1906 edition.)
132. **Jesaitis, A. J.** 1974. Linear dichroism and orientation of the *Phycomyces* photopigment. J. Gen. Physiol. **63**:1–21.
133. **Jolivette, H. D. M.** 1914. Studies on the reactions of *Pilobolus* to light stimuli. Bot. Gaz. (Chicago) **57**:89–121.
134. **Joyon, L., and B. Fott.** 1964. Quelques particularités infrastructurales du plaste des *Carteria* (Volvocales). J. Microsc. (Paris) **3**:159–166.
135. **Kivic, P. A., and M. Vesk.** 1972. Structure and function in the Euglenoid eyespot apparatus: the fine structure, and response to environmental changes. Planta **105**:1–14.
136. **Krebs, W., and H. Kühn.** 1977. Structure of isolated bovine rod outer segment membranes. Exp. Eye Res. **25**:511–526.
137. **Krinsky, N. I., and T. H. Goldsmith.** 1960. The carotenoids of the flagellated alga, *Euglena gracilis*. Arch. Biochem. Biophys. **91**:271–279.
138. **Kung, C.** 1979. Biology and genetics of *Paramecium* behavior, p. 1–26. *In* X. O. Breakefield (ed.), Neurogenetics: genetic approaches to the nervous system. Elsevier-North Holland Publishing Co., New York.
139. **Land, M.F.** 1972. The physics and biology of animal reflectors. Prog. Biophys. Mol. Biol. **24**: 75–106.
140. **Land, M. F.** 1978. Animal eyes with mirror optics. Sci. Am. **239**(6):126–134.
141. **Lang, N. J.** 1963. Electron microscopy of the Volvocaceae and Astrephomenaceae. Am. J. Bot. **50**:280–300.
142. **Leadbeater, B. S. C.** 1971. Observations on the life history of the Haptophycean alga *Pleurochrysis scherffelii* with special reference to the microanatomy of the different types of motile cells. Ann. Bot. **35**:429–439.
143. **Lee, Y. W.** 1960. Statistical theory of communication. John Wiley & Sons, Inc., New York.
144. **Leedale, G. F.** 1967. Euglenoid flagellates. Prentice-Hall, Inc., Englewood Cliffs, N.J.
145. **Lembi, C. A., and N. J. Lang.** 1965. Electron microscopy of *Carteria* and *Chlamydomonas*. Am. J. Bot. **52**:464–477.
146. **Lenci, F., and G. Colombetti.** 1978. Photobehavior of microorganisms: a biophysical approach. Annu. Rev. Biophys. Bioeng. **7**:341–361.
147. **Lewin, R.A.** 1976. The genetics of algae. Botanical monographs, vol. 12. University of California Press, Berkeley.
148. **Linder, J. C., and L. A. Staehelin.** 1979. A novel model for fluid secretion by the trypanosomatid contractile vacuole apparatus. J. Cell Biol. **83**:371–382.
149. **Lipetz, L. E.** 1971. The relation of physiological and psychological aspects of sensory intensity, p. 191–225. *In* W. R. Loewenstein (ed.), Principles of receptor physiology. Handbook of sensory physiology, vol. I. Springer-Verlag, Inc., New York.
150. **Lipson, E. D.** 1975. White noise analysis of *Phycomyces* light growth response system. II. Extended intensity ranges. Biophys. J. **15**:1013–1031.
151. **Litvin, F. F., O. A. Sineshchekov, and V. A. Sineshchekov.** 1978. Photoreceptor electric potential in the phototaxis of the alga *Haematococcus pluvialis*. Nature (London) **271**: 476–478.
152. **Lucas, I. A. N.** 1970. Observations on the fine structure of the Cryptophyceae. I. The genus *Cryptomonas*. J. Phycol. **6**:30–38.
153. **Ludwig, W.** 1929. Untersuchungen über die Schraubenbahnen niederer Organismen. Z. Vgl. Physiol. **9**:734–801.
154. **Luntz, A.** 1931. Untersuchungen über die Phototaxis. I. Mitteilung: die absoluten Schwellenwerte und die relative Wirksamkeit von Spektralfarben bei grünen und farblosen Einzelligen. Z. Vgl. Physiol. **14**:68–92.
155. **Lythgoe, J. N.** 1972. The adaptation of visual pigments to the photic environment, p. 566–603. *In* H. J. A. Dartnall (ed.), Photochemistry of vision. Handbook of sensory physiology, vol. VII/1. Springer-Verlag, New York.
156. **Macleod, H. A.** 1969. Thin-film optical filters. Elsevier-North Holland Publishing Co., New York.
157. **Maiwald, M.** 1971. A comparative ultrastructural study of *Pyramimonas montana* Geitler and a *Pyramimonas* spec. Arch. Protistenkd. **113**:334–344.
158. **Manton, I.** 1959. Electron microscopical observations on a very small flagellate: the problem of *Chromulina pusilla* Butcher. J. Mar. Biol. Assoc. U.K. **38**:319–333.
159. **Manton, I.** 1964. Observations on the fine structure of the zoospore and young germling of *Stigeoclonium*. J. Exp. Bot. **15**:399–411.
160. **Manton, I.** 1964. Die feinere Struktur von *Pedinomonas minor* Korschikoff. II. Electron microscopical investigation. Nova Hedwigia Z. Kryptogamenkd. **8**:441–451.
161. **Manton, I.** 1965. Some phyletic implications of flagellar structure in plants. Adv. Bot. Res. **2**: 1–34.
162. **Manton, I.** 1967. Electron microscopical observations on a clone of *Monomastix* Scherffel in culture. Nova Hedwigia Z. Kryptogamenkd. **14**:1–11.
163. **Manton, I.** 1968. Further observations on the microanatomy of the haptonema in *Chrysochromulina chiton* and *Prymnesium parvum*. Protoplasma **66**:35–53.
164. **Manton, I., and M. Parke.** 1960. Further observations on small green flagellates with special reference to possible relatives of *Chromulina pusilla* Butcher. J. Mar. Biol. Assoc. U.K. **39**: 275–298.
165. **Manton, I., and M. Parke.** 1965. Observations on the fine structure of two species of *Platymonas* with special reference to flagellar scales and the mode of origin of the theca. J. Mar.

Biol. Assoc. U.K. **45**:743–754.

166. **Manton, I., D. G. Rayns, H. Ettl, and M. Parke.** 1965. Further observations on green flagellates with scaly flagella: the genus *Heteromastix* Korshikov. J. Mar. Biol. Assoc. U.K. **45**:241–255.
167. **Marchant, H. J., and J. D. Pickett-Heaps.** 1972. Ultrastructure and differentiation of *Hydrodictyon reticulatum*. IV. Conjugation of gametes and the development of zygospores and azygospores. Aust. J. Biol. Sci. **25**:279–291.
168. **Marcus, M. A., and L. Aaron.** 1977. Kinetic resonance Raman spectroscopy: dynamics of deprotonation of the Schiff base of bacteriorhodopsin. Science **195**:1328–1330.
169. **Marcuse, D.** 1974. Theory of dielectric optical waveguides. Academic Press, Inc. New York.
170. **Marmarelis, P. Z., and V. Z. Marmarelis.** 1978. Analysis of physiological systems: the white noise approach. Plenum Publishing Corp., New York.
171. **Mast, S. O.** 1907. Light reactions in lower organisms. II. *Volvox globator*. J. Comp. Neurol. Psychol. **17**:99–180.
172. **Mast, S. O.** 1911. Light and the behavior of organisms. John Wiley & Sons, Inc., New York.
173. **Mast, S. O.** 1916. The process of orientation in the colonial organism, *Gonium pectorale*, and a study of the structure and function of the eye-spot. J. Exp. Zool. **20**:1–17.
174. **Mast, S. O.** 1917. The relation between spectral color and stimulation in the lower organisms. J. Exp. Zool. **22**:471–528.
175. **Mast, S. O.** 1927. The structure and function of the eye-spot in unicellular and colonial organisms. Arch. Protiskenkd. **60**:197–220.
176. **Mattox, K. R., and K. D. Stewart.** 1977. Cell division in the scaly green flagellate *Heteromastix angulata* and its bearing on the origin of the Chlorophyceae. Am. J. Bot. **64**:931–945.
177. **McCormick, D. B.** 1977. Interactions of flavins with amino acid residues: assessments from spectral and photochemical studies. Photochem. Photobiol. **26**:169–182.
178. **McCormick, D. B.** 1977. Spectral and photochemical assessments of interactions of the flavin ring system with amino acid residues, p. 233–245. *In* B. Pullman and N. Goldblum (ed.), Excited states in organic chemistry and biochemistry. Tenth Jerusalem Symposium on Quantum Chemistry and Biochemistry. Kluwer Boston, Inc., Hingham, Mass.
179. **McLachlan, J., and M. Parke.** 1967. *Platymonas impellucida* sp. nov. from Puerto Rico. J. Mar. Biol. Assoc. U.K. **47**:723–733.
180. **Melkonian, M.** 1975. The fine structure of the zoospores of *Fritschiella tuberosa* Iyeng. (Chaetophorineae, Chlorophyceae) with special reference to the flagellar apparatus. Protoplasma **86**:391–404.
181. **Melkonian, M..** 1978. Structure and significance of cruciate flagellar root systems in green algae: comparative investigations in species of *Chlorosarcinopsis* Chlorosarcinales). Plant Syst. Evol. **130**:265–292.
182. **Melkonian, M., and H. Robenek.** 1979. The eyespot of the flagellate *Tetraselmis cordiformis* Stein (Chlorophyceae): structural specialization of the outer chloroplast membrane and its possible significance in phototaxis of green algae. Protoplasma **100**:183–197.
183. **Mesibov, R., G. W. Ordal, and J. Adler.** 1973. The range of attractant concentrations for bacterial chemotaxis and the threshold and size of response over this range. J. Gen. Physiol. **62**: 203–223.
184. **Messer, G., and Y. Ben-Shaul.** 1969. Fine structure of *Peridinium westii* Lemm., a freshwater dinoflagellate. J. Protozool. **16**:272–280.
185. **Metzner, P.** 1929. Bewegungstudien an Peridineen. Z. Bot. **22**:225–265.
186. **Micalef, H., and P. Gayral.** 1972. Quelques aspects de l'infrastructure des cellules végétatives et des cellules reproductrices d'*Ulva lactuca* L. (Chlorophycées). J. Microsc. (Paris) **13**:417–428.
187. **Miller, W. H.** 1979. Ocular optical filtering, p. 69–143. *In* H. Autrum (ed.), Comparative physiology and evolution of vision in invertebrates. A: Invertebrate photoreceptors. Handbook of sensory physiology, vol. VII/6A. Springer-Verlag, Inc., New York.
188. **Mjaaland, G.** 1956. Some laboratory experiments on the coccolithophorid *Coccolithus huxleyi*. Oikos **7**:251–255.
189. **Moestrup, Ø.** 1978. On the phylogenetic validity of the flagellar apparatus in green algae and other chlorophyll a and b containing plants. BioSystems **10**:117–144.
190. **Moestrup, Ø., and H. A. Thomsen.** 1974. An ultrastructural study of the flagellate *Pyramimonas orientalis* with particular emphasis on Golgi apparatus activity and the flagellar apparatus. Protoplasma **81**:247–269.
191. **Mornin, L., and D. Francis.** 1967. The fine structure of *Nematodinium armatum*, a naked dinoflagellate. J. Microsc. (Paris) **6**:759–772.
192. **Murray, R. W.** 1974. The ampullae of Lorenzini, p. 125–146. *In* A. Fessard (ed.), Electroreceptors and other specialized receptors in lower vertebrates. Handbook of sensory physiology, vol. III/3. Springer-Verlag, Inc., New York.
193. **Nakamura, K., D. F. Bray, J. W. Costerton, and E. B. Wagenaar.** 1973. The eyespot of *Chlamydomonas eugametos*: a freeze-etch study. Can. J. Bot. **51**:817–819.
194. **Nichols, K. M., and R. Rikmenspoel.** 1978. Control of flagellar motion in *Chlamydomonas* and *Euglena* by mechanical microinjection of Mg^{2+} and Ca^{2+} and by electric current injection. J. Cell. Sci. **29**:233–247.
195. **Nikolayev, V. P., and V. G. Yakubenko.** 1978. Experimental research into the spatial structure of the fluctuations of the underwater light field. Izv. Akad. Nauk SSSR Atmos. Oceanic Phys. **14**:301–305.
196. **Nordli, E.** 1957. Experimental studies on the ecology of Ceratia. Oikos **8**:200–265.
197. **Norris, R. E., and B. R. Pearson.** 1975. Fine structure of *Pyramimonas parkeae*, sp. nov.

(Chlorophyta, Prasinophyceae). Arch. Protistenkd. **117**:192–213.

198. **Nultsch, W.** 1977. Effect of external factors on phototaxis of *Chlamydomonas reinhardtii*. II. Carbon dioxide, oxygen and pH. Arch. Microbiol. **112**:179–185.
199. **Nultsch, W.** 1979. Effect of external factors on phototaxis of *Chlamydomonas reinhardtii*. III. Cations. Arch. Microbiol. **123**:93–99.
200. **Nultsch, W., and D.-P. Häder.** 1979. Photomovement of motile microorganisms. Photochem. Photobiol. **29**:423–437.
201. **Nultsch, W., G. Throm, and I. von Rimscha.** 1971. Phototaktische Untersuchungen an *Chlamydomonas reinhardii* Dangeard in homokontinuierlicher Kultur. Arch. Mikrobiol. **80**: 351–369.
202. **Ohad, I., I. Goldberg, R. Broza, S. Schuldiner, and E. Gan-zvi.** 1969. Changes in lipid and pigment composition and photosynthetic activity during formation of chloroplast lamellae in a mutant of *Chlamydomonas reinhardi* y-1, p. 284–295. *In* H. Metzner (ed.), Progress in photosynthesis research, vol. 1. International Union of Biological Sciences, Tubingen.
203. **Ohad, I., P. Siekevitz, and G. E. Palade.** 1967. Biogenesis of chloroplast membranes. I. Plastid dedifferentiation in a dark-grown algal mutant (*Chlamydomonas reinhardi*). J. Cell Biol. **35**: 521–552.
204. **Paintal, A. S.** 1972. Cardiovascular receptors, p. 1–45. *In* E. Neil (ed.), Enteroreceptors. Handbook of sensory physiology, vol. III/1. Springer-Verlag, Inc., New York.
205. **Papoulis, A.** 1977. Signal analysis. McGraw-Hill Book Co., New York.
206. **Parke, M., and I. Adams.** 1960. The motile (*Crystallolithus hyalinus* Gaarder and Markali) and non-motile phases in the life history of *Coccolithus pelagicus* (Wallich) Schiller. J. Mar. Biol. Assoc. U.K. **39**:263–274.
207. **Parke, M., and I. Manton.** 1965. Preliminary observations on the fine structure of *Prasinocladus marinus*. J. Mar. Biol. Assoc. U.K. **45**: 525–536.
208. **Parke, M., and I. Manton.** 1967. The specific identity of the algal symbiont in *Convoluta roscoffensis*. J. Mar. Biol. Assoc. U.K. **47**:445–464.
209. **Parke, M., and D. G. Rayns.** 1964. Studies on marine flagellates. VII. *Nephroselmis gilva* sp. nov. and some allied forms. J. Mar. Biol. Assoc. U.K. **44**:209–217.
210. **Parratt, L. G.** 1961. Probability and experimental errors in science. Dover Publications Inc., New York.
211. **Piccinni, E., and M. Mammi.** 1978. Motor apparatus of *Euglena gracilis*: ultrastructure of the basal portion of the flagellum and the paraflagellar body. Boll. Zool. **45**:405–414.
212. **Piccinni, E., and P. Omodeo.** 1975. Photoreceptors and phototactic programs in protista. Boll. Zool. **42**:57–79.
213. **Pickett-Heaps, J. D.** 1970. Some ultrastructural features of *Volvox*, with particular reference to the phenomenon of inversion. Planta **90**:174–190.
214. **Pickett-Heaps, J. D., and D. W. Ott.** 1974. Ultrastructural morphology and cell division in *Pedinomonas*. Cytobios **11**:41–58.
215. **Pocock, M. A.** 1932. Volvox in South Africa. Ann. S. Afr. Mus. **16**:523–656.
216. **Rabinowitch, E. I.** 1951. Photosynthesis and related processes, vol. 2, part 1, p. 605. Interscience Publishers, Inc., New York.
217. **Retallack, B., and R. D. Butler.** 1972. Reproduction in *Bulbochaete hiloensis* (Nordst.) Tiffany. I. Structure of the zoospore. Arch. Mikrobiol. **86**:265–280.
218. **Rushton, W. A. H.** 1972. Visual pigments in man, p. 364–394. *In* H. J. A. Dartnall (ed.), Photochemistry of vision. Handbook of sensory physiology, vol. VII/1. Springer-Verlag, Inc., New York.
219. **Rushton, W. A. H., and G. H. Henry.** 1968. Bleaching and regeneration of cone pigments in man. Vision Res. **8**:617–631.
220. **Sager, R., and G. E. Palade.** 1954. Chloroplast structure in green and yellow strains of *Chlamydomonas*. Exp. Cell Res. **7**:584–588.
221. **Sakaguchi, H., and K. Iwasa.** 1979. Two photophobic responses in *Volvox carteri*. Plant Cell Physiol. **20**:909–916.
222. **Sakaguchi, H., and K. Tawada.** 1977. Temperature effect on the photoaccumulation and phobic response of *Volvox aureus*. J. Protozool. **24**:284–288.
223. **Salisbury, J. L., and G. L. Floyd.** 1978. Molecular, enzymatic, and ultrastructure characterization of the pyrenoid of the scaly green monad *Micromonas squamata*. J. Phycol. **14**:362–368.
224. **Schell, A. C.** 1969. The antenna as a spatial filter, p. 557–579. *In* R. E. Collin and F. J. Zucker (ed.), Antenna theory, part 2. McGraw-Hill Book Co., New York.
225. **Schenck, H., Jr.** 1957. On the focusing of sunlight by ocean waves. J. Opt. Soc. Am. **47**:653–657.
226. **Schletz, K.** 1976. Phototaxis bei *Volvox*. Pigmentsysteme der Lichtrichtungsperzeption. Z. Pflanzenphysiol. **77**:189–211.
227. **Schmidt, J. A., and R. Eckert.** 1976. Calcium couples flagellar reversal to photostimulation in *Chlamydomonas reinhardtii*. Nature (London) **262**:713–715.
228. **Schnepf, E., and G. Deichgräber.** 1972. Über den Feinbau von Theka, Pusule und Golgi-Apparat bei dem Dinoflagellaten *Gymnodinium* spec. Protoplasma **74**:411–425.
229. **Silverberg, B. A., and T. Sawa.** 1974. Cytochemical localization of oxidase activities with diaminobenizidine in the green alga *Chlamydomonas dysosmos*. Protoplasma **81**:177–188.
230. **Snyder, A. W.** 1975. Photoreceptor optics—theoretical principles, p. 38–55. *In* A. W. Snyder and R. Menzel (ed.), Photoreceptor optics. Springer-Verlag, Inc., New York.
231. **Song, P.-S.** 1970. Molecular orbital treatment of the intramolecular complexes in flavin adenine dinucleotide (FAD), p. 358–380. *In* E. D. Berg-

mann and B. Pullman (ed.), Quantum aspects of heterocyclic compounds in chemistry and biochemistry. Second Jerusalem Symposium on Quantum Chemistry and Biochemistry. Israel Academy of Sciences and Humanities, Jerusalem.

232. **Song, P.-S., P. Koka, B. B. Prézelin, and F. T. Haxo.** 1976. Molecular topology of the photosynthetic light-harvesting pigment complex, peridinin-chlorophyll a-protein, from marine dinoflagellates. Biochemistry **15**:4422–4427.
233. **Springer, M. S., M. F. Goy, and J. Adler.** 1979. Protein methylation in behavioural control mechanisms and in signal transduction. Nature (London) **280**:279–284.
234. **Stewart, K. D., and K. R. Mattox.** 1975. Comparative cytology, evolution, and classification of the green algae with some consideration of the origin of other organisms with chlorophylls a and b. Bot. Rev. **41**:104–135.
235. **Stoeckenius, W., R. H. Lozier, and R. A. Bogomolni.** 1979. Bacteriorhodopsin and the purple membrane of Halobacteria. Biochim. Biophys. Acta **505**:215–278.
236. **Throndsen, J.** 1973. Fine structure of *Eutreptiella gymnastica* (Euglenophyceae). Norw. J. Bot. **20**:271–280.
237. **Throndsen, J.** 1976. Occurrence and productivity of small marine flagellates. Norw. J. Bot. **23**:269–293.
238. **Tomas, R. N., and E. R. Cox.** 1973. Observations on the symbiosis of *Peridinium balticum* and its intracellular alga. I. Ultrastructure. J. Phycol. **9**:304–323.
239. **Treviranus, L. C.** 1817. Fernere Beobachtungen über die Bewegung der grünen Materie im Pflanzenreiche, p. 72–92. *In* G. R. Treviranus and L. C. Treviranus (ed.), Vermischte Schriften anatomischen und physiologischen Inhalts, vol. II. J.G. Heyse, Bremen.
240. **Vetter, W., G. Englert, N. Rigassi, and U. Schwieter.** 1971. Spectroscopic methods, p. 189–266. *In* O. Isler (ed.), Carotenoids. Birkhäuser-Verlag, Basel.
241. **Wait, J. R.** 1962. Electromagnetic waves in stratified media. Macmillan Publishing Co., Inc., New York.
242. **Wald, G., and P. K. Brown.** 1953. The molar extinction of rhodopsin. J. Gen. Physiol. **37**: 189–200.
243. **Walne, P. L., and H. J. Arnott.** 1967. The comparative ultrastructure and possible function of eyespots: *Euglena granulata* and *Chlamydomonas eugametos*. Planta **77**:325–353.
244. **Watanabe, M., and M. Furuya.** 1974. Action spectrum of phototaxis in a cryptomonad alga, *Cryptomonas* sp. Plant Cell Physiol. **15**:413–420.
245. **Watson, M. W.** 1975. Flagellar apparatus, eyespot and behavior of *Microthamnion kuetzingianum* (Chlorophyceae) zoospores. J. Phycol. **11**:439–448.
246. **Weisskopf, V. F.** 1968. How light interacts with matter. Sci. Am. **219**(3):60–71.
247. **White, R. H.** 1978. Insect visual pigments. Adv. Insect Physiol. **13**:35–67.
248. **Wolken, J. J.** 1977. *Euglena*: the photoreceptor system for phototaxis. J. Protozool. **24**:518–522.